



FACULTY OF SCIENCE AND TECHNOLOGY

MASTER THESIS

Study programme / specialisation:
Marine and Offshore Technology

The spring semester, 2022

Author:
Jonatan Kwan-Soo Byman

Open / Confidential

Jonatan Byman.....
(Signature author)

Course coordinator:
Professor Yihan Xing, Ph.D.

Supervisor(s):
Professor Daniel Karunakaran, Ph.D.
(University of Stavanger and Subsea7, Norway)

Thesis title:

Steel Catenary Riser with Residual Curvature in Deepwater and Harsh Environment

Credits (ECTS): 30

Keywords:
Residual Curvature Method, RCM, Steel Catenary Riser, SCR, Extreme Response Analysis, Fatigue Analysis, Deepwater, Harsh Environment

Pages: 120
+ appendix: 6

Stavanger, June 15/2022
date/year

Abstract

The exploration and production of oil and gas are still high in demand. With the advancement of subsea technology, it is possible to move into deeper waters and harsher environments. It highlights the importance of finding riser configurations that is suitable but also cost-effective. This thesis aims to find a riser configuration that can handle the large vessel motions of the Floating Production, Storage and Offloading (FPSO) in a remote, deepwater and harsh environment.

The conventional Steel Catenary Riser (SCR) has been a favored concept for deep and ultradeep water developments. However, the SCR is very sensitive to large vessel motions, impacting the downward velocity at the hang-off point. This translates to a higher velocity in the Touch Down Zone (TDZ) that can induce excessive levels of stress and fatigue.

An alternative that has been considered is the implementation of residual curvature sections in the riser using the Residual Curvature Method (RCM). These sections create a small deformation in the pipe that works as triggers for lateral buckling and aids in absorbing compressive forces generated. A comparison between the conventional SCR and the Residual Curvature Steel Catenary Riser (RCSCR) is performed to evaluate how the residual curvature affects the response in the TDZ.

According to previous works, the conventional SCR with a coating is not able to cope with a downward velocity above 2.33 m/s. The implementation of Residual Curvature (RC) to the riser showed that it could cope with downward velocities up to 3.35 m/s at the hang-off point. Moreover, the fatigue performance was analyzed for wave-induced fatigue. Neither the SCR nor the RCSCR had an expected fatigue life above the acceptance criteria of 250 years.

Overall, this thesis has shown that the RCSCR improved the strength performance in the TDZ and improved the riser's ability to cope with large vessel motions. For fatigue performance, the RCSCR did not meet the design requirements and still requires more study.

Keywords: Residual Curvature Method, RCM, Steel Catenary Riser, SCR, Extreme Response Analysis

Acknowledgments

I want to express my most profound appreciation to my faculty supervisor in the Department of Mechanical Engineering and Structural Engineering and Materials Science, Professor Daniel Karunakaran, Ph.D., for the opportunity to write my master thesis under his supervision. His knowledge, guidance, and comments have been important in developing this thesis.

Moreover, I would like to thank Adekunle Peter Orimolade, Ph.D., for his valuable input, explanations, and aid in simulations and analysis.

Many thanks to Subsea7 Stavanger for providing the office space and resources required for the thesis work. Moreover, I would like to thank the Hydrodynamics and Ocean Technology group of Subsea 7 Stavanger for the help, discussions, and guidance on the thesis topic and the use of Orcaflex.

To my lovely parents, who raised me to become who I am today. Thank you very much.

To my beloved girlfriend, Marina Silva, for all your support, assistance, motivation and love. You have made this semester special and unforgettable. You are a truly amazing person.

Moreover, thank you to my fellow students at the University of Stavanger for all the good memories during my master's study.

Contents

Abstract	i
Acknowledgment	ii
Contents	iii
List of Figures	vii
List of Tables	x
Abbreviations	xii
1 Introduction	1
1.1 Scope and objectives	3
2 Deepwater Riser Systems	4
2.1 Riser systems	4
2.1.1 Compliant risers	5
2.1.2 Top tensioned riser	7
2.1.3 Hybrid riser	8
2.2 Rigid risers	8
2.3 Flexible risers	9
2.4 Riser components	9
2.4.1 Flex joint	9
2.4.2 Tapered stress joint	10
2.4.3 Strakes	11
2.5 Riser challenges	12
2.5.1 Deep-water challenges	12
2.5.1.1 Increased weight of the riser	12
2.5.1.2 Sizing of the riser	12
2.5.1.3 Area of spreading	12
2.5.1.4 Current	13
2.5.2 Harsh environment challenges	13
2.5.2.1 Floater motions	13
2.5.2.2 Fatigue	13
2.5.2.3 Installation	13

3	Steel Catenary Riser	15
3.1	Conventional SCR	15
3.2	Weight distributed SCR	17
3.3	Steel Lazy Wave Riser	18
3.4	Material selection for SCR's	19
4	FPSO	20
4.1	Introduction	20
4.2	Mooring system	21
4.2.1	Spread mooring system	21
4.2.2	Turret mooring system	21
4.2.3	Comparison of mooring systems	22
4.3	Selected FPSO for the thesis	23
5	Design loads and standards	24
5.1	Pressure loads	24
5.2	Functional loads	24
5.2.1	Marine growth	25
5.3	Environmental loads	25
5.3.1	Waves	25
5.3.2	Current	25
5.3.3	Floater motions	26
5.4	Design codes and standards	26
5.4.1	Introduction	26
5.4.2	Load and resistance factor design - DNV-ST-F201	27
5.4.2.1	Accidental Limit State	27
5.4.2.2	Serviceability Limit State	27
5.4.2.3	Ultimate Limit State	28
5.4.2.4	Fatigue Limit State	31
5.4.3	Working stress design	33
6	Residual Curvature Method	35
6.1	Introduction	35
6.2	Bending moment and curvature	37
6.3	Curvature and residual strain	37
6.4	Residual curvature using the Reel lay method	39
6.4.1	Reeling and unreeling of the riser	39
6.4.2	Straightening of the riser	40

6.5	Application of residual curvature	41
6.5.1	Calculation of residual curvature	42
6.5.2	Example of project installed with RCM	42
6.5.2.1	Skuld	42
6.5.3	Use case scenarios for local residual curvatures	43
7	Design basis and methodology	45
7.1	Introduction	45
7.2	Scope	45
7.3	Data for design	45
7.3.1	FPSO	45
7.3.2	Motions of the FPSO	46
7.3.2.1	FPSO static offsets	46
7.3.2.2	Wave frequency motions	47
7.3.2.3	Low frequency motions	48
7.3.3	Environmental data	48
7.3.3.1	Water depths	48
7.3.3.2	Current	48
7.3.3.3	Waves	48
7.3.4	Riser properties	49
7.3.5	Design life	50
7.3.6	Hydrodynamic data	50
7.3.7	Soil-riser interaction	51
7.4	Wall thickness	51
7.5	Design cases	52
7.6	Acceptance criteria	52
8	Extreme response analysis	54
8.1	Introduction	54
8.2	Static analysis	55
8.3	Static analysis of the conventional steel catenary riser	56
8.3.1	Analysis with coating	56
8.3.2	Analysis without coating	58
8.4	Seed components	60
8.5	Dynamic analysis for the steel catenary riser	61
9	Parametric study for the RCSCR	62
9.1	Section length sensitivity	64

9.2	Radius of curvature sensitivity study	67
9.2.1	Analysis of 60 m section with RC	67
9.2.2	Analysis of 140 m section with RC	69
9.3	Distance to seabed sensitivity study	71
9.3.1	Analysis of 60 m section	71
9.3.2	Analysis for 140 m section	72
9.4	Sensitivity for several sections in a row	73
9.4.1	Analysis of 60 m section	74
9.4.2	Analysis of 140 m section	75
9.5	Two separated sections sensitivity study	76
9.5.1	Analysis of 60 m section	77
9.5.2	Analysis of 140 m section	77
9.6	Different curvature for the residual curvature sections	78
9.7	Response analysis of the RCSCR	79
9.8	Fine tuning of parameters	81
9.8.1	Downward velocity of 3.63 m/s	81
9.8.2	Downward velocity of 3.42 m/s	82
9.8.3	Downward velocity of 3.35 m/s	82
9.9	Static analysis of the revised RCSCR configuration	85
9.10	Dynamic analysis of the revised RCSCR configuration	87
9.11	Summary of the parametric study and response analyses	88
10	Fatigue analysis	91
10.1	Introduction	91
10.2	S-N curves	91
10.2.1	Stress concentration factor	93
10.3	Wave induced fatigue	94
10.4	Results of the fatigue analysis	97
10.4.1	Conventional SCR	97
10.4.2	RCSCR	98
11	Conclusion and recommendations	101
11.1	Conclusion	101
11.2	Recommendations	103
	References	104
	Appendix	A. 6

List of Figures

1.1	Deep-water production concepts [2]	1
2.1	Compliant riser configurations [8]	6
2.2	Top Tensioned Riser (TTR) used on a SPAR and Tension Leg Platform (TLP) [14]	7
2.3	A typical hybrid riser configuration [3]	8
2.4	Cross section of a flexible riser [3]	9
2.5	Flex joint [11]	10
2.6	Tapered stress joint [8]	11
2.7	VIV suppression strakes [15]	11
3.1	Illustration of free hanging SCR [14]	16
3.2	Weight distributed SCR for harsh environments [16]	17
3.3	Illustration of a SLWR layout [24]	18
4.1	BP's Glen Lyon's FPSO [26]	20
4.2	Internal turret on an FPSO [28]	22
4.3	External turret on an FPSO [29]	22
6.1	Illustration of reel lay vessel and pipeline	35
6.2	Section with residual curvature [32]	36
6.3	Straightener tracks configuration for straight pipe (left) and under-straightened residual curvature section (right) [31]	36
6.4	The relation between bending moment and curvature [33]	37
6.5	The relationship between residual strain and curvature [35]	38
6.6	Pipeline reeling setup [36]	40
6.7	Unreeling of the riser [36]	40
6.8	Illustration of straightener equipment [36]	40
6.9	DNV-ST-F101 straight pipe criterion [36]	41
6.10	Residual curvature in the riser [38]	42
6.11	Local residual curvature locations [9]	43
6.12	Tie-in using RCM [39]	44
6.13	Riser configuration with local residual curvature versus nominal catenary [40]	44
7.1	FPSO mean, far and near offsets	47

8.1	Static effective tension with coating for the SCR	56
8.2	Static bending moment with coating for the SCR	57
8.3	Static utilization factor with coating for the SCR	58
8.4	Static effective tension without coating for the SCR	58
8.5	Static bending moment without coating for the SCR	59
8.6	Static utilization factor without coating for the SCR	59
8.7	Gumbel distribution for the maximum downward velocity at the hang-off point	60
9.1	Residual curvature sections	63
9.2	Compression versus section lengths with respect to residual curvature . .	65
9.3	Utilization factor versus section lengths with respect to residual curvature	66
9.4	Comparison of RC section lengths	66
9.5	Utilization factor versus radius of curvature with respect to residual cur- vature for 60 m section	68
9.6	Comparison of implemented curvature to the RC sections for 60 m section	69
9.7	Utilization factor versus radius of curvature with respect to residual cur- vature for 140 m section	70
9.8	Comparison of implemented curvature to the RC sections for 140 m section	70
9.9	Comparison of distance to seabed sensitivity for 60 m section	72
9.10	Comparison of distance to seabed sensitivity for 140 m section	73
9.11	Curvature setup in Orcaflex for the 60 m section	74
9.12	Sensitivity analysis of multiple 60 m sections of RC in a row	75
9.13	Curvature setup in Orcaflex for the 140 m section	76
9.14	Sensitivity analysis of multiple 140 m sections of RC in a row	76
9.15	Sensitivity analysis of multiple 60 m sections of RC in spread out loca- tions	77
9.16	Sensitivity analysis of multiple 140 m sections of RC in spread out loca- tions	78
9.17	RCSCR and SCR utilization factor comparison	80
9.18	The minimum effective tension for RCSCR and SCR	81
9.19	Strength response for RCSCR with for a downward velocity of 3.35 m/s	83
9.20	Effective tension for the RCSCR	86
9.21	Bending moment for the RCSCR	87
9.22	DNV utilization factor for the RCSCR	87
10.1	S-N curves in seawater with cathodic protection [47]	93
10.2	Blocking of the wave scatter diagram	96

10.3	Total fatigue damage of the SCR	97
10.4	Fatigue life for the SCR	98
10.5	Total fatigue damage of the RCSCR	99
10.6	Fatigue life for the RCSCR	99
A-1	The Orcaflex main window [49]	A. 2
A-2	Orcaflex toolbar [49]	A. 3
A-3	Orcaflex model states [49]	A. 4
A-4	Orcaflex coordinate system [49]	A. 5
A-5	Orcaflex headings and directions [49]	A. 5
A-6	Time and simulation stages [49]	A. 6

List of Tables

4.1	Comparison of spread moored versus turret moored FPSO [27]	23
5.1	Simplified design check for accidental loads	27
5.2	Design fatigue factors (DFF)	32
6.1	Residual strains versus radius of curvature	39
7.1	FPSO parameters	46
7.2	FPSO offsets for operational and accidental mooring conditions	47
7.3	Significant wave height and period data	49
7.4	Wave and current data for the North Sea location	49
7.5	Riser properties	50
7.6	Hydrodynamic coefficients	50
7.7	Soil-riser interaction parameters	51
7.8	Matrix of the load cases	52
8.1	Load factors for ULS check against DNV-ST-F201	55
8.2	Strength response of the SCR with a downward velocity of 3.81 m/s	61
9.1	Selected section lengths for RCSCR	64
9.2	Residual curvature sensitivity with respect to section length	65
9.3	Residual curvature sensitivity for the 60 m section	67
9.4	Residual curvature sensitivity for the 140 m section	69
9.5	Distance to seabed sensitivity for residual curvature of 60 m section	71
9.6	Distance to seabed sensitivity for residual curvature of 140m section	73
9.7	Sensitivity to different residual curvature for each of the sections	79
9.8	Strength response for the RCSCR	80
9.9	Dynamic strength responses for the RCSCR with a downward velocity of 3.63 m/s	82
9.10	Dynamic strength responses for the RCSCR with a downward velocity of 3.42 m/s	82
9.11	Dynamic strength responses for the RCSCR with a downward velocity of 3.35 m/s	83
9.12	Fine tuning of residual curvatures section for the near offset position	84
9.13	Fine tuning of residual curvatures section for the far offset position	85
9.14	Static result for revised RCSCR configuration	86

9.15 Dynamic strength responses for the revised RCSCR with a downward velocity of 3.35 m/s	88
10.1 Parameters for D-curve in seawater with cathodic protection	92
10.2 Parameters for C2-curve in seawater with cathodic protection	92
10.3 Sector probability for each of the wave directions	94
10.4 Lumped probability of occurrence for the representative sea states	96
10.5 SCR Fatigue life at the critical location	97
10.6 RCSCR Fatigue life at the critical location	98

Abbreviations

ALS	Accidental Limit State
API	American Petroleum Institute
ASME	American Society of Mechanical Engineers
CALM	Catenary Anchor Leg Mooring
DNV	Det Norske Veritas
FLS	Fatigue Limit State
FPS	Floating Production System
FPSO	Floating Production, Storage and Offloading
JONSWAP	Joint North Sea Wave Project
LF	Low Frequency Motions
LRFD	Load and Resistance Factor Design
NCS	Norwegian Continental Shelf
RAO	Response Amplitude Operator
RC	Residual Curvature
RCM	Residual Curvature Method
RCSCR	Residual Curvature Steel Catenary Riser
SCF	Stress Concentration Factor
SCR	Steel Catenary Riser
SLS	Serviceability Limit State
SLWR	Steel Lazy Wave Riser
SPM	Single Point Mooring
TDP	Touch Down Point
TDZ	Touch Down Zone
TLP	Tension Leg Platform
TSJ	Tapered Stress Joint
TTR	Top Tensioned Riser
UF	Utilization Factor
ULS	Ultimate Limit State
VIV	Vortex Induced Vibration
WDSCR	Weight Distributed Steel Catenary Riser
WF	Wave Frequency Motions
WSD	Working Stress Design

Chapter 1

Introduction

The world depends on the oil and gas industry as it is supplying over 64 % of the total energy consumed as of 2020 [1]. An increase in renewable energy sources has been emerging. However, all of them combined provide less than ten percent of the world's energy supply [1]. Energy consumption increases yearly, highlighting the importance of finding new and more productive methods for exploration and production in the oil and gas sector.

In the past decades, oil and gas production has moved from onshore into deep and ultra-deepwater depths offshore. Naturally, the exploration and development of the fields offshore are more challenging than an onshore field, mainly due to the environmental conditions of the sea. The advancement of subsea technology has facilitated and accelerated the production in deeper waters in areas such as the Norwegian Continental Shelf (NCS), Gulf of Mexico, Brazil, and West Africa.

A range of deepwater production concepts is presented in Figure 1.1, with the Floating Production, Storage, and Offloading (FPSO) being the preferred option. The main challenge for the FPSO in deep waters in combination with harsh environments are the vessel motions, especially the pitch and heave motions, as these have an enormous impact on the riser.

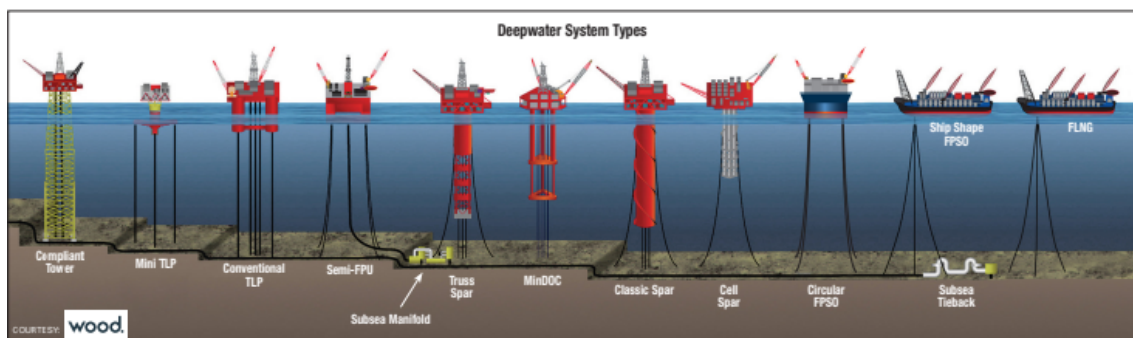


Figure 1.1: Deep-water production concepts [2]

Risers are a key component of oil and gas production which are used to transfer the hydrocarbons from the wells to the topside of the production unit. It is critical that the riser design is robust, safe in addition to being cost-effective. There are two main configurations, rigid and flexible risers. A third configuration can be obtained by combining these two, making a hybrid riser [3]. However, the simplest and preferred solution is the free-hanging Steel Catenary Riser (SCR) [4]. The SCR's primary advantages over the other concepts are the ease of construction and installation. In addition, they can be fabricated in longer sections at an overall lower cost. Furthermore, it has a high resistance to temperature and external and internal pressures [5] [6].

The drawback to the SCR is its sensitivity to the vessel motions. Harsher environments and deep water induce large downward velocity at the hang-off point. With the SCR being a rigid element, the downward velocity causes critical compressive and bending loads in the TDZ. In addition, the fatigue performance close to the hang-off point and in the TDZ is a critical issue in these environmental conditions, making this concept unfeasible [7]. In order to reduce the loads, several concepts have been proposed, with the most used one being the Steel Lazy Wave Riser (SLWR) which protects the TDZ by absorbing the vessel's motions with a geometrical spring [8]. This concept is well established. However, the main disadvantages are the cost of the buoyancy modules and the installation challenges.

Thus, a different alternative to the SLWR, is proposed in this thesis, known as the Residual Curvature Method (RCM). It is a straightforward and cost-effective method to control lateral buckling by creating intermittent residual curvature to certain sections of the pipe [9]. These sections absorb part of the energy generated by the FPSO's motion, resulting in a significant improvement in risers strength performance in the TDZ [4].

In addition to reducing stresses in the TDZ, the cost of implementation is low while the installation is simple. The residual curvature is created onboard the vessel by adjusting the straightener system during installation. These adjustments are made in less than 20 minutes; hence the low-cost [10]. On the other hand, the main disadvantage of the RCM is the fatigue life performance [4]. The performance increases compared to the SCR. However, more research and studies into fatigue performance for the RCSCR are required.

1.1 Scope and objectives

The thesis mainly focuses on establishing and assessing the RCSCR configuration and its capability to cope with the harsh environmental conditions and large vessel motions. This assessment considers the static and dynamic strength responses of the riser, in addition to fatigue performance. All of which are compared to a conventional SCR, in order to see the effect of the implementation RC in the riser. Moreover, how this method affects the riser's maximum effective tension, compression load, bending moment, and utilization factor considering the Load and Resistance Factor Design (LRFD) described by Det Norske Veritas (DNV) [11].

The study focuses on the strength performance of the RCSCR, which entails a parametric study for the geometry and parameters affecting the sections with RC. Analyses will be performed to establish an optimum configuration for the RCSCR and investigate the behavior of the parameters on the riser. The results of the parametric study provide a base case to consider. The simulations will be performed using the Orcaflex software for strength and fatigue analyses. The scope of the thesis is as follows:

- **Chapter 2** presents a general description of deepwater riser systems.
- **Chapter 3** discusses in more detail the SCR and its variations, along with challenges in deepwater and harsh environments.
- **Chapter 4** provides information for the FPSO and compares the mooring systems considered.
- **Chapter 5** presents information regarding the design loads and standards considered for the riser design.
- **Chapter 6** specifies the background theory for the RCM and its applicability.
- **Chapter 7** provides the design basis which includes analysis methodology, design data, and acceptance criteria for the riser design.
- **Chapter 8** presents the extreme response analysis for the conventional SCR
- **Chapter 9** consists of a parametric study, in addition to presenting the extreme responses analysis of the RCSCR
- **Chapter 10** presents the fatigue analyses for the SCR and RCSCR
- **Chapter 11** provides the conclusions and recommendations of the study

Chapter 2

Deepwater Riser Systems

2.1 Riser systems

The riser is the pipeline connecting the facilities from the topside to the seabed. They are important in all the different phases of the exploration and production of oil and gas. According to DNV the primary functions depending on their use of purpose and area of application, include [11]:

- Transportation of fluid from and to the well, with auxiliary support lines, guide tools, and drilling string. Moreover, it serves as a running and retrieving string for the blowout preventer.
- Transfer of processed fluids between the floater and the structure.
- Transportation of produced fluids from the reservoir
- Convey fluids to the reservoir from the topside facility

There are four main categories of risers, which is commonly divided into [11]:

- Production risers
- Drilling risers
- Export/injection risers
- Completion/workover risers

Production risers transports the fluids from the reservoir. It could also be utilized for other operations, including well workovers, injection, and completion [11].

Drilling risers isolates the wellbore fluid from the surroundings. The main functions of this riser are to provide fluid transportation from and to the well, guiding

of tools and drilling strings, support the auxiliary lines and be used as a running and retrieval string for the BOP [11].

Export risers provide transport of the processed fluids from the topside facility to an off-site unit or processing facility. While the **injection risers** provide transportation of fluid from the topside facility to the reservoir or a suitable disposal formation [11].

Completion/workover risers are used in temporary completion and workover operations, and it includes all of the equipment between the workover floaters tensioning system, and the subsea tree [11].

2.1.1 Compliant risers

The compliant riser offers flexibility for the floater to displace in the horizontal direction. It is designed to absorb floater motions without using additional heave motion compensation systems [12], making them suitable for harsh and deepwater environments.

The material used for the compliant riser can be either rigid or flexible pipe, where the most common rigid pipe is the SCR. Depending on the configuration required, there are several compliant configurations available according to the location's environmental conditions. Examples of such flexible configurations include Steep Wave, Lazy Wave, Steep S, Lazy S, and Free Hanging, as shown in Figure 2.1. To decide which of the configurations would be suitable for the development, one must perform analyses and consider the materials, costs, and structural integrity.

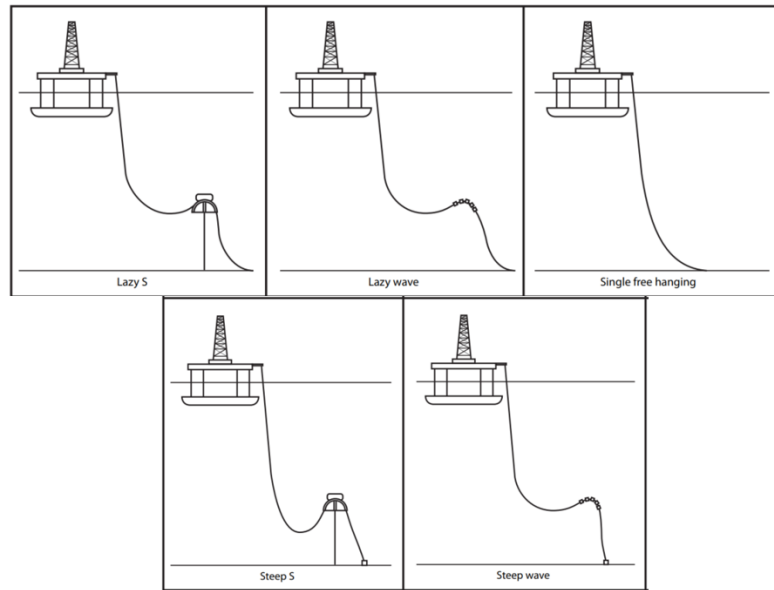


Figure 2.1: Compliant riser configurations [8]

Steep- and lazy wave: This configuration has buoyancy elements attached to a section length of the riser. The lazy wave setup requires less subsea infrastructure than the steep wave configuration, thus being the preferred configuration. The steep wave configuration must be installed with a subsea base and bend stiffener.

Steep- and lazy S: Similarly to the steep and lazy wave, where buoyancy elements are added to a section of the riser, but over a shorter distance. It is either installed with a fixed subsea buoy or a floating buoy.

The primary reason to install risers with buoyancy elements for both wave and S configurations is the reduction of top tension while absorbing heave motion and protecting the Touch Down Point (TDP).

Free hanging: The simplest form of the riser configuration and the cheapest. It requires minimal, if any, subsea infrastructure. The installation is either lowered onto the seabed or lifted from the seabed. These risers are exposed to loads while experiencing floater motions as the water depths increase and the riser's length and top tension increase. For free-hanging risers, the floater motion directly impacts the TDP, the critical point on the riser.

The connection point between the riser and the topside facility is a critical design issue for the compliant riser configurations. In order to minimize pipe stresses and bending moments in the hang off-area, components such as tapered joints and flex joints are installed [11].

2.1.2 Top tensioned riser

TTR are vertical risers that allow for floater motions in the vertical direction with the aid of heave compensation systems [13]. Ideally, the top tension is constant regardless of the floater motions. This reduces the risk of buckling and bending stresses due to the heave motion and minimizes the occurrence of Vortex Induced Vibration (VIV).

One of the main design parameters regarding the mechanical behavior of the riser is the top tension, in addition to the floater motion limitations. As a result, TTR's are best suited for structures/floaters with minimal heave motion. Spar's and TLP's are two structures commonly used and are shown in Figure 2.2

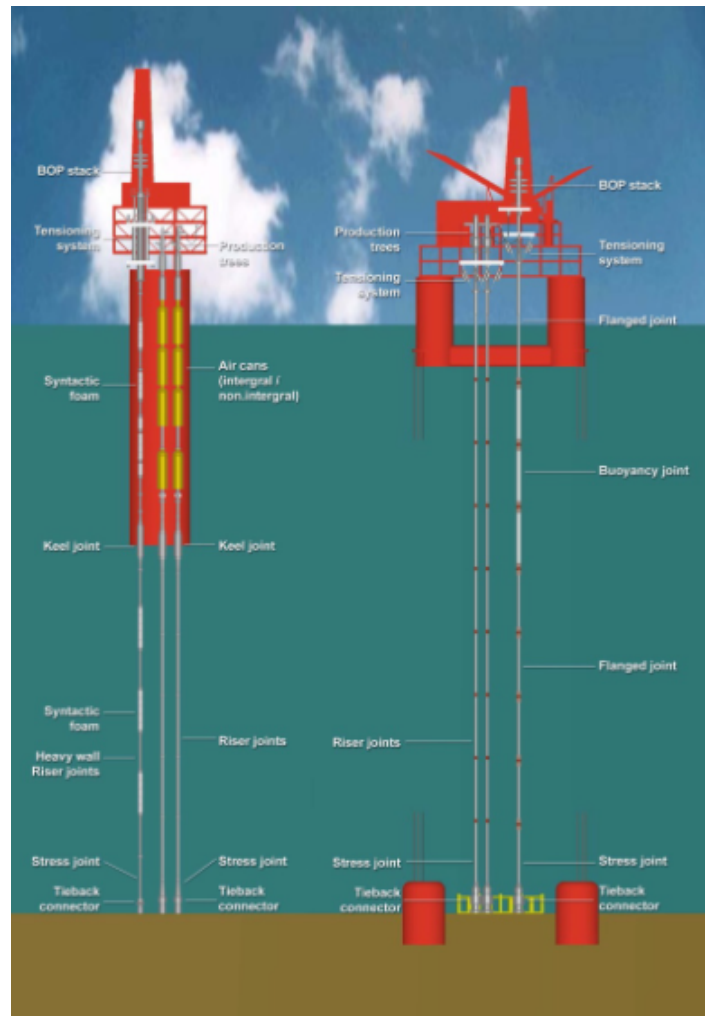


Figure 2.2: TTR used on a SPAR and TLP [14]

2.1.3 Hybrid riser

A hybrid riser is a combination of a compliant riser and a TTR where the TTR is connected to the seabed and a submerged buoy on the other end. At the same time, the compliant section of the riser is connected to the buoy and the topside facility. An illustration of a typical hybrid riser configuration is shown in Figure 2.3.

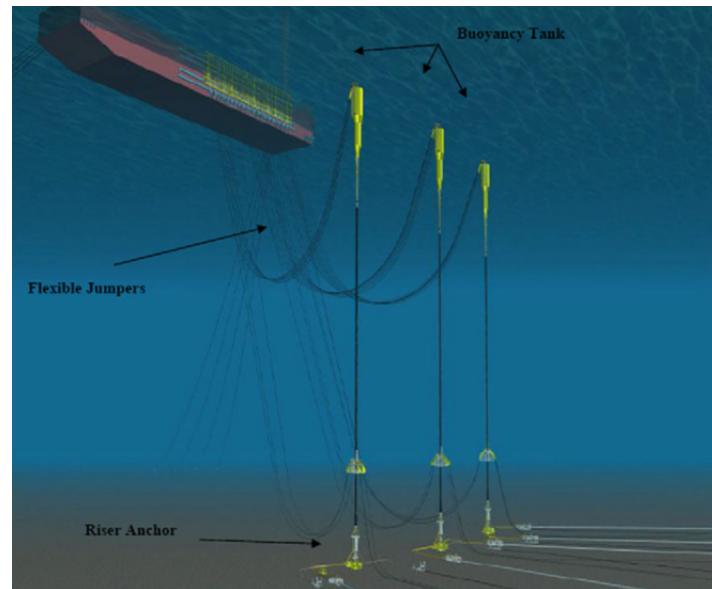


Figure 2.3: A typical hybrid riser configuration [3]

Using a hybrid configuration allows the floating structure to move in case of emergencies and leave the risers subsea. Additionally, the TTR section is located at depths where it experiences significantly less wave and current loading. On the other hand, the compliant section comprises flexible pipes that can withstand harsher environments.

2.2 Rigid risers

Rigid risers are made up of sections of metallic pipes joined together by welding, bolted connections, or threads in materials such as low carbon steel, titanium, or aluminum alloys. Low-carbon steel, most commonly referred to as steel risers, is the typical choice for a material in today's industry. It is popular due to its extensive knowledge of the material and mechanical properties. Additionally, they are available in large diameters, and the cost is relatively low compared to flexible risers [3].

2.3 Flexible risers

Flexible risers consist of several layers of composite pipes with a low bending stiffness to increase the compliant performance. Figure 2.4 shows a typical configuration of the layers. The carcass shall resist the external pressure. The pressure sheath between the carcass and the zeta spiral prevents fluid from leaking. Moreover, the armours prevent axial stress/hoop stress and resist internal pressure. Lastly, the outer external sheath prevents fluid from leaking and acts as an abrasion protection [3].

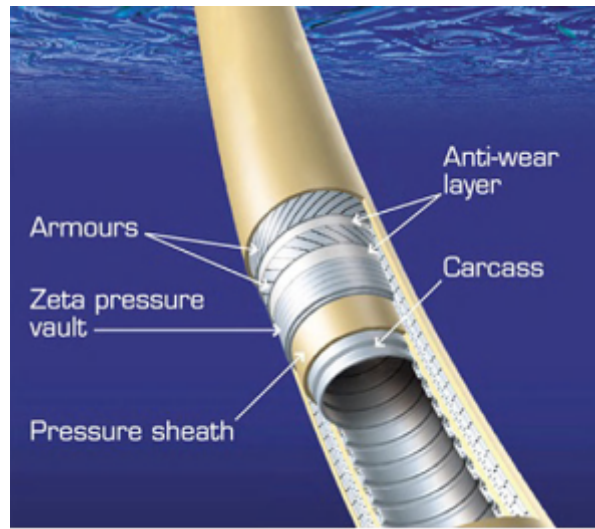


Figure 2.4: Cross section of a flexible riser [3]

2.4 Riser components

A complete riser system includes many components, such as strakes, connectors, flex joints, stress joints, and ball joints. All of which are essential to a fully working and optimized system. A few of the key components will be described in this section.

2.4.1 Flex joint

The flex joint is used at the top of SCR acting as the interface between the vessel and riser. It allows the riser system to rotate with a minimum bending moment, thus reducing the bending stresses at the hang-off point [3].

In the design, it is important to consider the flex joint stiffness, as this regulates the maximum stress and fatigue in the hang-off area. For large rotations, which typically occurs during storm conditions, the flex joint stiffness is much less compared to small amplitudes that occur in fatigue analysis [3]. The flex joint stiffness is affected by

variations in temperature and residual torque after installation of the joint. An illustration of the flex joint is presented in Figure 2.5.

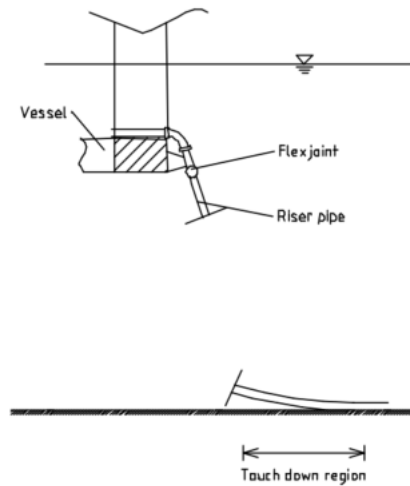


Figure 2.5: Flex joint [11]

2.4.2 Tapered stress joint

The Tapered Stress Joint (TSJ) can be used as a replacement for the flex joint. It also contributes to lower bending and fatigue issues between rigid sections of the riser in connection with less rigid sections. Furthermore, this reduces the local bending stresses and fatigue between the two sections [8][7].

The TSJ in one end has the bending stiffness close to the rigid section of the riser, while in the other end, the bending stiffness is lower than the less rigid section of the riser. This variation is usually achieved by having a different wall thickness, creating the taper of the joint [8] as shown in Figure 2.6.

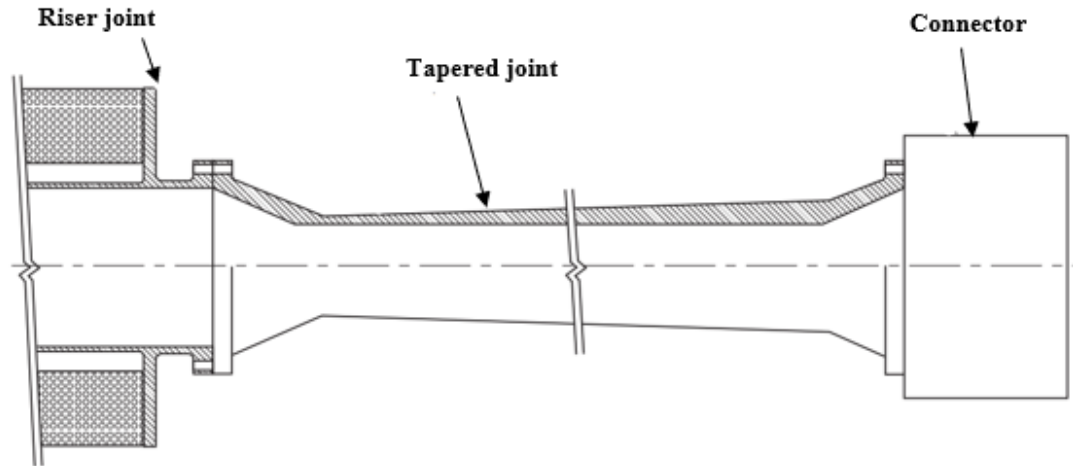


Figure 2.6: Tapered stress joint [8]

2.4.3 Strakes

A strong current creates VIV, caused by the shedding of vortices in the wake region of the downstream side of the flow [7]. The VIV can significantly impact the fatigue damage on the riser, reducing the expected life drastically. In order to avoid this, suppression devices against VIV including helical strakes and fairings, are added to sections of the riser as shown in Figure 2.7. These devices are designed to control the flow pattern around the riser, effectively decreasing the vibrations.



Figure 2.7: VIV suppression strakes [15]

2.5 Riser challenges

The risers being studied in this thesis are located in deepwater and harsh environments, which increases the complexity of the riser systems design [16]. The design of the riser system must consider the water depth, floater motions, pressure, thermal management, hydraulic issues, and more. The following sections will discuss the challenges associated with deepwater and harsh environments.

2.5.1 Deep-water challenges

2.5.1.1 Increased weight of the riser

The increased length of the riser is directly proportional to the weight increase of the riser with water depth. This results in a larger top tension at the floater, which is a key parameter in the selection of floater type. The capacity of the floater must be able to handle all the mooring and riser systems, where the top tension is the limiting factor [17].

2.5.1.2 Sizing of the riser

The sizing of the risers depends on two main parameters: the internal diameter and the wall thickness. The wall thickness is often selected for production and injection risers based on the internal pressure. However, the installation procedure also plays a role for larger export risers. The installment of the risers is usually done with no fluid in the riser, in which case the wall thickness must resist the external pressure to avoid collapsing. Overall, the riser must be able to handle the internal pressure from the transported hydrocarbons and the external hydrodynamic pressure from the seawater and avoid burst and collapse [17].

2.5.1.3 Area of spreading

In deepwaters, the riser system requires a large radial spreading area. As the depth increases, the distance from the floater to the TDP increases to get the risers' proper configurations. According to Howells and Hatton [17], the typical radial spreading of the risers is 1 to 1.5 times the water depth. For instance, at 1500 m water depth, the total diametrically spread between opposing risers would be 3000 and 4500m. The spreading area is one of the key factors considered while selecting the riser and production system and the positioning.

2.5.1.4 Current

The suspended length of the riser increases proportionally to the water depth. As the suspended length increases, the riser becomes more vulnerable to VIV, particularly where the current is strong. The VIV may cause large fatigue damage to the risers. This can be reduced by using suppression devices such as strakes or fairings along the exposed areas of the riser.

2.5.2 Harsh environment challenges

2.5.2.1 Floater motions

Displacement of the risers due to the motions of the surface floater is an important factor. The displacement could occur at varying depths, depending on the selected floater (Semi-submersible, TLP, SPAR or vessel etc.). Moreover, the displacement increases the stress that the riser is subjected to, which could lead to critical failures such as bending and collapsing. When it comes to designing a riser, the following floater motions must be considered [11]:

- The static offset - mean offset due to wave, wind, and current loading
- The wave frequency motions - first-order wave-induced motions
- The low-frequency motions - motions to wind gust and second-order wave forces
- Pulldown/set down - due to the combined effect of the mooring lines/tether constraints and floater offset

2.5.2.2 Fatigue

One of the fundamental challenges for SCR designs in harsh environments such as the North Sea is the fatigue in the hang-off area and the TDZ [18]. The current generates vortex shedding on the backside of the riser and VIV, and as mentioned in the previous section, this massively decreases the expected lifetime of the riser.

2.5.2.3 Installation

Execution of marine operations in the North Sea and harsh environmental conditions is only possible during small weather windows of the year, as the weather conditions have to be quite calm. This adds another challenge to the riser installation, with

more uncertainty about the weather windows. Installations are usually limited to the summer season when the air pressure and temperature remain constant. According to a study performed on the weather windows, the month with the highest likelihood of a weather window lasting more than three days was July [19].

Chapter 3

Steel Catenary Riser

The SCR has been and continues to be a very attractive solution for deepwater field developments. The first SCR was installed and deployed back in 1994 at Shell's TLP at a water depth of 872m [20]. Since then, the offshore industry has improved existing systems while implementing new technology, making it feasible for SCR's to be installed in depths of up to 8000 ft (2438 m) [21]. However, there are significant challenges in greater water depths due to the large vessel motions in harsher operating conditions. The different types of SCR configuration and the main challenges for the riser and deepwater will be discussed.

3.1 Conventional SCR

The conventional SCR is a simple free-hanging configuration. It forms a catenary shape due to its self-weight, starting at the floater at around 20 degrees of the vertical, curving to a nearly horizontal orientation on the seabed. As the SCR, is a compliant riser, it is self-compensated regarding heave movement without any heave compensation. An illustration of a SCR with is shown Figure 3.1

SCR are known to be economical in terms of construction and installation. In addition, it has a high resistance to external and internal pressure for deepwater installation due to the strength of the material. In order to accommodate for the rotation and deflection between the riser and the floater, the flex joint is installed.

The riser can be connected at the seabed without any specialized bottom system connection. It is required that some length of the pipe is laying horizontally on the seabed before it is connected to the seabed connection/termination point to allow for any horizontal movement due to vessel offsets. Alternatively, in order to reduce the complexity and cost, the riser can be extended to be part of the subsea pipeline [7].

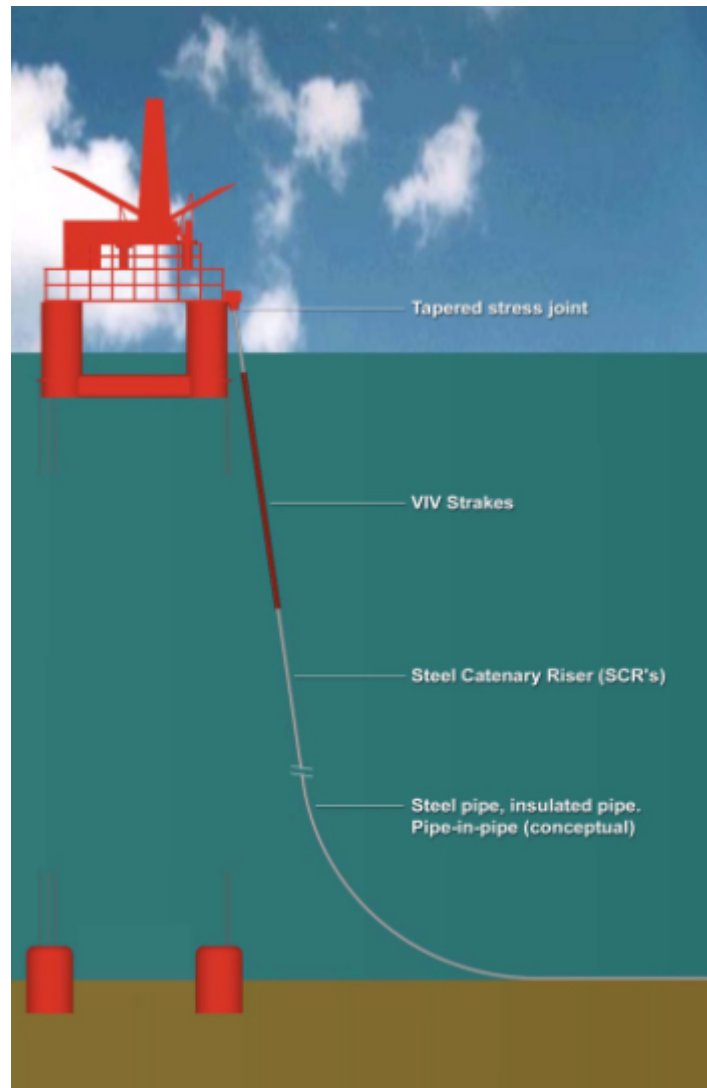


Figure 3.1: Illustration of free hanging SCR [14]

The vessel motions can be severe for deepwater applications in harsh environments. This makes it a difficult challenge for the riser to satisfy the strength and the fatigue design acceptance criteria, particularly for the TDZ. In extreme conditions, the vessel offset is large, which results in variations of the suspended length of the riser, thus changing the position of the TDP as well. This, in combination with the heave motion of the vessel, causes the riser to continuously lift-off and laying down of the riser on the seabed. Thus, making the TDZ a critical area for fatigue and buckling issues. The soil-riser interaction also impacts the fatigue damage on the riser.

To deploy the conventional SCR in a deepwater and harsh environment, multiple modified concepts of the SCR have been developed. This includes the use of weight-distributed sections of the riser and the use of buoyancy modules, as will be discussed

3.3 Steel Lazy Wave Riser

This concept was first proposed by Karunakaran et al. [8]. The SCR is modified by attaching buoyancy modules to sections of the riser, creating a wave shape of the riser. This essentially de-couples the vessel motions from the TDZ, which reduces the vessel's payload. The SLWR configuration allows for substantially larger horizontal offsets of the floater without changing the TDP compared to the traditional SCR. Thus, with less movement of the TDP, the riser's strength and fatigue performance improve substantially [23][7].

In comparison to the conventional SCR, the SLWR has a smoother approach to the seabed. This results in lower stresses in the TDP. However, due to the buoyancy modules, there is an increase in stresses at the sag and hog bend regions. These regions are areas important to the design in lazy wave configurations [8].

Furthermore, the price of the buoyancy modules is expensive, and the installation is trickier than for the conventional SCR. Thus, the SLWR configuration must be optimized to meet the riser performance target while minimizing the use of buoyancy elements for the development to be economically feasible. A typical configuration of an SLWR is shown in Figure 3.3.

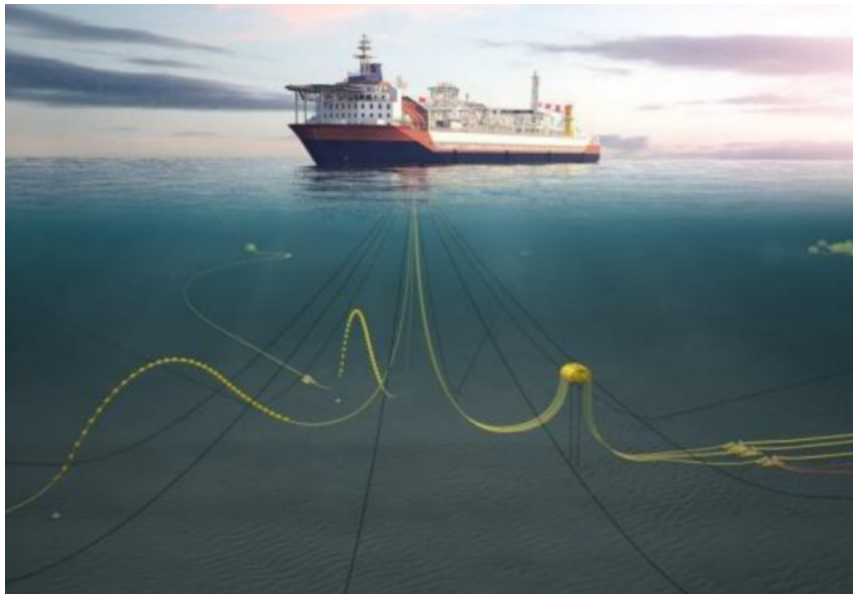


Figure 3.3: Illustration of a SLWR layout [24]

3.4 Material selection for SCR's

The standard choice for SCR's has been low carbon steel for the majority of riser systems, where common material grades are X60, X65, and X70. While moving into deeper waters, materials such as aluminum and titanium alloys are also implemented to reduce the total weight of the riser.

Titanium alloy expands the possibilities for metallic risers compared to traditional low-carbon steel. It has a 50 % of the steel's Young's modulus. At the same time, it has an increased yield, tensile strength, and better fatigue performance [25]. Using titanium which is highly resistant to corrosive environments, should also be considered and not just the cost per unit weight of the material to the low carbon steel, as normal steel requires corrosive resistant measures such as coating.

Chapter 4

FPSO

4.1 Introduction

In applications in deepwater, the floating production systems have grown increasingly more popular in the oil and gas production. This is due to their competitiveness and suitability in these deepwater developments compared to the fixed platforms used for shallower waters. The differentiating factor between the floating production system and the fixed system lies in the fact that the floaters are held up by the buoyancy of displaced water, while the fixed has a supporting structure extending to the seabed. Thus, for a fixed platform system, the increase in cost and weight increases exponentially with the water depth. On the other hand, for a floating production system, the weight and cost increase more linearly [6]. Hence, for the thesis, a floating production system will be considered. This chapter presents the FPSO, which has been successfully deployed in projects and areas with harsh environments and deepwaters. A photo of a FPSO is shown in Figure 4.1.



Figure 4.1: BP's Glen Lyon's FPSO [26]

4.2 Mooring system

Installing FPSO's in deepwater areas is commonly done using one of the mooring systems, the spread mooring or the turret mooring. The mooring system selection depends on the region's environmental condition. For example, outside the coast of Africa, the spread mooring system is dominant, as the conditions there are relatively calm. On the other hand, for fields off the coast of Brazil and Norway, the turret moored system is more suitable for the environmental conditions and the commonly used system.

4.2.1 Spread mooring system

The mooring lines are connected to the bow and the stern of the FPSO to maintain a fixed orientation of the vessel during production. It is tethered using 12 to 22 mooring lines anchored to the seabed. Due to the fixed orientation, the vessel's heading is extremely important. Hence, the spread mooring system is an obvious choice for calm environmental conditions with a monotonous wind direction. Attaching the risers to a spread moored FPSO is dependent on the layout of the field but also the number of the risers to be installed. As the mooring lines are connected to the bow and the stern, the risers have to be connected to the port, or starboard sides of the vessel [27].

4.2.2 Turret mooring system

Turret mooring is a variation of the Single Point Mooring (SPM) concept, which utilizes a turret as the connection point for both the mooring lines and the risers. The turret allows the vessel to change its orientation depending on the weather direction, making it superior to a spread mooring in moderate to harsh environments with multi-directional weather directions.

The placement of the turret can be either located inside the hull of the FPSO also known as an internal turret system, or it can protrude from the bow of the FPSO commonly called an external turret system and are shown in Figure 4.2 and Figure 4.3 respectively.

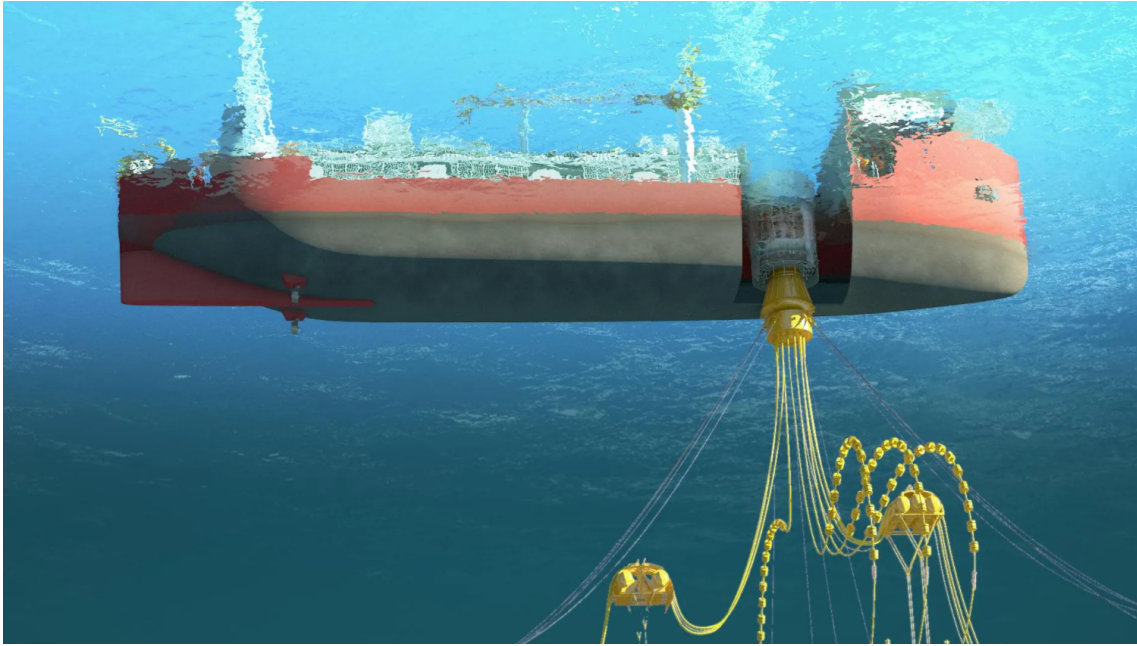


Figure 4.2: Internal turret on an FPSO [28]



Figure 4.3: External turret on an FPSO [29]

For both concepts, the turrets can be permanently installed or dis-connectable, allowing the FPSO to detach in an emergency and leave the area. A disadvantage of the disconnectable turret is the decreased maximum load-bearing capacity compared to the permanently installed turret. The disconnectable turret must be able handle the entire loading of the risers, umbilicals and mooring lines if the FPSO has to disconnect during an emergency, hence the lowered capacity [27].

4.2.3 Comparison of mooring systems

Overall the turret mooring system has more advantages compared to the spread mooring system, such as reduced loads on the mooring lines and increased performance in offloading. It also utilizes the seafloor area more efficiently, resulting in a reduced span of the flowlines, which improves the flow assurance and minimizes cost [27]. A direct comparison between them is shown in Table 4.1.

Table 4.1: Comparison of spread moored versus turret moored FPSO [27]

Characterstic	Spread moored	Turret moored
Vessel orientation	Fixed	360 degree weathervaning
Vessel motions	Alters between small to large, dependant on vessel direction and environmental conditions	Smaller motions, as vessel is oriented in the optimal direction given the environmental direction
Environment	Mild to moderate - mono directional	Moderate to harsh - multi directional
Field layout	Not applicable for crowded field	Adaptable and applicable for crowded field
No. of risers and arrangement	Suitable for a large number of risers and capability for tie in solutions	Suitable for a medium number of risers with a reduced capability for tie ins
Riser connection	Free hanging from star/port side of the FPSO	Hanging from the turret connection
Station keeping performance	Large number of anchoring points and varying offsets	Fewer anchoring points and offset is reduced
Offloading performance	Depends on the vessel and environmental orientation	Increased performance, FPSO is heading toward the optimal direction
Storage capacity	Large storage capacity	Reduced due to the internal turret

4.3 Selected FPSO for the thesis

The selected concept for this thesis is the turret moored FPSO system. A FPSO is the preferred vessel due to the remote field, with limited existing infrastructure and exposure to harsh environments. Additionally, it may be challenging to perform inspections, maintenance, and repairs due to the location.

Being able to weathervane into the direction with the least loads from currents, waves and wind is the main reason for choosing a turret moored FPSO. The turret itself is a permanent internal turret chosen because the field is remote, in deepwater, harsh environments, where icebergs and cyclones are not of concern.

Chapter 5

Design loads and standards

The various loads for the riser system are key input parameters to determine the design loads or predict the vessel motions. The loads to be considered according to the DNV-ST-F201 standard are [11]:

- Pressure loads
- Functional loads
- Environmental loads
- Accidental loads

5.1 Pressure loads

Pressure loads (P) are the combined loading effect due to the hydrostatic internal and external pressures. The riser components must be designed to withstand the maximum differential pressure between the internal and external pressure to which the components would be exposed to during operations [11].

5.2 Functional loads

Functional loads (F) are the loads the system is exposed to during the transportation, storage, installation, testing, and operations phases, without any environmental or accidental loads. Typical functional loads to be considered for design are:

- Weight and buoyancy
- Marine growth
- Applied tension
- Thermal loads

The loads can be categorized into dead, live and deformation loads. Dead loads are the weight of the structures (e.g. pipes, coating, anodes, etc.) in the air. At the same time, the live loads vary during operations due to flow, weight, pressure, and temperature. Lastly, the deformation loads are a consequence of the deformations imposed on the risers through the use of reeling, stingers, rock-berms, seabed contours, or constraints from the floater.

5.2.1 Marine growth

The accumulation of marine growth on the riser must be considered in the design. It influences the mass, hydrodynamic diameter, and hydrodynamic loading. Marine growth will occur in the euphotic zone, which is the region where the photosynthesis can happen (approximately 200m depth) [30]. Estimates for the marine growth rate and its extent may be calculated based on previous experience and available data.

5.3 Environmental loads

Environmental (E) loads are imposed directly or indirectly by the ocean environment. Where the principal loads are waves, currents, and floater motions [11].

5.3.1 Waves

As stated in DNV-ST-F201, the wind-driven surface waves are a major source of dynamic environmental forces on the risers. The wave shapes are irregular in shape and varies in height and length, and impacts the riser from one or more direction at the same time.

Wave conditions is usually described by the deterministic design wave or by random wave described by wave spectra, where most spectra is given in terms of significant wave height, spectral period, spectral shape and directionality [11].

5.3.2 Current

The current imposes large loading on the riser system, and the main effects include:

- direct current loading on the riser
- mean floater position

- vortex induced vibrations

For design current velocities, the profile and direction must be based on the best statistics available for that area. This includes data from tidal current, wind-induced current, storm surge current, density-induced current, global ocean current, etc. Additionally, the velocity and magnitude as a function of water depth is also important to consider. As the current and velocity and direction usually does not change rapidly with time, they seen as time independent for each sea state, simplifying the calculations.

5.3.3 Floater motions

Floater motions are important to consider for the loading conditions and have been described more thoroughly in Section 2.5.2.1.

5.4 Design codes and standards

5.4.1 Introduction

The risers are exposed to various loading conditions throughout their lifetime, from normal loading caused by currents, wind, and waves to accidental loads. For the risers to handle all these loads, they must be designed in accordance with recommended practices and standards. The standards and recommended practices can be national, regional, or international. Additionally, it could be made by standard developing organizations. Design requirements must consider the different phases of the life cycle, such as; construction, installation, commissioning, operations & maintenance, and abandonment.

The minimum requirements for the given conditions must be met to consider a design safe. For example, the standard riser design looks at the criteria for burst, collapse, and buckling. Moreover, in addition to the minimal requirements, a safety factor is added to cover any uncertainty and inaccuracy made in the analyses stages. In the offshore industry, and for risers there are two core design principles; LRFD and Working Stress Design (WSD).

5.4.2 Load and resistance factor design - DNV-ST-F201

”The fundamental principle of LRFD method is to verify that factorized design load effects do not exceed factored design resistance for any of the considered limit states (i.e., failure modes)” [11]. There are four limit states to consider which are as follows; Accidental Limit State (ALS), Serviceability Limit State (SLS), Ultimate Limit State (ULS), and the Fatigue Limit State (FLS).

5.4.2.1 Accidental Limit State

Accidental loads are loads that the riser may be subjected to in abnormal conditions, incorrect operation, or technical failure, all of which affect the safety of personnel, equipment, and the environment. Moreover, the design of the riser should be able to handle a direct accidental load for an event with a frequency of occurring larger than 0.01. For ALS some of the most common accidental loads are [11]:

- Fires and explosions
- Impact & collisions
- Hook & drag loads
- Failure of support system
- Exceedance of incidental internal overpressure
- Environmental events

The data in Table 5.1 can be used to perform a simplified design check of the riser.

Table 5.1: Simplified design check for accidental loads

Prob. of occurrence	Safety class low	Safety class medium	Safety class high
$>10^{-2}$	Accidental loads may be regarded similar to environmental loads and may be evaluated similar to ULS design check		
$10^{-3} - 10^{-4}$	$\gamma_e = 1.0$	$\gamma_e = 1.0$	$\gamma_e = 1.0$
$10^{-4} - 10^{-5}$	Accidental loads or event may be disregarded	$\gamma_e = 0.9$	$\gamma_e = 0.9$
$10^{-5} - 10^{-6}$	Accidental loads or events may be disregarded		$\gamma_e = 0.8$
$<10^{-6}$	Accidental loads or events may be disregarded		

5.4.2.2 Serviceability Limit State

The serviceability limit state governs the acceptable limitations to normal operation for the riser. The system’s functional requirements define these limitations. The SLS criteria cover the global riser behavior, such as the displacement, deflections, rotation, and ovalization of the riser. Exceeding the SLS does not necessarily lead to failure, as this should be governed by the ALS [11].

In addition to the global riser actions mentioned, the standard also outlines limitations regarding the ovalization limit due to bending and riser stroke. The ovalization is a measure of the deviation of the round pipe section. This is commonly visible as an elliptic cross-section. In order to prevent the riser from premature buckling due to bending with the out-of-roundness tolerance from fabrication, the pipe must fulfill the following requirement:

$$f_0 = \frac{D_{max} - D_{min}}{D_0} \leq 0.03 \quad (5.1)$$

For a top tensioned riser, such as the SCR, a tensioner pulls on the top end of the riser to maintain a constant tension and avoid bending. The tensioner pulls continuously as the floater and riser move relative to each other, where the travel distance of the tensioner is the stroke. Riser stroke are important for the design requirements for the tensioner, draw works, and clearance of surface equipment and the drill floor. It should be designed with a sufficient stroke, to avoid any damage to the riser, components, and equipment [11].

5.4.2.3 Ultimate Limit State

The ULS requires the risers to withstand a maximum load combination for an annual exceedance probability of 10^{-2} . Failing to meet the requirements of the ULS for the riser will result in a structural collapse. According to DNV, the typical failure modes for ULS to be considered in the riser design include:

- Bursting
- Hoop buckling
- Gross plastic deformation and local buckling
- Gross plastic deformation, local buckling, and hoop buckling
- Unstable fracture and gross plastic deformation
- Liquid tightness
- Global buckling
- Propagation buckling

Bursting

The riser's main task is transporting the hydrocarbons safely from the seabed to the topside facility. Thus, it is important to avoid pipe bursting to internal overpressure. For risers, the critical area for bursting is located at the top-end, as the hydrostatic pressure is equal to the atmospheric pressure and the internal pressure is at a maximum.

The design must satisfy Equation 5.2 at all cross-sections:

$$(p_{li} - p_e) \leq \frac{p_b \times t}{\gamma_m \times \gamma_{SC}} \quad (5.2)$$

where:

- p_{li} = local incidental pressure
- p_e = external pressure
- t = Pipe wall thickness
- γ_{SC} = Safety class factor
- γ_m = Material resistance factor

The burst pressure (p_b) is the minimum burst resistance required to prevent the riser from bursting. It is dependent on the mechanical properties of the material selected. Moreover, the burst pressure is given by Equation 5.3.

$$p_b(t) = \frac{2}{\sqrt{3}} \times \frac{2 \times t}{D - t} \times \min\left(f_y; \frac{f_u}{1.15}\right) \quad (5.3)$$

Where:

- D = Outer pipe diameter
- f_y = Yield strength
- f_u = Tensile strength

The minimum required wall thickness t_1 to be replaced for t in Equation 5.3 is given by Equation 5.4.

$$t_1 = \frac{D}{\frac{4}{\sqrt{3}} \times \frac{\min\left(f_y; \frac{f_u}{1.15}\right)}{\gamma_m \times \gamma_{SC} \times (p_{li} - p_e)} + 1} \quad (5.4)$$

Hoop buckling (collapse)

The collapse resistance is dependent on the external pressure. Should the external pressure exceed the internal pressure significantly, the riser could collapse and must be designed against, for example, increasing the wall thickness.

Opposite to buckling, the critical area for collapse is at the bottom section of the riser, where the external pressure is at its maximum and vice versa for the internal pressure. For risers subjected to external pressure, the design criteria in Equation 7.3 must be satisfied.

$$(p_e - p_{min}) \leq \frac{p_c \times t_1}{\gamma_{SC} \times \gamma_m} \quad (5.5)$$

where:

p_e = External pressure

p_{min} = Minimum internal pressure

p_c = Hoop buckling resistance (Given by Equation 5.6)

$$\left(p_c(t) - p_{el}(t) \right) \times \left(P_c^2(t) - P_p^2(t) \right) = p_c(t) \times p_{el}(t) \times p_p(t) \times f_0 \times \frac{D}{t} \quad (5.6)$$

where:

$f_0 = \frac{D_{max} - D_{min}}{D} =$ Initial ovality

p_{el} = Elastic collapse pressure of the pipe, which is given by Equation 5.7.

$$P_{el}(t) = \frac{2E \times \left(\frac{t}{D} \right)^3}{1 - \nu^2} \quad (5.7)$$

P_p = Plastic collapse pressure (given by Equation 5.8.)

$$P_p = 2 \times \frac{t}{D} \times f_y \times \alpha_{fab} \quad (5.8)$$

where:

α_{fab} = Fabrication factor

Propagating buckling

Propagating buckling is a failure mode caused by local buckling. The local buckling propagates until the external pressure drops. This criterion ensures that a buckling remains local and does not spread to the neighboring pipe sections. Thus, the propagating must be checked against Equation 5.9.

$$(p_e - p_{min}) \leq \frac{P_{pr}}{\gamma_c \times \gamma_m \times \gamma_{SC}} \quad (5.9)$$

where:

P_e = External pressure

P_{min} = Minimum internal pressure

γ_c = Special condition factor for buckle propagation, value is 1.0 if no propagation is allowed or 0.9 if short distance of buckling is allowed

γ_{SC} = Safety class factor

γ_m = Material resistance factor

P_{pr} = Buckling resistance (Given by Equation 5.10)

$$P_{pr} = 35 \times f_y \times \alpha_{fab} \left(\frac{t_2}{D} \right)^{2.5} \quad (5.10)$$

where:

$t_2 = t_{nom} - t_{corr}$

t_{nom} = nominal thickness

When these riser design criteria for propagating buckling are met, the hoop buckling criterion is also satisfied. The criterion for propagating buckling commonly results in a thicker wall thickness compared to the other criteria, which may result in a conservative riser design if this is required. For practical purposes, this is only used for critical regions where propagation can occur, which reduces the weight and cost of the riser significantly.

5.4.2.4 Fatigue Limit State

The riser system is exposed to cyclic loading that could cause excessive fatigue, crack growth, or damage, causing degradation of the system. All the cyclic loading imposed during the entire service life must be considered, including the phases such

as transportation, towing, installation, running, and hang-off. As such, the riser system must be designed with adequate safety against fatigue for all phases of the service life [11].

There are two fatigue assessment methods which are:

- methods based on the S-N curves
- methods based on fatigue crack propagation calculations

While following the method using S-N curves, this fatigue criterion must be satisfied:

$$D_{fat} \times DFF \leq 1.0 \tag{5.11}$$

where:

D_{fat} = accumulated fatigue damage

DFF = design fatigue factor (use Table 5.2)

Table 5.2: Design fatigue factors (DFF)

Safety class		
Low	Medium	High
3.0	6.0	10.0

For the method based on crack propagation calculations, the riser components must be designed and inspected so that the maximum expected initial defect size would not grow to a critical size during its service life. The fatigue crack growth must satisfy Equation 5.12:

$$\frac{N_{tot}}{N_{cg} \times DFF} \tag{5.12}$$

where:

N_{tot} = total number of applied stress cycles during service or to in-service inspection

N_{cg} = number of stress cycles necessary to increase the defect from the initial to the critical defect size

DFF = design fatigue factor (see Table 5.2)

5.4.3 Working stress design

”The WSD method is a design format where the structural safety margin is expressed by one central safety factor or usage factor for each limit state” [11]. According to the standard, DNV-OS-F201 WSD is less superior to the LRFD and a more easy-to-use and conservative alternative. If the diameter to wall thickness ratio is less than 30, the WSD can be used for combined loading checks. Opposite to LRFD, the WSD approach utilizes a single usage factor for combined loading factors.

The general WSD design format according to DNV is given by Equation 5.13.

$$g(S, R_k, \eta, t) \leq 1 \quad (5.13)$$

Where:

S = total load affect

R_k = resistance

η = usage factor

$g()$ = generalized load effect

Moreover, for the combined loading criteria for pipe members subjected to a combination of effective tension, bending moment and net internal overpressure the following Equation 5.14 is applicable:

$$\{\gamma_{SC} \times \gamma_m\} \left\{ \frac{|M_d|}{M_k} \times \sqrt{1 - \left(\frac{p_{id} - p_e}{p_b(t_2)} \right)^2 + \left(\frac{T_{ed}}{T_k} \right)^2} \right\} \left(\frac{p_{id} - p_e}{p_b(t_2)} \right)^2 \leq 1 \quad (5.14)$$

On the other side, if the pipe is subjected to a combination of effective tension, bending moment, and net external overpressure the

$$\{\gamma_{SC} \times \gamma_m\}^2 \left\{ \left(\frac{|M_d|}{M_k} \right) + \left(\frac{T_{ed}}{T_k} \right)^2 \right\}^2 + \{\gamma_{SC} \times \gamma_m\}^2 \left(\frac{p_e - p_{min}}{p_c(t_2)} \right)^2 \leq 1 \quad (5.15)$$

Where:

γ_{SC} = resistance factor dependent on safety class (consequence of failure)

γ_m = resistance factor to take into account uncertainties in material properties

M_d = design bending moment = $\gamma_F \times M_F + \gamma_E \times M_E + \gamma_A \times M_A$

M_F, M_E, M_A = bending moment from functional, environmental and accidental

loads respectively

$\gamma_F, \gamma_E, \gamma_A$ = load effect factor for functional environmental and accidental loads respectively

M_k = plastic bending moment resistance = $f_y \times \alpha_c \times (D - t_2)^2 \times t_2$

α_c = flow stress parameter for strain hardening

p_{id} = local internal pressure

p_e = external pressure

p_b = burst resistance pressure

p_c = collapse pressure

p_{min} = local minimum internal pressure taken as the most unfavorable internal pressure plus static head of the internal fluid

t_2 = pipe wall thickness

T_{ed} = design effective tension (force) = $\gamma_F \times T_{eF} + \gamma_E \times T_{eE} + \gamma_A \times T_{eA}$

T_{eF}, T_{eE}, T_{eA} = effective tension from functional, environmental and accidental loads respectively

T_k = plastic axial force resistance

Chapter 6

Residual Curvature Method

6.1 Introduction

The RCM is a method for laying pipe in a controlled manner, with a pre-defined residual curvature. It was patented by Equinor back in the early 2000s, but as of January 2022, the patent is expired [31].

For RCM, the reel lay is the preferred installation method. However, it can also be installed using S-lay or J-lay methods. The residual curvature is implemented by temporarily adjusting the straightener settings for a limited section of the pipe over regular or varying intervals along the riser. An illustration of the reel laying method is shown in Figure 6.1.

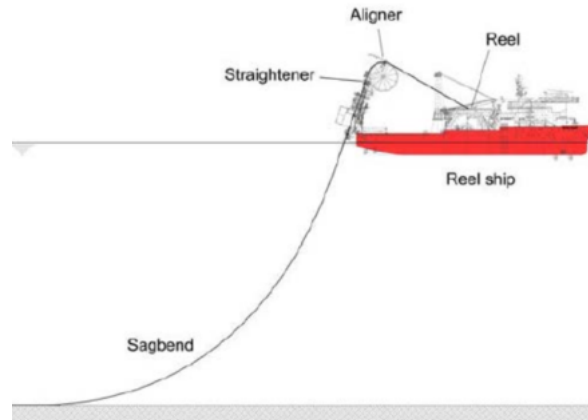


Figure 6.1: Illustration of reel lay vessel and pipeline

As the straightener creates imperfections in the riser, adjusting the settings will allow for a variation in the residual curvature generated. An ideal residual strain is between 0.15 % and 0.25 % over a pre-defined curvature length. The lengths range from 40-meter sections to 100-meter sections over a one-kilometer distance, as illustrated in Figure 6.2.

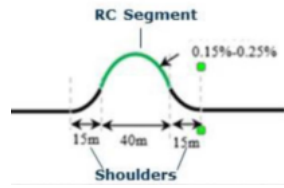


Figure 6.2: Section with residual curvature [32]

There is an upper limit to the achievable residual curvature. This depends on the lay system characteristics (the aligner wheel, straightener, and tensioner), the pipe properties (cross-section geometry and material properties), and the catenary shape and tension.

In order to reach the desired residual strain between 0.15 and 0.25 %, two options are available: under-straight or over-straight the pipelines. A photo showing the pipe being laid with and straight and under-straightened is shown in Figure 6.3.



Figure 6.3: Straightener tracks configuration for straight pipe (left) and under-straightened residual curvature section (right) [31]

The main advantages of using the RCM for initiating the buckling for global expansion and buckling control using the reel lay method include:

- Robust and predictable in-place behavior
- Low cost (compared to other buckle initiation methods)

6.2 Bending moment and curvature

In the installation phase, the pipes are regularly subjected to bending. For the reel lay method, the pipes are bent when spooled onto the reel, while the process is reversed when it goes through the straightener, and bent again in the sagbend. The bending moment's relation to the curvature is shown in Figure 6.4 for a pipe that has been plastically deformed.

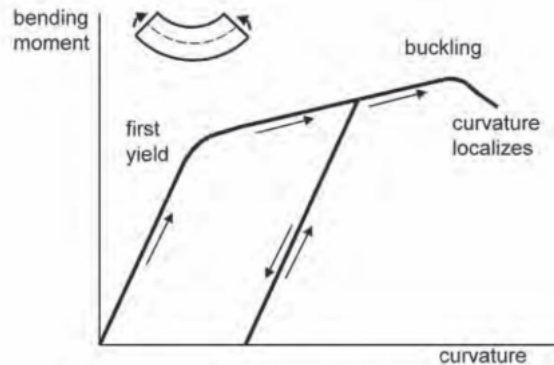


Figure 6.4: The relation between bending moment and curvature [33]

For small curvatures, the pipe bends elastically, where the ratio of the bending moment to the curvature is known as the flexural rigidity (F). Furthermore, as the curvature increases above the yield curvature, it starts to yield plastically, and the relationship starts to curve over [33].

As the curvature increases, the bending moment continues to increase at a slow rate, which is controlled by the interaction between the strain hardening and the ovalization. When the curvature is reduced, the bending moment decreases linearly. As the bending moment reaches zero, there is residual curvature [34].

Surpassing the curvature limit results in an unstable bending process, causing the pipe to wrinkle and buckle unevenly. The result is a curvature that is not uniform but rather localized at the buckle forming a kink [33].

6.3 Curvature and residual strain

The residual strain is suitable for measuring the residual curvature, and the relationship between them is shown in Figure 6.5.

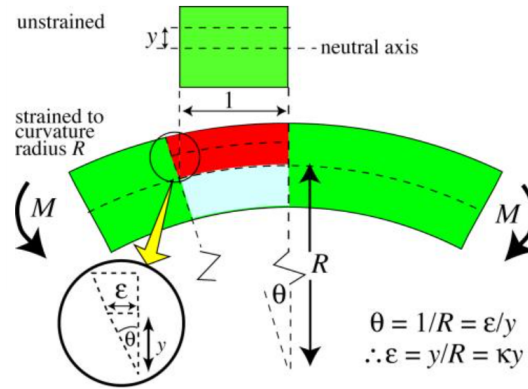


Figure 6.5: The relationship between residual strain and curvature [35]

The radius of the curvature R is given by Equation 6.1.

$$\tan\theta = \frac{1}{R} \quad (6.1)$$

However, for small values of θ this can be simplified to $\tan\theta = \theta$

Using this relation, Equation 6.1 yields Equation 6.2:

$$\theta = \frac{1}{R} \quad (6.2)$$

Moreover, using the same relation for the small triangle in Figure 6.5, gives Equation 6.3.

$$\tan\theta = \frac{\epsilon}{r} \rightarrow \theta = \frac{\epsilon}{r} \quad (6.3)$$

Combining Equation 6.2 and Equation 6.3, ϵ is given by Equation 6.4.

$$\epsilon = \frac{r}{R} \quad (6.4)$$

The strain and curvature can be defined by the term in Equation 6.4 in Equation 6.5 and Equation 6.6 respectively.

$$\epsilon = \frac{r}{R} = \frac{d}{2R} \quad (6.5)$$

$$\theta = \kappa = \frac{1}{R} \quad (6.6)$$

Using the results from Equation 6.5 and Equation 6.6, the relation between the residual strain and curvature can be made by Equation 6.7.

$$\epsilon = \frac{r}{R} = r \times \kappa \quad (6.7)$$

Where:

ϵ = strain

r = radius of pipeline

d = outer diameter of pipeline

κ = curvature

R = radius of curvature

In Table 6.1, three different risers have been selected, with a wall thickness of one inch for the calculations. It summarizes the residual strains versus the corresponding residual radiuses.

Table 6.1: Residual strains versus radius of curvature

Residual strain	Radius of residual curvature [m]		
	10" ID	12" ID	14" ID
0.15 %	102	119	135
0.20 %	76	89	102
0.25 %	61	71	81

6.4 Residual curvature using the Reel lay method

6.4.1 Reeling and unreeling of the riser

Reeling the riser onto the spool is shown in Figure 6.6 and has to be performed at a suited spool base. The riser is under tension as it goes to the aligner on the inclined ramp given by the angle (θ). It passes the aligner and is then spooled onto the reel [36].

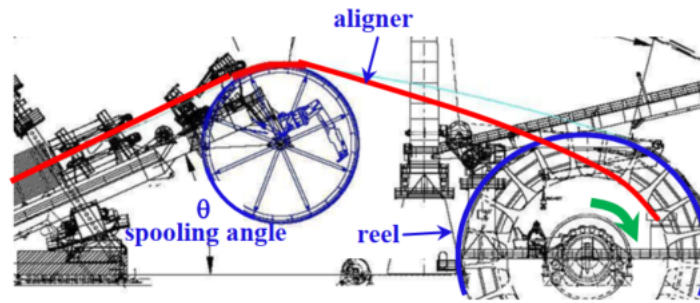


Figure 6.6: Pipeline reeling setup [36]

The unloading operation of the riser from the spool is a reverse operation of the reeling operation. The tower angle has to be increased to the appropriate lay-angle, as can be seen in Figure 6.7.

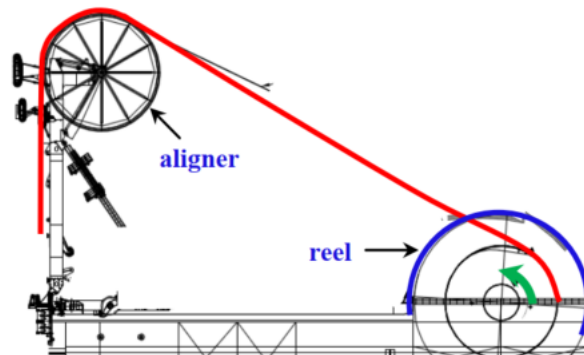


Figure 6.7: Unreeling of the riser [36]

6.4.2 Straightening of the riser

As the riser passes the aligner and reaches the straightener, it is reverse bent to the exact curvature of the upper track. Passing the upper tracks, it enters the tensioner that guides the riser to the lower tracks that prevent the riser from any misalignment, as shown in Figure 6.8.

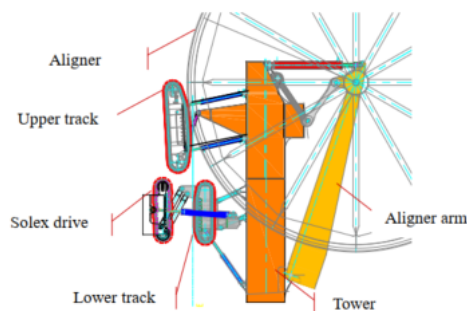


Figure 6.8: Illustration of straightener equipment [36]

Following the DNV-ST-F101, the riser can be defined as straight if the criterion given in Equation 6.8 is fulfilled.

$$OOS < 0.0015 \times L \quad (6.8)$$

Where:

OOS = Out-of-straightness

L = full length of the riser

Using this criterion, a 6m long pipe joint must not exceed 9 mm, shown in Figure 6.9 or interpreted such that the radius of curvature must be over 500m.

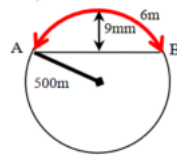


Figure 6.9: DNV-ST-F101 straight pipe criterion [36]

6.5 Application of residual curvature

The first application of RCM was in the Skuld project for Equinor back in 2012. Since then, Subsea 7 alone has installed more than 116 residual curvature sections. It has quickly become a more favorable and economical option for lateral buckling design using the reel lay method. Other advantages using RCM over different methods include [37]:

1. Reduced installation costs
2. Allows for late design changes since there is no need for additional procurement or logistics for the implementation of RCM
3. This design removes "rogue buckling" completely and is a reliable buckling initiator at low axial force
4. Using RCM avoids the need for special welding and the use of automatic ultrasonic testing as the post-buckle strains are low compared to alternative methods

6.5.1 Calculation of residual curvature

The residual curvature in a riser can be determined based on Figure 6.10, given by Equation 6.9 and Equation 6.10.

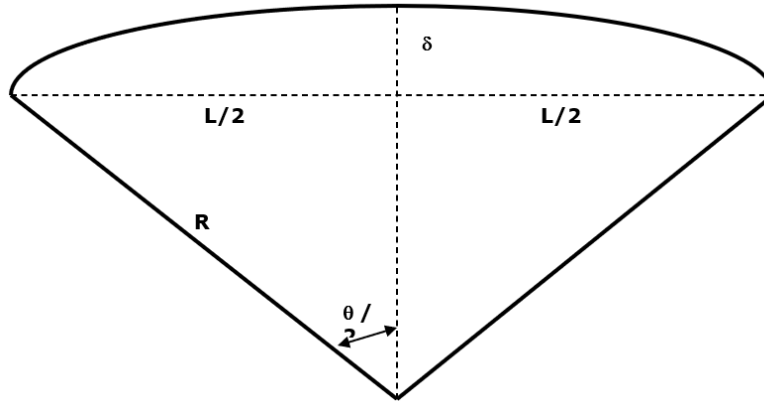


Figure 6.10: Residual curvature in the riser [38]

$$\delta = R \times \left(1 - \cos\left(\frac{\theta}{2}\right) \right) \quad (6.9)$$

$$\sin\left(\frac{\theta}{2}\right) = \frac{L/2}{R} \quad (6.10)$$

Where:

δ = Residual Out-of-Straightness

R = Residual radius of curvature

θ = Included angle

L = Measured length

6.5.2 Example of project installed with RCM

6.5.2.1 Skuld

The Skuld Project was, as mentioned in previous sections, the first application of RCM. Its located in the Norwegian Sea at 360 m water depth, where Equinor is the owner and operator. There were 26 kilometers of 14" and 16" pipelines installed with 25 sections of residual curvature along the whole length, where examples can be seen in Figure 6.11.

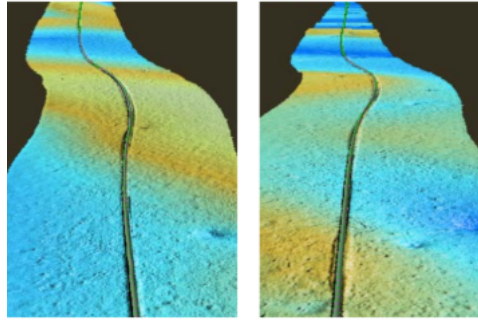


Figure 6.11: Local residual curvature locations [9]

The residual curvature sections were 70m long and installed with 1 km spacing. For the 70 m section, it included a 15 m transitioning section in both ends, where the residual curvature strain goes from 0 to 0.2 %, as were the target strain [9].

All of the residual curvature sections were triggered, and results also showed that the residual curvature dominated the global buckling response and not the pipe-soil interaction. Moreover, conventional methods such as intermittent rock cover, triggering berms, or snake lay were evaluated but found to be significantly more costly than using RCM [9].

6.5.3 Use case scenarios for local residual curvatures

RCM could be utilized for other methods rather than just controlling the pipeline expansion and global buckling. It could also be used for [39]:

- Enabling of direct tie-in of risers as shown in Figure 6.12
- Adaption to seabed topography as shown in Figure 6.13
- Reduction of stress and fatigue of the SCR's
- Elimination of straightening trials for reel-laid pipelines

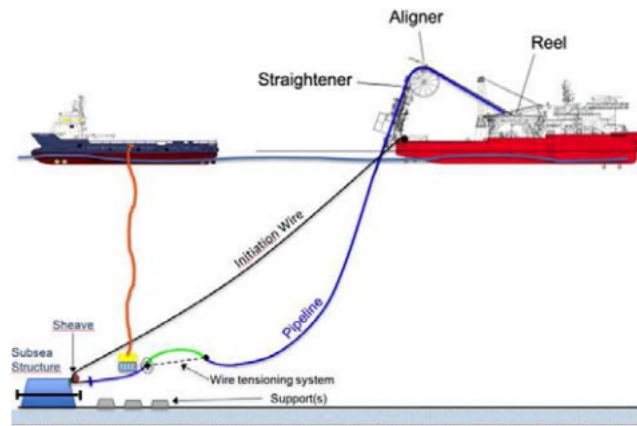


Figure 6.12: Tie-in using RCM [39]

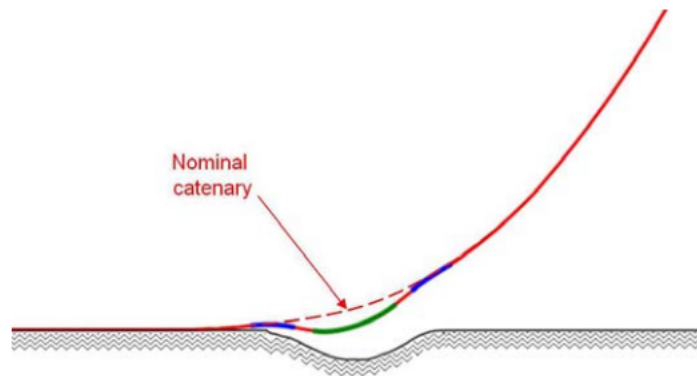


Figure 6.13: Riser configuration with local residual curvature versus nominal catenary [40]

Chapter 7

Design basis and methodology

7.1 Introduction

This section will cover the implementation of the RCM to the selected riser, which in this scenario is a free-hanging SCR. The analysis will cover the SCR with and without a coating and compare it to a conventional SCR with no RCM implemented. Moreover, the following section will describe all of the riser properties, data, and methodology used for the implementation.

7.2 Scope

The scope of this thesis is parameters for the North Sea with harsh environmental conditions. Moreover, the field has a water depth of 1500 m, considered deep-water operational conditions.

Given that the field is deep-water, there are limited options when it comes to selecting an appropriate vessel or floater. In this thesis, the selected floater is a ship-shaped FPSO, commonly used for deepwater, and is well proven in fields worldwide. The selected turret moored FPSO and its corresponding Response Amplitude Operator (RAO) data are for a typical FPSO used for operations in this area of the North Sea. There will be analyzes performed for various scenarios with and without implementing RCM for the SCR's using Orcaflex, the software.

7.3 Data for design

7.3.1 FPSO

The input required for the FPSO in Orcaflex includes :

- Origin = located at the center of the FPSO

- X-axis = longitudinal axis positive to FPSO bow (direction of surge)
- Y-axis = transversal axis (direction of sway)
- Z-axis = vertical axis (direction of heave)

All of the dimensions for the FPSO and turret position can be seen in Table 7.1.

Table 7.1: FPSO parameters

Parameters of FPSO	Value	Unit
Length	295	m
Width	46	m
Height	27	m
Turret diameter	12	m
Location of turret	0 (center of FPSO)	m

7.3.2 Motions of the FPSO

To properly analyze the global riser response the following motions must be considered [11]:

- Low Frequency Motions (LF)
- Wave Frequency Motions (WF)
- FPSO static offsets

7.3.2.1 FPSO static offsets

Considering that the FPSO is impacted by the environmental loads such as waves, wind, and current, the FPSO will have varying positions or offsets. The commonly used static offsets are near, mean, and far. The near position indicates the FPSO displacement towards the connection point of the riser at the seabed. Moreover, the far offset is the opposite of the near offset, where the displacement of the FPSO away from the connection of the riser at the seabed.

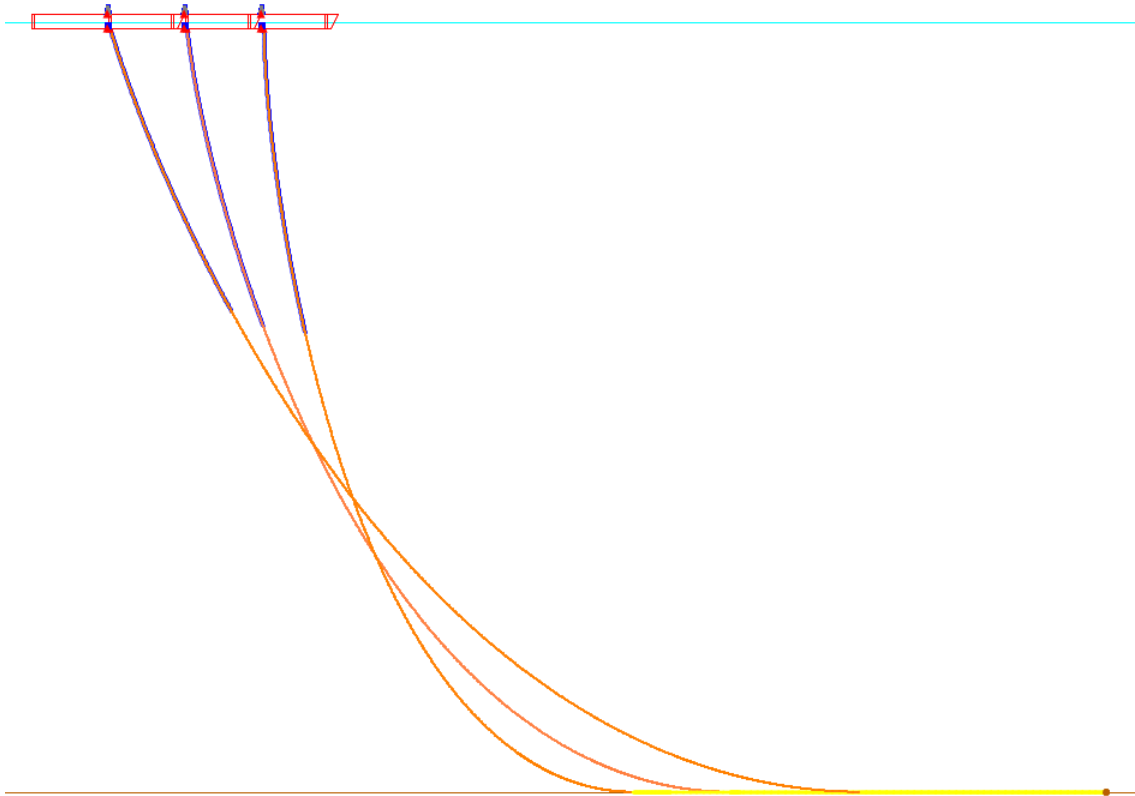


Figure 7.1: FPSO mean, far and near offsets

The operational and accidental conditions are considered for the static and dynamic analyses. For the operational condition, the FPSO's maximum offset is ten percent of the water depth. On the other hand, the maximum offset is 12 % of the water depth for accidental conditions. The offsets are summarized in Table 7.2.

Table 7.2: FPSO offsets for operational and accidental mooring conditions

Condition	FPSO offset (%)	FPSO offset (\pm m)
Operational	10	150
Accidental	12	180

7.3.2.2 Wave frequency motions

WF are a result of the first-order wave forces acting on the FPSO, causing it to move in periods between 3-25 seconds [41]. The motions of WF are given by the RAO's. For the RAO's used in this thesis, the FPSO will be analyzed with six degrees of freedom (surge, sway, heave, roll, pitch and yaw). Moreover, the origin of the RAO is at the vessel's center of gravity.

7.3.2.3 Low frequency motions

LF is the motion response for frequencies below the wave frequencies coming from near surge, sway, and yaw Eigenperiods for the FPSO. Furthermore, the LF usually have a period of 30 to 300 seconds [41].

7.3.3 Environmental data

7.3.3.1 Water depths

As mentioned in the introduction, the water depth of the selected field is 1500m, based on the average depth for the field in the North Sea. Moreover, the selected density for the seawater is 1025 kg/m³ with an average temperature of 10°C.

7.3.3.2 Current

For the Norwegian sector, a combination using wind and wave periods of a 100-years together with a 10-year current return period is usually acceptable [42]. The data used in this thesis considers a regular current profile for the North Sea. The maximum current velocity is located at the sea surface, and the minimum is close to the seabed.

Typical sea states with a return period of 100 years are given in DNVGL-OS-E301 for the Northern North Sea and the North Sea.

7.3.3.3 Waves

The thesis aims to analyze the performance and limitations of a conventional SCR before and after applying residual curvature. The implementation should increase the riser's ability to handle larger floater motions. Thus, the wave data must be applied to calculate the floater heave motion responses.

Irregular wave theory has been used to model the extreme-sea state using the Joint North Sea Wave Project (JONSWAP) spectrum. JONSWAP is an alternation of the Pierson-Moskowitz spectrum that includes the limited fetch conditions and is described by Equation 7.1.

$$S_j(\omega) = A_\gamma S_{PM}(\omega) \gamma \exp\left(-0.5\left(\frac{\omega-\omega_p}{\sigma\omega_p}\right)^2\right) \quad (7.1)$$

Where:

$S_{PM}(\omega)$ = Pierson-Moskowitz spectrum

γ = non - dimensional peak shape parameter

σ = spectral width parameter

$A_\gamma = 1 - 0.287 \ln(\gamma)$ which is a normalizing factor

The model in Equation 7.1 is conditional on that the criterion in Equation 7.2 is fulfilled.

$$3.6 < \frac{T_p}{\sqrt{H_s}} < 5 \quad (7.2)$$

This study's ULS design is based on the combination of an extreme sea state of a 100-year wave with a 10-year current. Data for both wave and wind for a general North Sea location are presented in Table 7.3 and Table 7.4.

Table 7.3: Significant wave height and period data

Parameter	100-year wave	10-year current
H_s (m)	17.7	14.9
T_p (s)	18.6	17.3

Table 7.4: Wave and current data for the North Sea location

Water depth (m)	Omni directional current speed (m/s)	
	100 -year	10 -year
0	1.67	1.47
-70	1.31	1.16
-110	1.05	0.93
-150	0.83	0.74
-325	0.54	0.48
-490	0.39	0.34
-650	0.23	0.23
-1200	0.23	0.23
-1500	0.23	0.23

7.3.4 Riser properties

The properties of the selected riser for the design and analysis are presented in Table 7.5

Table 7.5: Riser properties

Riser properties	Value	Unit
Internal diameter	10/254	in/mm
Steel grade	X65	
Steel density	7850	kg/m ³
Specified minimum yield strength	448.2	MPa
Specified minimum tensile strength	530.9	MPa
Modulus of Elasticity	207	GPa
Poisson ratio	0.3	
Internal fluid density	500	kg/m ³
External coating thickness	75	mm
Coating density	700	kg/m ³

7.3.5 Design life

For the production riser, the typical design life is 25 years. Considering a high safety class, a safety factor of 10 will be used on the wave-induced fatigue life, where the minimum criterion for fatigue life for the SCR is 250 years.

7.3.6 Hydrodynamic data

The hydrodynamic loading on the SCR can be expressed using the Morison equation, which is a function of the relative fluid velocities and accelerations. The coefficients such as drag, inertia, and added mass vary with the Reynolds number, Keulegan-Carpenter number, and the surface roughness.

A drag coefficient between 0.7 and 1.0 is standard, and an inertia coefficient of 2.0 is generally used for cylindrical bare pipes [11]. The hydrodynamic coefficients are presented in Table 7.6. Using a conservative approach, the value is assumed constant over the entire depth.

Table 7.6: Hydrodynamic coefficients

Hydrodynamic data	Value
Normal drag coefficient	1.0
Axial drag coefficient	0.0
Normal added mass coefficient	1.0
Axial added mass coefficient	0.0

7.3.7 Soil-riser interaction

Compared to a pipeline laying on the seabed, the SCR has a much more complex behavior as a result of the dynamic movements from the vessel's motions and the hydrodynamic loading. Studies have shown that the seabed soil directly influences the riser's fatigue and strength responses and the local geometry in the TDZ [43]. Thus, it is essential to consider the soil-riser interactions in the design, where the important parameters are listed in Table 7.7.

Table 7.7: Soil-riser interaction parameters

Parameter	Value	Unit
Normal friction parameter	0.5	
Axial friction coefficient	0.3	
Horizontal laterl/axial soil stiffness	200	kN/m ²
Vertical soil stiffness	50	kN/m ²

7.4 Wall thickness

To avoid critical failure of the riser in terms of burst and collapse, the wall thickness must be correctly dimensioned. The wall thickness can be calculated from the fundamental hoop stress given by Equation 7.3.

$$t = \frac{P_i D_i - P_o D_o}{2\sigma_n} \quad (7.3)$$

Where:

P_i = Internal pressure

P_o = External pressure

D_i = Internal diameter

D_o = External diameter

σ_n = Normal stress = $\sigma_n = f_1 \times \sigma_y$

f_1 = Design factor = 0.72

σ_y = Yield stress

The internal pressure is 500 bar at the top of the riser for the design. The maximum pressure difference is located at the top of the riser. As the external pressure at sea level is equal to the atmospheric pressure, P_o becomes 0.

Implementing this into Equation 7.3, it can be simplified and the wall thickness calculated based on Equation 7.4.

$$t = \frac{P_i D_i}{2f_1 \sigma_y} \quad (7.4)$$

Using the data are given in Table 7.5 and internal pressure of 500 bar, a minimum wall thickness for the riser has to be 19.7 mm. This thesis will consider a wall thickness of 30 mm for further analysis.

7.5 Design cases

The load cases to be considered in this thesis for the SCR and RCSCR designs are presented in Table 7.8. Based on previous work by Orimolade [6], the combination of a 100 - year wave and 10 - year current results in a more extreme response behavior compared to a 10 - year wave in combination with a 100 - year current. Thus, as the location of the field is similar to Orimolade, the 10 - year wave and 100 - year current will not be considered in the load cases.

Table 7.8: Matrix of the load cases

Load case	Limit state	Load type	Wave	Current	Offset
1	Static	Functional	-	-	Mean
2	Dynamic - ULS	Functional + environmental	100 - year	10 - year	Near
3	Dynamic - ULS	Functional + environmental	100 - year	10 - year	Far
4	Dynamic - ALS	Functional + environmental	100 - year	10 - year	Near
5	Dynamic - ALS	Functional + environmental	100 - year	10 - year	Far

7.6 Acceptance criteria

The acceptance criteria follow the DNV-ST-F201 recommendations, which include:

- The SCR strength performance must be in accordance with the standards combined loading criteria for bending moment, effective tension, net internal pressure, and net external pressure
- The LRFD format must be less than unity (1) for both the static and the dynamic responses

Moreover, the generalized load effect for the LRFD is given by Equation 7.5

$$g(t) = g(M_d(t), T_{ed}(t), \Delta p, R_k, \wedge) \leq 1 \quad (7.5)$$

where:

M_d = Bending moment

T_{ed} = Effective tension

Δp = Local differential pressure

R_k = Vector of cross-sectional capacities

Λ = Vector of the safety factors

Should $g(t)$ exceed one, the design will lead to the failure of the structure. Thus a design must always be below one, also known as the unity or utilization factor.

Furthermore, the maximum allowable static stress allowed is 2/3 of the SMYS, corresponding to 300 MPa. In ULS design, a design factor of 0.8 is considered, resulting in maximum allowable stress of 358 MPa. On the other hand, for ALS design, a design factor of 1.0 is considered. Thus the maximum allowable stress is 448 MPa.

The riser must not experience negative tension, which is compression, or at least be kept to a minimum. Additionally, the fatigue shall be designed against a combined loading from WF, and LF motions and the acceptance criteria are ten times the SCR's design life.

Chapter 8

Extreme response analysis

8.1 Introduction

Taking into account the design basis from the previous chapter, the extreme response analyses are performed. Analyses for the SCR will be presented in this chapter. For the SCR with the implementation of residual curvature, from now called RCSCR, a parametric study is executed for the extreme analysis, which will be presented in the next chapter. The software used for the modeling and analysis in this study is called Orcaflex. A brief general description of Orcaflex is presented in Appendix A.

The procedure used for the analysis are listed below and are similar to the approach used in theses by Gemilang, Vesga and Orimolade [7] [44] [6]:

- Determining the optimum configuration for RCSCR
- Static analysis
- Dynamic analysis
- LRFD check against DNV standard
- Fatigue analysis

The load factors used for the checking the ULS LRFD conditions against the DNV standard is presented in Table 8.1.

Table 8.1: Load factors for ULS check against DNV-ST-F201

Parameter	Value
Functional (γF)	1.10
Environmental (γE)	1.30
Condition (γc)	1.00
Moment Condition (γcm)	1.00
Reduced Functional (γRF)	0.91
Reduced Environmental (γRE)	0.77
Safety Class Factor (γSC)	1.26
Material Resistance Factor (γm)	1.15
Fabrication Factor (αfab)	1.00
WSD Usage Factor (η)	0.75

8.2 Static analysis

This section covers the static analysis for the conventional SCR at the far, near, and mean offset positions. The general riser properties were mentioned in Table 7.5, and the riser itself is attached 5 meters from the turret center and 12 meters below the water surface on the FPSO. Moreover, the horizontal span from the upper termination point at the turret to the anchoring point on the seabed there is 2094 meters: Additionally, the horizontal span to the TDP from the upper termination point is 1066 meters.

The static analysis was performed with and without the coating to understand better how the coating impacts the static configuration. As mentioned in Section 7.3.2.1, the offsets for the near and far positions of the FPSO refer to the in-plane displacement towards the TDP for the near offset and opposite for the far offset.

The static analysis considers the functional load, such as self-weight, buoyancy, and hydrostatic effect. However, it does not consider environmental loads. These analyzes aim to verify the base design and check that the strength designs for effective tension, bending moment, and the DNV utilization factor are within the acceptable limits.

8.3 Static analysis of the conventional steel catenary riser

The SCR's optimal configuration for the North-Sea environment using an FPSO is a top angle of 10° relative to the mean vertical position. The anchoring point is 2094 meters away, giving a total riser length of 3100 meters from the hang-off point for the mean offset position.

8.3.1 Analysis with coating

Evaluating the plot in Figure 8.1, it is clear that the effective static tension is a function of the riser length. The maximum effective tension appears at the hang-off point due to the entire weight of the riser being considered at this point. Thus, it is logical that the far offset has the highest top effective tension due to the longest suspended length. Moreover, the near position has the shortest suspended length and should have the lowest effective top tension.

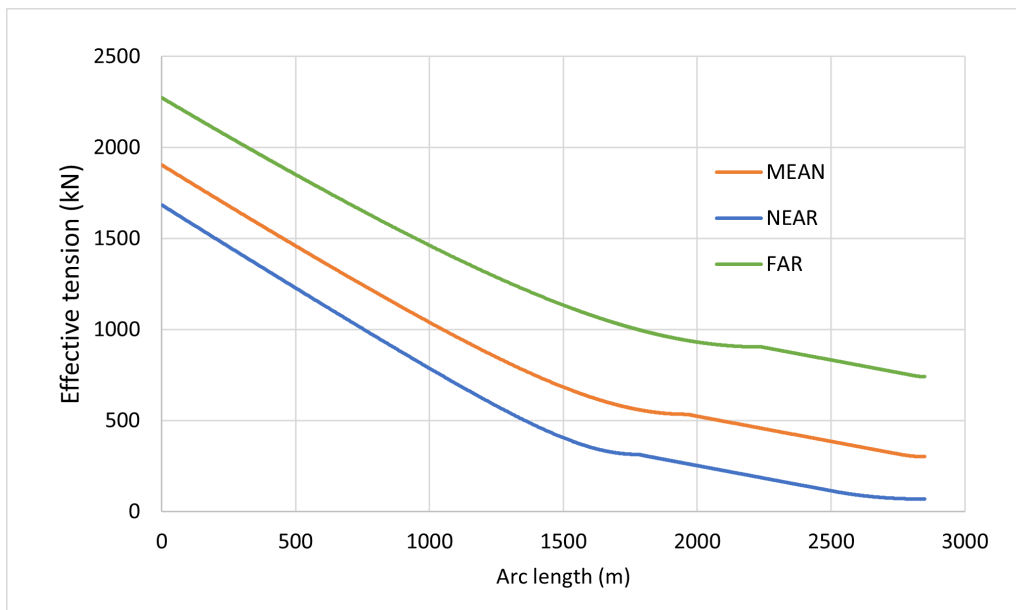


Figure 8.1: Static effective tension with coating for the SCR

The maximum bending moment is located at the TDP, as is shown in Figure 8.2, due to the riser bending from an almost vertical position to a horizontal position.

Furthermore, the near offset position gives the highest static bending moment. This is caused by the small sag-bend curvature that occurs when the FPSO is at the near offset position. Oppositely, the bending moment for the far offset position

is the minimum due to the large sag-bend curvature in the TDZ. There is a clear correlation between the bending moment and the angle at which the riser approaches the seabed.

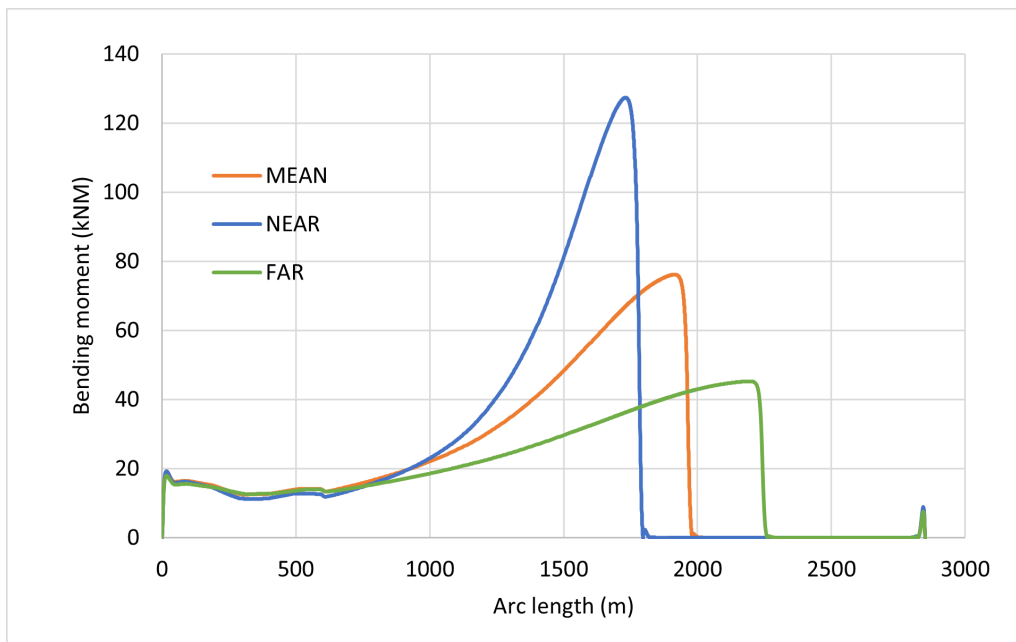


Figure 8.2: Static bending moment with coating for the SCR

The highest utilization factor is in the TDZ of the near offset position, as seen in Figure 8.3. On the other hand, the maximum utilization factor is located at the hang-off point for the far offset position. Based on the graphs, the bending moment is the main parameter for the maximum utilization factor for the near offset position, and the effective tension is the main parameter for the far offset position.

Considering that the utilization factor is larger for the near offset position than the far offset, the critical offset in the design against extreme responses is at the near position. Thus, the bending moment impacts the design more than the effective tension and has to be the main design parameter of the two for the riser.

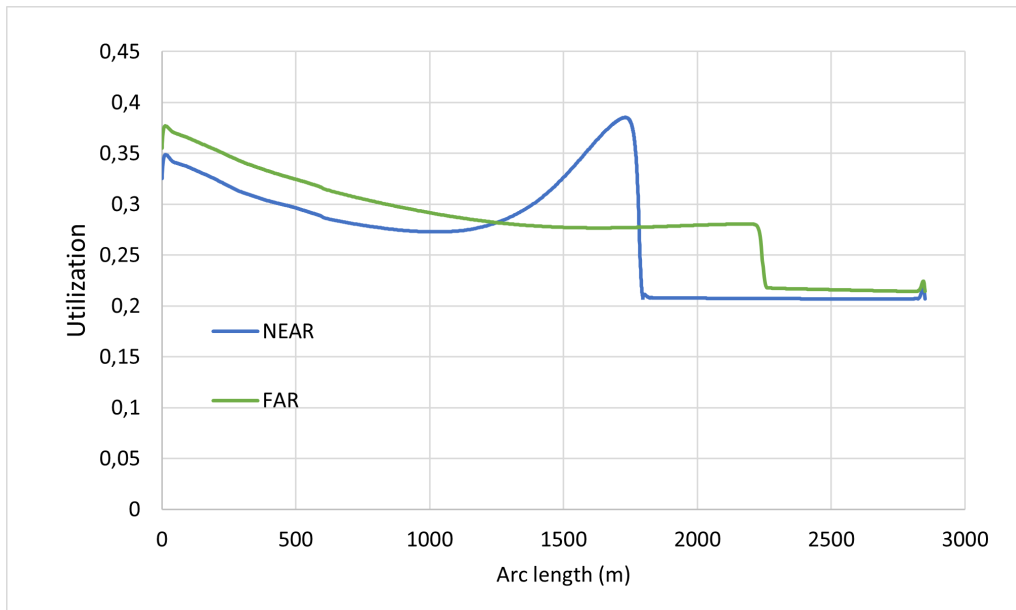


Figure 8.3: Static utilization factor with coating for the SCR

8.3.2 Analysis without coating

When comparing the graphs in Figure 8.4 to Figure 8.1, the effective tension without coating is considerably higher. This is because the coating has a density of 700 kg/m^3 , causing a positive buoyancy for the riser. Thus, the SCR with the coating is lighter than the SCR without coating.

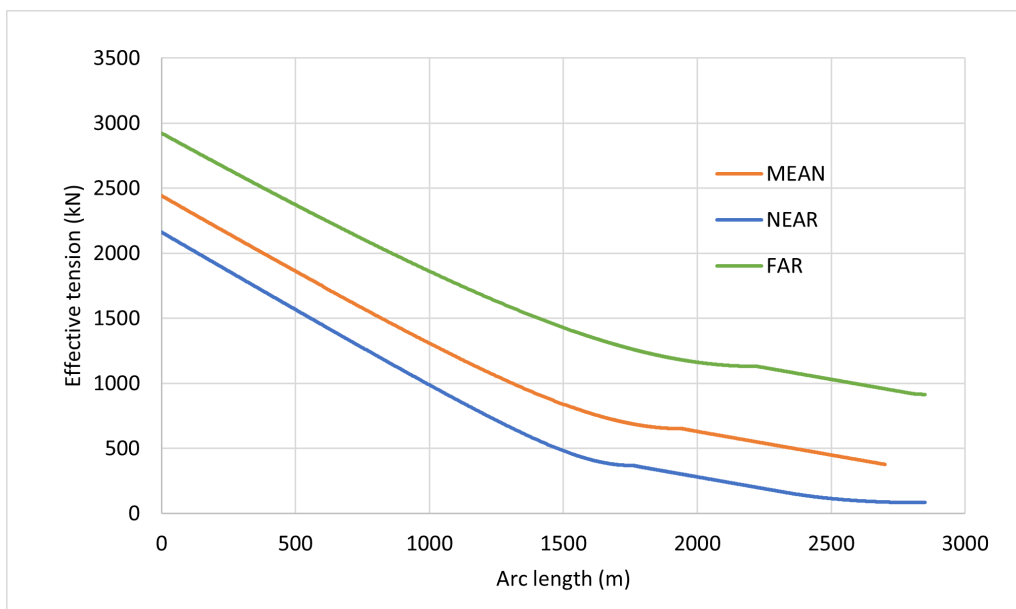


Figure 8.4: Static effective tension without coating for the SCR

The bending moment shown in Figure 8.5 is almost identical to the riser with coating as shown in Figure 8.2. Without coating, the bending moment is higher, again

caused by the increased weight of the riser without the coating. Moreover, the maximum bending moment is still in the TDZ as expected.

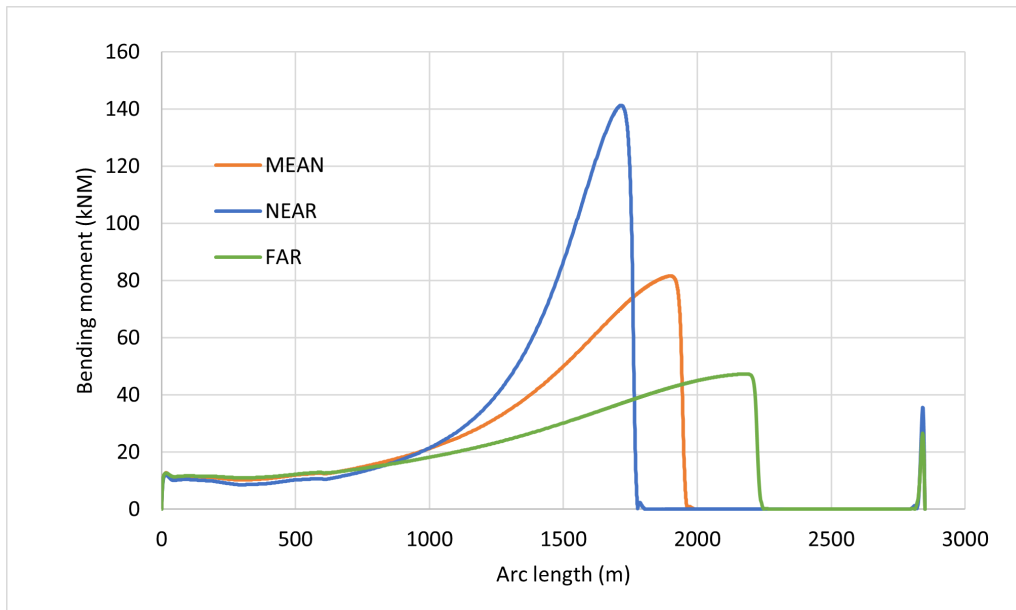


Figure 8.5: Static bending moment without coating for the SCR

The utilization factor is slightly larger for the SCR without coating, as shown in Figure 8.6. This is due to the increased effective tension and bending moment caused by the removal of the coating.

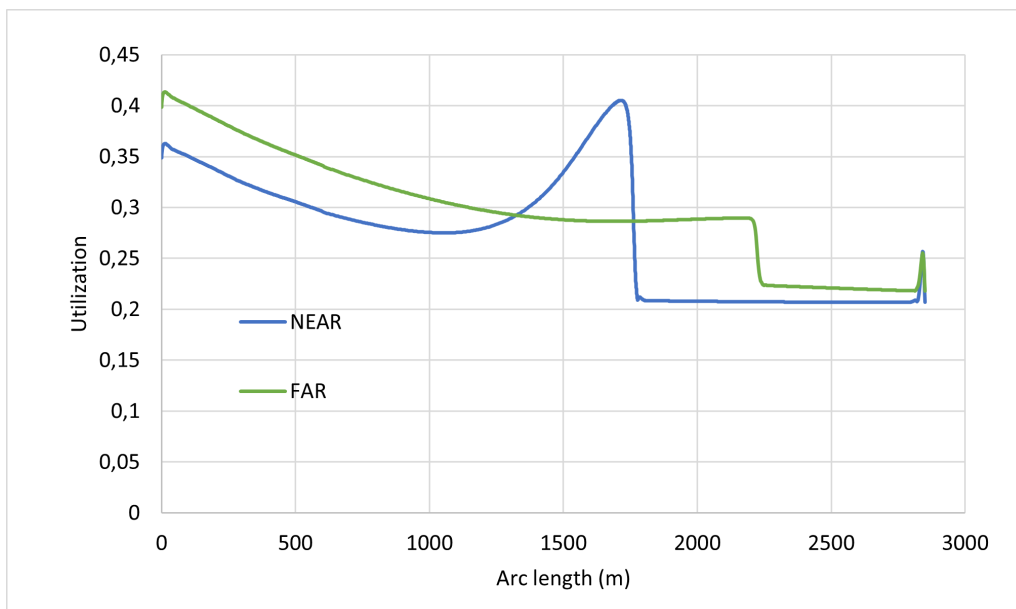


Figure 8.6: Static utilization factor without coating for the SCR

8.4 Seed components

The main analysis was performed using 20 simulations of a 3-hours storm duration for an extreme sea state response. A randomly selected component yields a different sea state for each of the 20 simulations. To simplify the simulations, the seed numbers are sorted from 1 to 20.

Running these dynamic simulations outputs 20 different downward velocities at the hang-off point, which are plotted into an extreme value distribution, in this case, a Gumbel distribution. From this distribution, a 90 % percentile response can be obtained and selected as seen from Figure 8.7. The plot shows that the maximum acceptable downward velocity without exceeding the 90 % response is 3.95 m/s. For seed number 18, the downward velocity was 3.81 m/s, and this seed number will be used for the dynamic analysis.

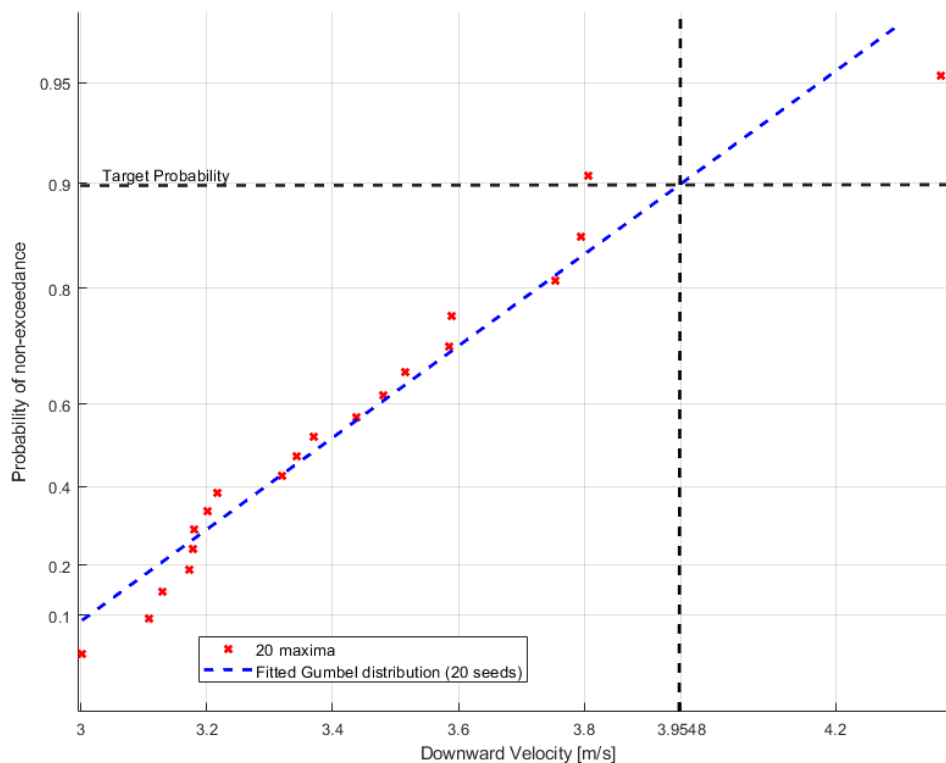


Figure 8.7: Gumbel distribution for the maximum downward velocity at the hang-off point

8.5 Dynamic analysis for the steel catenary riser

As mentioned in the previous section, 20 full 3-hour simulations were done to find the maximum downward velocity, which usually coincides with the peak sea-state. However, as this is not always the case, the full simulations help identify the worst response interval. Using the worst response interval, a simplified and shorter analysis method can be implemented according to the industrial standard procedures. The simulation is reduced to 135 seconds, capturing the worst response for the SCR. The simulation time is set to five wave periods before the worst response time and two periods after.

In the analyses the current and waves are assumed to be coming in the same direction, impacting the FPSO at the bow. This combination is considered to account for the worst response in a 3-hour storm condition. The dynamic simulations only consider the far and near offset positions for the FPSO as one of these will result in the worst response.

The dynamic results for the SCR are presented in Table 8.2. Analyses performed by Gemilang [7] show that a SCR with a coating is not feasible above a downward velocity of 2.33 m/s. Thus, there is no surprise that the DNV utilization factor is much more significant than one for all the load cases. There are large compression forces and bending moments for all load cases, making none of them acceptable based on the utilization factor. The largest utilization is for the ULS Near offset position, which indicates that this is the critical offset while considering the extreme responses with a factor of 2.81. Thus, the study of implementing the residual curvature to the riser will be focused on the ULS near offset.

Table 8.2: Strength response of the SCR with a downward velocity of 3.81 m/s

Offset	ULS		ALS	
	Near	Far	Near	Far
Max. Eff. Top tension [kN]	2067.00	4253.11	2034.33	4244.87
Max. Compression [kN]	497.88	1127.37	432.40	1282.08
Max. Bending moment [kNm]	1620.97	1184.64	1638.39	1184.72
Max. DNV Utilization factor	2.81	2.19	2.28	1.75

Chapter 9

Parametric study for the RCSCR

The parametric study covers the optimal geometry of the residual curvature and location for it to be implemented in the riser. There are several key parameters to the implementation, such as the arc length, radius of curvature, the distance from the seabed, and more. In order to find the optimal parameters for the RCSCR the procedure follows the previous thesis work done by Vesga and Ramiro which is as follow [44][45].

- Step 1: Select a load case - Harsh North Sea conditions during a 3-hour storm.
- Step 2: Obtain the maximum downward velocity at the hang-off point
- Step 3: Specify the parameters - Determine the location for implementation of residual curvature by varying the arc lengths, the radius of curvature, and distance from the seabed.
- Step 4: Sensitivity study for the parameters - Selection of the best parameter settings in accordance with the DNV utilization factor.
- Step 5: Optimizing design - Using the combination of the optimal parameters, find a utilization factor less than one. Reiterate design or lower downward velocity.
- Step 6: RCSCR selection - Continue with the design that yields the lowest utilization factor below one.

For the selected load case, the maximum downward velocity at the hang-off point is 3.8 m/s. The base case for the sensitivity analysis has the section with residual curvature implemented before the 45 meters before the TDZ. Thus, the arc length of the riser must be determined using the Orcaflex software.

- TDZ start at arc length: 1563 m
- TDZ end at arc length: 1669 m

- TDZ length: 106 m

Using this data, the end of the residual curvature section is located at 1518m in the arc length of the riser. The residual curvature used for the sensitivity analysis consists of one under-straightened section followed by a section with no residual curvature into an over-straightened section. There is a transition section before and after the under and over-straightened sections, as seen in the gradual curvature (pink line) in Figure 9.1. The residual curvature in the transitional sections is calculated using Equation 9.1.

$$K_{res} = \frac{\epsilon_{res}}{r} \quad (9.1)$$

where:

K_{res} = desired residual curvature

ϵ_{res} = residual strain

r = outer radius of the pipeline

The residual strain increases linearly for every 5-meter length until the desired residual curvature is achieved.

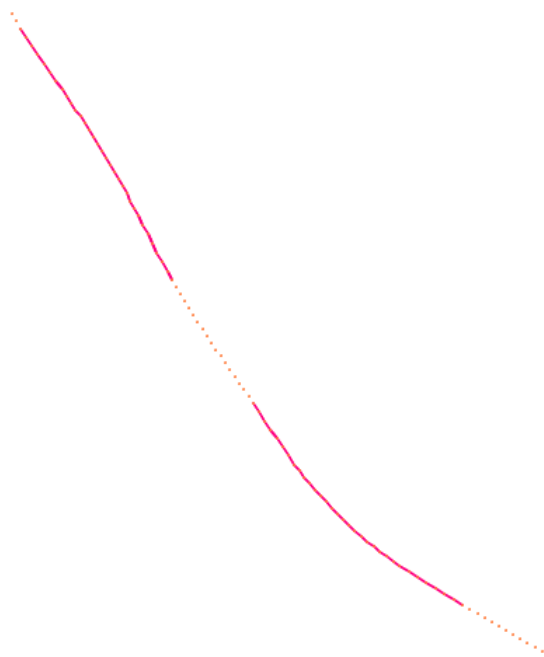


Figure 9.1: Residual curvature sections

9.1 Section length sensitivity

This study is performed for a downward velocity of 3.8 m/s, as previously mentioned. The section lengths implemented with residual curvature are selected based on a percentage of the water depth. The selected lengths are presented in Table 9.1.

Table 9.1: Selected section lengths for RCSCR

Section lengths based for RCSCR	
Percentage of water depth	Section lengths [m]
4	60
7	100
9	140
14	200
16	240
20	300
27	400
33	500
47	700
67	1000

The total length listed in Table 9.1 is the total length for the under and over-straightened sections combined. An example of the sectional setup for the 60 m section would be: 3.75 m - 3.75 m - 15 m - 3.75 m - 3.75 m for each of the sections. Where the 15 m section has the selected residual curvature, while the other lengths (3.75m) are ramp up and down transitional sections, linearly increasing and decreasing the RC. The number of sections needed in the transitional build-up increases as the section with residual curvature increases.

The utilization factor decreases depending on the section length with the residual curvature implemented, as shown in Table 9.2. Having a section length of 60 m reduces the utilization to a minimum of 1.81. On the other hand, without residual curvature, the utilization factor is 2.83 for the conventional SCR. All the sections were implemented 45 m before the touchdown zone. The end of the section were located at the arc length of 1518 m as mentioned above and implemented with a curvature of 0.02 equivalent to a radius of curvature of 50 m.

Table 9.2: Residual curvature sensitivity with respect to section length

Section length with curvature [m]	Max utilization	Max compression [kN]
60	1.81	257.53
100	1.96	247.67
140	1.90	218.08
200	2.12	248.49
240	2.27	259.59
300	2.32	300.14
400	2.42	344.74
500	2.16	376.80
700	2.12	375.78
1000	2.14	382.65

Figure 9.2 and Figure 9.3 show that the lowest utilization factor does not exactly correspond to the minimum compression forces at a section length of 60 m. However, the compression is reduced from 497.88 kN for the SCR without residual curvature to 257.53 kN.

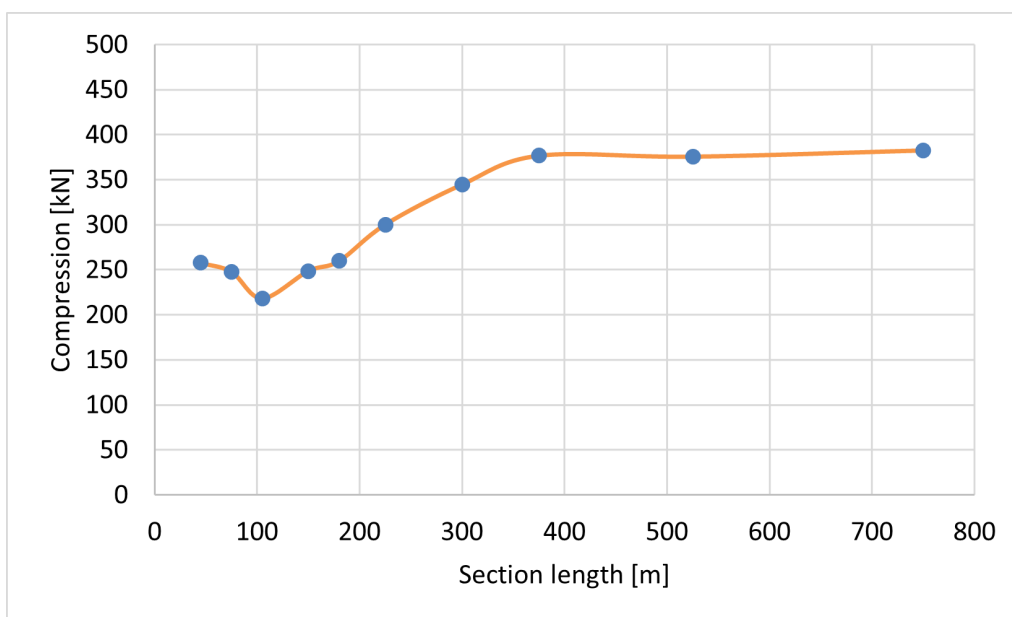


Figure 9.2: Compression versus section lengths with respect to residual curvature

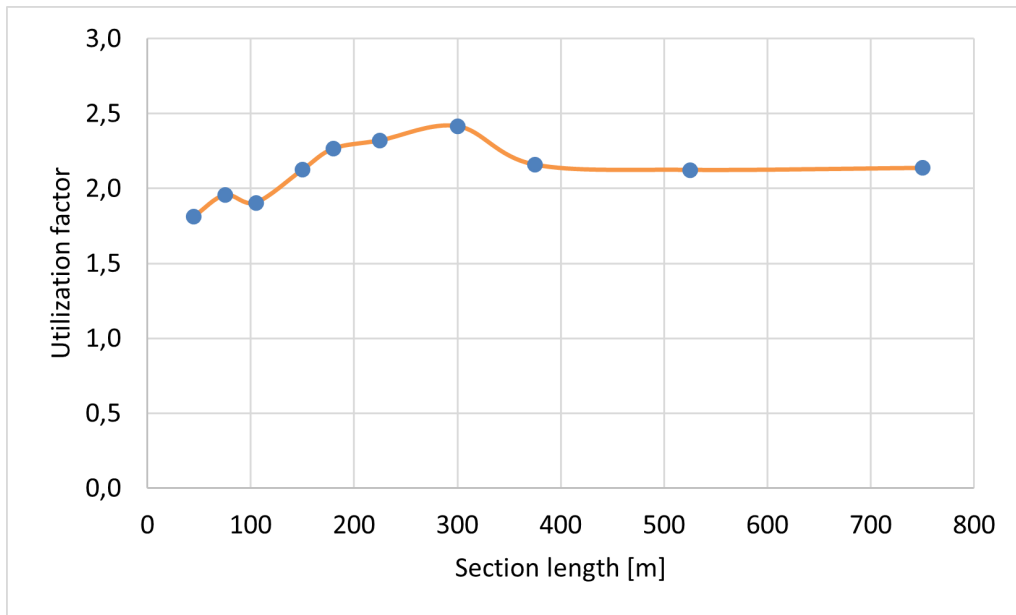


Figure 9.3: Utilization factor versus section lengths with respect to residual curvature

In Figure 9.4, the DNV utilization factor is plotted against the sections with residual curvature implemented for all the analyzed lengths. By comparing the base case without RC implemented, it is clear that the peak of utilization is transitioned away from the sagbend to the sections with RC as intended.

The section length does impact the design. Thus the two sections with the lowest utilization factor will be used for the next sensitivity analysis in order to see how the section lengths impact the other parameters.

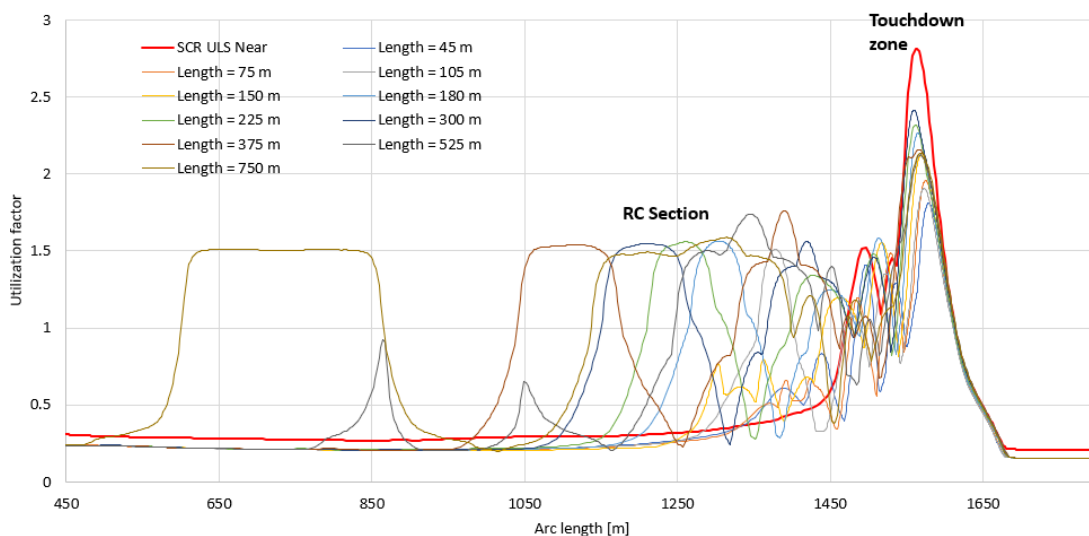


Figure 9.4: Comparison of RC section lengths

9.2 Radius of curvature sensitivity study

The curvatures used for the sensitivity study range from 0.01 to 0.03 as shown in Tables, 9.3 and 9.4. These curvatures represent the peak of the section, where there is a transition zone before and after to ramp up and ramp down the curvature. To implement the residual curvature in the pipe during installation, it is required to have a gradual increase and decrease of the curvature. The purpose of the study is to analyze how the DNV utilization factor and compression in the riser is affected by the curvature.

9.2.1 Analysis of 60 m section with RC

The sensitivity analyses for the radius of curvature implemented for the 60 m section are presented in Table 9.3. For the analyses the radius of curvature is in the range of 33 to 100 m, with the corresponding curvature. The utilization factor is lowest with a curvature of 0.025, which corresponds to a radius of 40 m, which is also visualized in Figure 9.5. A low and high radius of curvature increases the utilization factor, where the lowest values are in the 0.02 curvature area.

According to the results presented in Table 9.3, the lowest utilization factor occurs at a curvature of 0.025. On the other hand, the lowest compression force is for a curvature of 0.03. As the main acceptance criteria are the utilization factor, a curvature of 0.025 is more optimal.

Table 9.3: Residual curvature sensitivity for the 60 m section

Curvature [1/m]	Radius of curvature [m]	Max compression [kN]	Max utilization
0.01	100.0	313.63	1.98
0.0125	80.0	286.50	1.89
0.015	66.7	262.42	1.78
0.016	62.5	253.40	1.75
0.017	58.8	244.37	1.72
0.0175	57.1	240.22	1.70
0.018	55.6	236.21	1.69
0.019	52.6	228.98	1.66
0.02	50.0	221.78	1.63
0.0225	44.4	204.72	1.58
0.025	40.0	188.11	1.57
0.0275	36.4	173.57	1.69
0.03	33.3	160.64	1.82

According to the results presented in Table 9.3, the lowest utilization factor occurs at a curvature of 0.025. On the other hand, the lowest compression force is for

a curvature of 0.03. As the main acceptance criteria are the utilization factor, a curvature of 0.025 is more optimal.

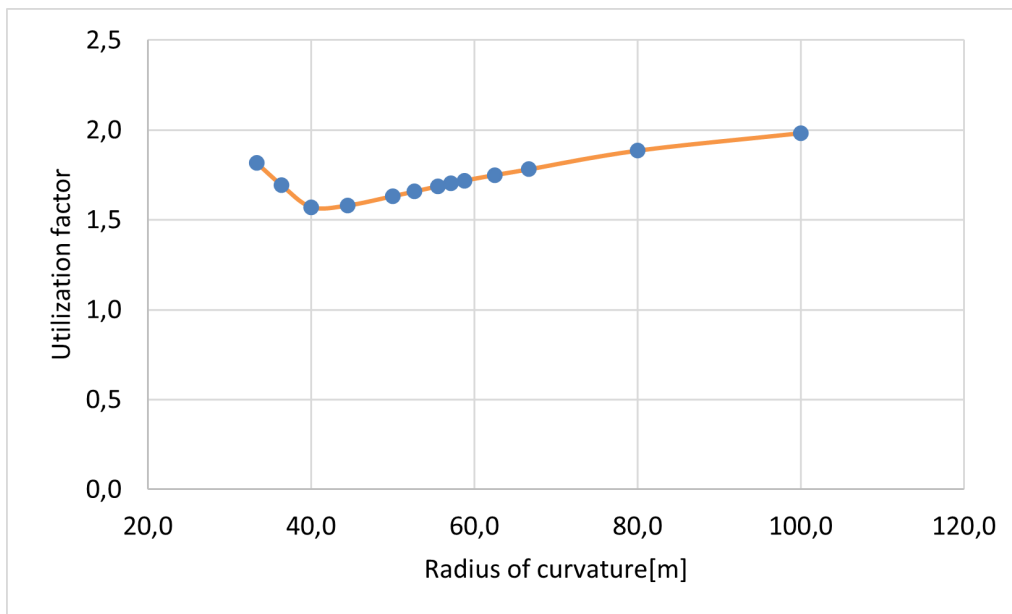


Figure 9.5: Utilization factor versus radius of curvature with respect to residual curvature for 60 m section

Figure 9.6 shows all of the tested curvatures, where the thicker red line represents the SCR without any curvature. It is clear that the utilization factor decreases in the TDZ by increasing the curvature. On the other hand, in the section with residual curvature the utilization increases beyond acceptable values. The best result for the 60 m section was 0.025 in curvature marked with a blue dotted line in the graph, and it can be seen that the utilization factor is higher in the section with RC than in the TDZ.

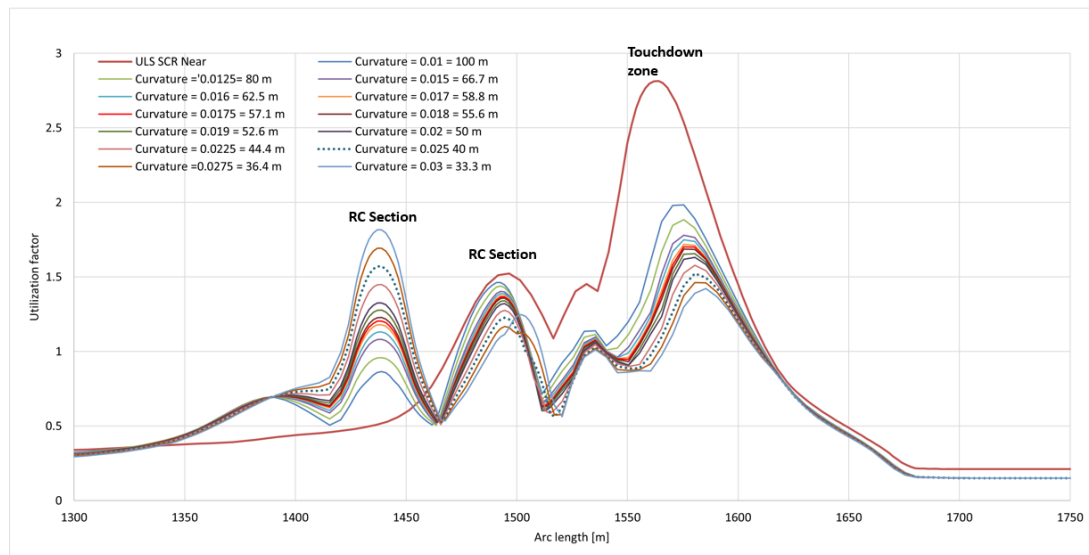


Figure 9.6: Comparison of implemented curvature to the RC sections for 60 m section

9.2.2 Analysis of 140 m section with RC

Similar to the 60 m section, the same range of radius of curvature was tested for the 140 m section. The results are presented in Table 9.4, where the lowest utilization factor was 1.57, to a corresponding 0.02 curvature or a radius of curvature of 50 m, also illustrated in Figure 9.7. Furthermore, the lowest utilization factor is for curvatures around 0.02, similar to the 60 m section. Again, the compression is not lowest at the same curvature, resulting in the lowest utilization factor.

Table 9.4: Residual curvature sensitivity for the 140 m section

Curvature [1/m]	Radius of curvature [m]	Max compression [kN]	Max UF
0.01	100.0	313.25	2.27
0.0125	80.0	282.95	2.16
0.015	66.7	258.75	2.07
0.016	62.5	249.98	2.03
0.017	58.8	241.37	2.00
0.0175	57.1	237.31	1.98
0.018	55.6	233.24	1.96
0.019	52.6	225.56	1.93
0.02	50.0	218.04	1.81
0.0225	44.4	200.64	1.83
0.025	40.0	184.87	1.90
0.0275	36.4	170.40	1.97
0.03	33.3	156.79	2.12

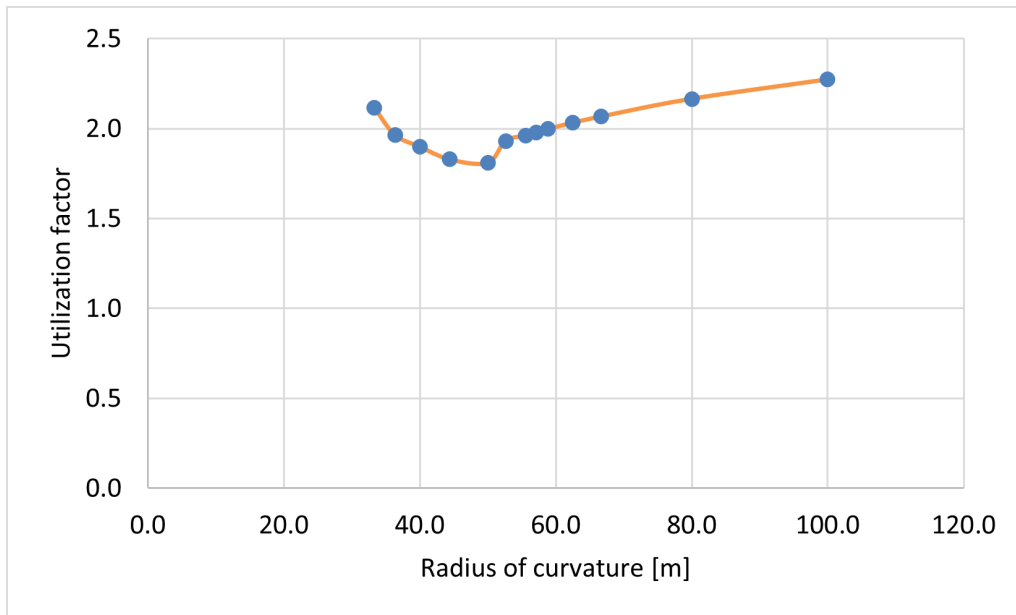


Figure 9.7: Utilization factor versus radius of curvature with respect to residual curvature for 140 m section

In Figure 9.8 the same pattern emerges, where the utilization drops in the TDZ with a higher curvature, and at the same time it increases more as the curvature increases in the sections with the residual curvature is implemented.

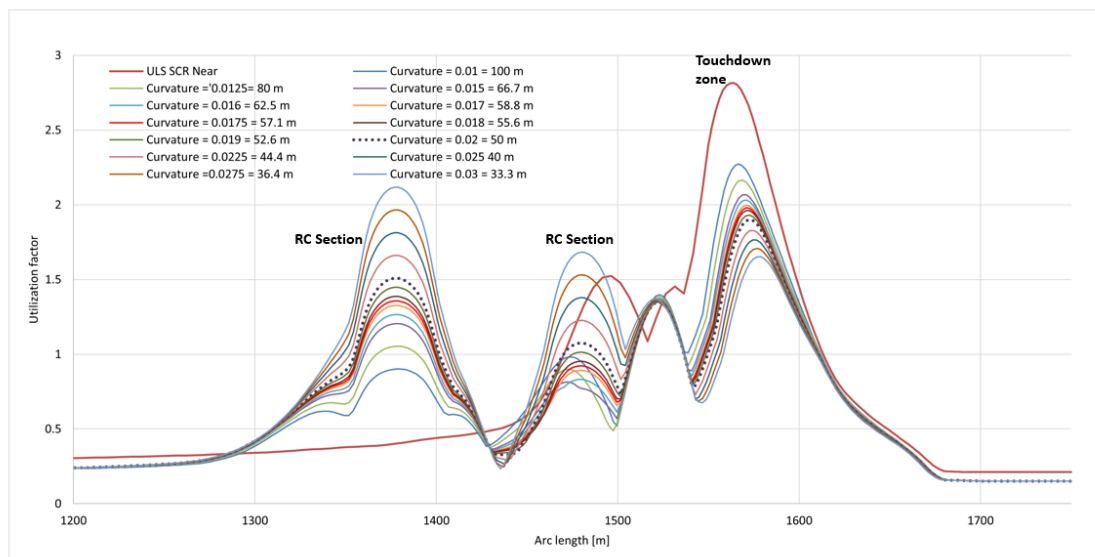


Figure 9.8: Comparison of implemented curvature to the RC sections for 140 m section

The results from the 60 m section and the 140 m section coincide. It shows that the utilization continues to decrease in the TDZ with a larger curvature, but in the process, the utilization factor increases in the RC sections. Thus, it can be

concluded that the residual curvature section improves the utilization factor overall, but it also transitions the worst responses to the residual curvature sections. This indicates that the RCM is applicable to the riser. However, further parameters must be tested to find an optimum configuration.

9.3 Distance to seabed sensitivity study

The distance to the seabed was analyzed to find the optimal distance from the seabed to the lowest part of the section with residual curvature, in the vertical distance and how this impacts the compression and the DNV utilization factor. These analyses use the curvature that resulted in the lowest utilization factor based on the sensitivity analyses above 0.025 for the 60 m section and 0.02 for the 140 m, respectively.

9.3.1 Analysis of 60 m section

The tested distances range from 11 m over the seabed to 500 m over the seabed. In Table 9.5 the results for the section are presented, and the lowest curvature was at 35 m above the seabed. By increasing the distance from the seabed to 500 m, there is almost no reduction from not having any RC implemented. On the other hand, having a distance between 125 m and 18 m from the seabed for this section length does not vary more than 0.26 in utilization.

Table 9.5: Distance to seabed sensitivity for residual curvature of 60 m section

Arc length [m]	V. Distance to seabed for static NEAR position of RCSCR [m]	Max compression [kN]	Max utilization
1000	500	454.50	2.63
1261	250	284.04	1.92
1402	125	252.04	1.80
1425	105	236.51	1.71
1438	95	227.22	1.72
1451	85	215.99	1.80
1466	75	201.65	1.84
1479	65	188.36	1.84
1492	55	188.36	1.84
1509	45	182.19	1.79
1524	35	187.34	1.58
1539	27	178.75	1.60
1559	18	150.53	1.64
1579	11	227.18	2.15

Figure 9.9 shows the distance variation to the seabed for all the distances. The thick red line represents the SCR for the ULS near offset position without any RC while

the red dotted line shows lowest utilization factor at 35 meters above the seabed, effectively decreasing the utilization factor from 2.81 to 1.58.

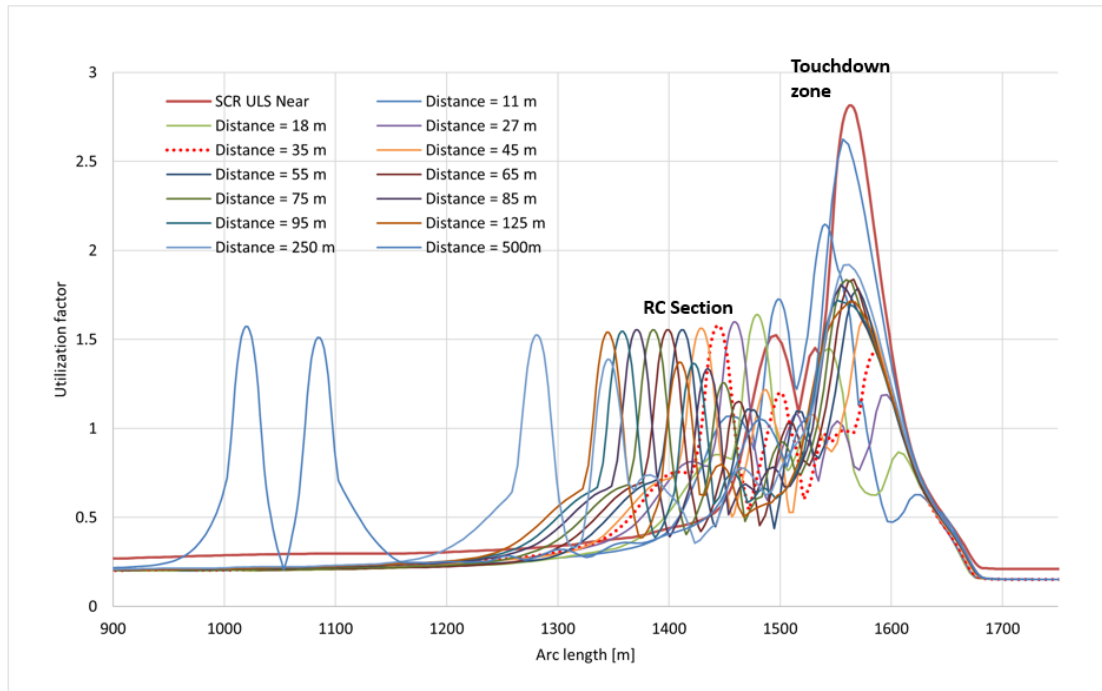


Figure 9.9: Comparison of distance to seabed sensitivity for 60 m section

9.3.2 Analysis for 140 m section

Opposite to the 60 m section, the lowest utilization factor for this length was 11 meters above the seabed, with a utilization of 1.54 as shown in Table 9.6. In this case, this also has the most decrease in compression of the riser, reducing it to 186.58 kN from 496 kN in the SCR.

Similar to the 60 m section, the utilization factor is seen to be quite similar between 27 m to 125 m above the seabed, highlighted in Figure 9.10. Again, the residual curvature transitions the peak of the utilization away from the TDZ to the sections with RC, but still above the acceptable criteria of one.

For both section lengths it is apparent that the implementation of the RC high up in the riser from 250 meters and above, has limited effect on the utilization in the TDZ. Having the RC applied closer to the seabed will have a more positive impact on the configuration and lower the utilization.

Table 9.6: Distance to seabed sensitivity for residual curvature of 140m section

Arc length [m]	V. Distance to seabed for static NEAR position of RCSCR [m]	Max compression [kN]	Max utilization
1000	500	486.53	2.72
1261	250	379.07	2.27
1402	125	284.29	1.84
1425	105	269.51	1.77
1438	95	263.29	1.74
1451	85	258.14	1.71
1466	75	248.80	1.80
1479	65	236.98	1.89
1492	55	222.57	1.94
1509	45	209.43	1.94
1524	35	225.18	1.85
1539	27	239.16	1.65
1559	18	230.17	1.55
1579	11	186.58	1.54

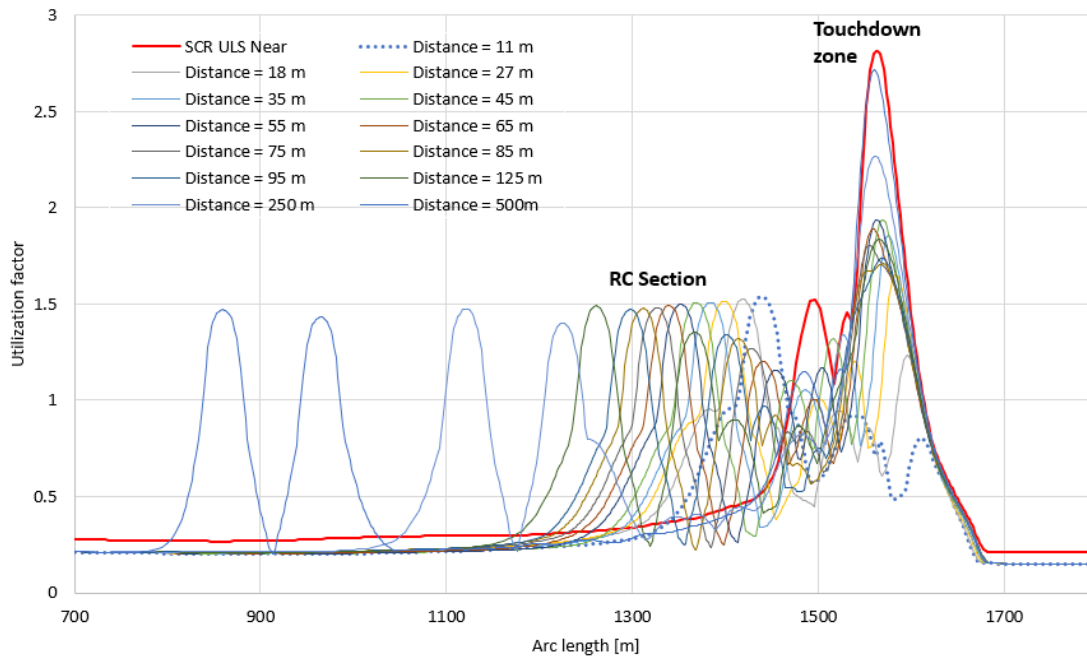


Figure 9.10: Comparison of distance to seabed sensitivity for 140 m section

9.4 Sensitivity for several sections in a row

This analysis was performed to see the influence of multiple RC sections in a row and how this impacts the utilization factor. In this analysis, the sections have the same curvature, and the lowest section location is based on the analysis in the previous section.

9.4.1 Analysis of 60 m section

For the 60 m section, the residual curvature resulting in the lowest utilization factor are:

- Curvature of 0.025 m^{-1} equivalent to a radius of curvature of 40 m
- Distance from the seabed for the lowest part of 35 m
- Residual curvature section (3.75 m - 3.75m - 15 m - 3.75m - 3.75 m)

How the transition curvature was setup in Orcaflex is shown in Figure 9.11.

Sections: Total length = 3100,0m

No.	Line type	Section length (m)	Target segment length (m)	Number of segments	Pre-bend curvature (rad/m)		Cumulative values	
					x	y	Length (m)	Segments
9	Residual curvature pipe	3,75	2,0	2	0,0	0,0125	1432,75	468
10	Residual curvature pipe	3,75	2,0	2	0,0	0,025	1436,5	470
11	Residual curvature pipe	15,0	2,0	8	0,0	0,025	1451,5	478
12	Residual curvature pipe	3,75	2,0	2	0,0	0,025	1455,25	480
13	Residual curvature pipe	3,75	2,0	2	0,0	0,0125	1459,0	482
14	10" ID Steel Pipe	35,0	2,0	18	0,0	0,0	1494,0	500
15	Residual curvature pipe	3,75	2,0	2	0,0	-0,0125	1497,75	502
16	Residual curvature pipe	3,75	2,0	2	0,0	-0,025	1501,5	504
17	Residual curvature pipe	15,0	2,0	8	0,0	-0,025	1516,5	512
18	Residual curvature pipe	3,75	2,0	2	0,0	-0,025	1520,25	514
19	Residual curvature pipe	3,75	2,0	2	0,0	-0,0125	1524,0	516

Figure 9.11: Curvature setup in Orcaflex for the 60 m section

The analysis was performed for one to four sections in a row. According to Figure 9.12, having multiple sections in a row with the same curvature does not significantly impact the maximum utilization in the TDZ. The utilization reduces slightly TDZ. However, the sections where the RC has been implemented have a higher value making this a more critical area than the TDZ for the design.

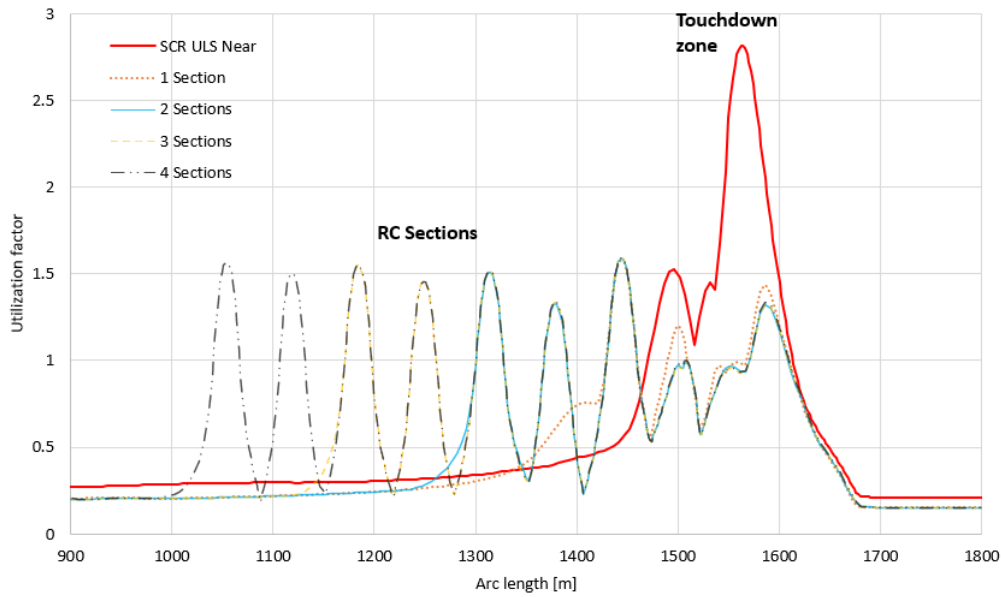


Figure 9.12: Sensitivity analysis of multiple 60 m sections of RC in a row

9.4.2 Analysis of 140 m section

For the 140 m section, the residual curvature that results in the lowest utilization factor are:

- Curvature of 0.02 m^{-1}
- Distance to seabed of 11 m
- Residual curvature section (5 m - 5 m - 5 m - 2.5 m - 35 m - 2.5 m - 5 m - 5 m)

Figure 9.13 shows how each curvature section's curvature was implemented in Orcaflex.

The results for the 140 m section coincide with the results found for the 60 m section. Increasing the number of sections in a row has a negligible impact on the utilization factor in the TDZ, also presented in Figure 9.14.

Sections: 39 Total length = 3100,0m

No.	Line type	Section length (m)	Target segment length (m)	Number of segments	Pre-bend curvature (rad/m)		Cumulative values	
					x	y	Length (m)	Segments
9	Residual curvature pipe	5,0	2,0	2	0,0	0,005	1409,0	520
10	Residual curvature pipe	5,0	2,0	2	0,0	0,00667	1414,0	522
11	Residual curvature pipe	5,0	2,0	2	0,0	0,01	1419,0	524
12	Residual curvature pipe	2,5	2,0	1	0,0	0,02	1421,5	525
13	Residual curvature pipe	35,0	2,0	18	0,0	0,02	1456,5	543
14	Residual curvature pipe	2,5	2,0	1	0,0	0,02	1459,0	544
15	Residual curvature pipe	5,0	2,0	2	0,0	0,01	1464,0	546
16	Residual curvature pipe	5,0	2,0	2	0,0	0,00667	1469,0	548
17	Residual curvature pipe	5,0	2,0	2	0,0	0,005	1474,0	550
18	10" ID Steel Pipe	35,0	2,0	18	0,0	0,0	1509,0	568
19	Residual curvature pipe	5,0	2,0	2	0,0	-0,005	1514,0	570
20	Residual curvature pipe	5,0	2,0	2	0,0	-0,00667	1519,0	572
21	Residual curvature pipe	5,0	2,0	2	0,0	-0,01	1524,0	574
22	Residual curvature pipe	2,5	2,0	1	0,0	-0,02	1526,5	575
23	Residual curvature pipe	35,0	2,0	18	0,0	-0,02	1561,5	593
24	Residual curvature pipe	2,5	2,0	1	0,0	-0,02	1564,0	594
25	Residual curvature pipe	5,0	2,0	2	0,0	-0,01	1569,0	596
26	Residual curvature pipe	5,0	2,0	2	0,0	-0,00667	1574,0	598
27	Residual curvature pipe	5,0	2,0	2	0,0	-0,005	1579,0	600

Figure 9.13: Curvature setup in Orcaflex for the 140 m section

Based on the analysis of both sections, it is not beneficial to implement more than one section with residual curvature for the configuration. The location of the section has more impact than the number of sections.

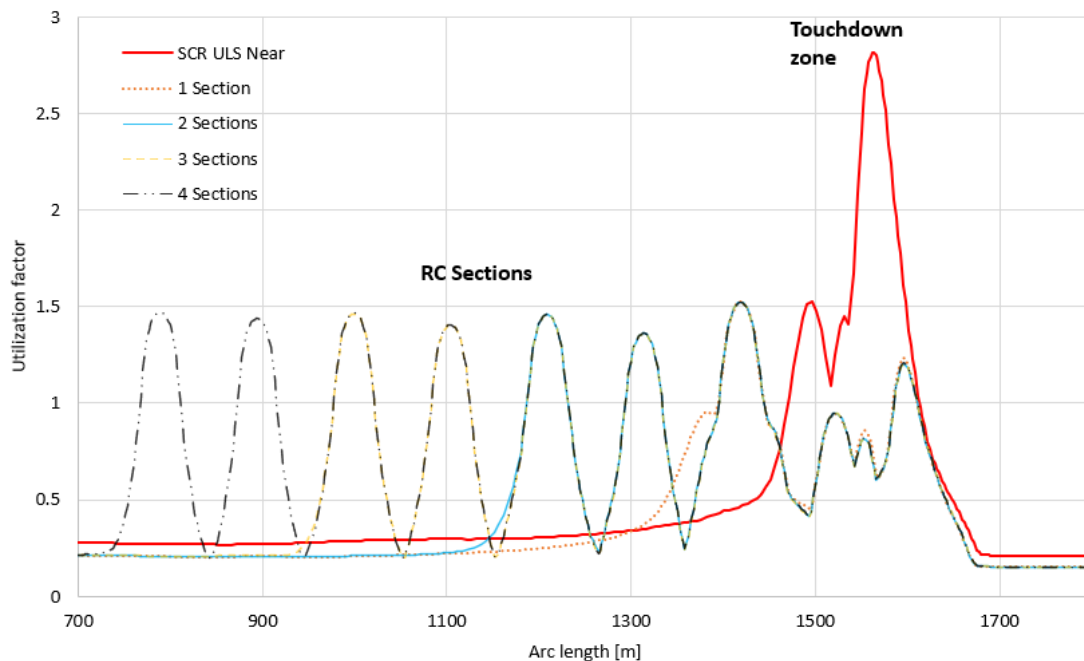


Figure 9.14: Sensitivity analysis of multiple 140 m sections of RC in a row

9.5 Two separated sections sensitivity study

This analysis studies the effect of two sections of residual curvature in two different locations of the riser. The bottom section is located at the optimum distance above

the seabed, which was found and discussed in Section 9.3 and the top section is moved upward in the riser by a distance ranging from 100 m - 700 m.

9.5.1 Analysis of 60 m section

The curvature for both sections are identical to those used in Section 9.4.1. The utilization for two sections for any of the distances spread apart does not impact the TDZ as shown in Figure 9.15 in comparison to only having one section. Moreover, as the distance increase, there is a slight increase in the utilization for the second section closer to the FPSO.

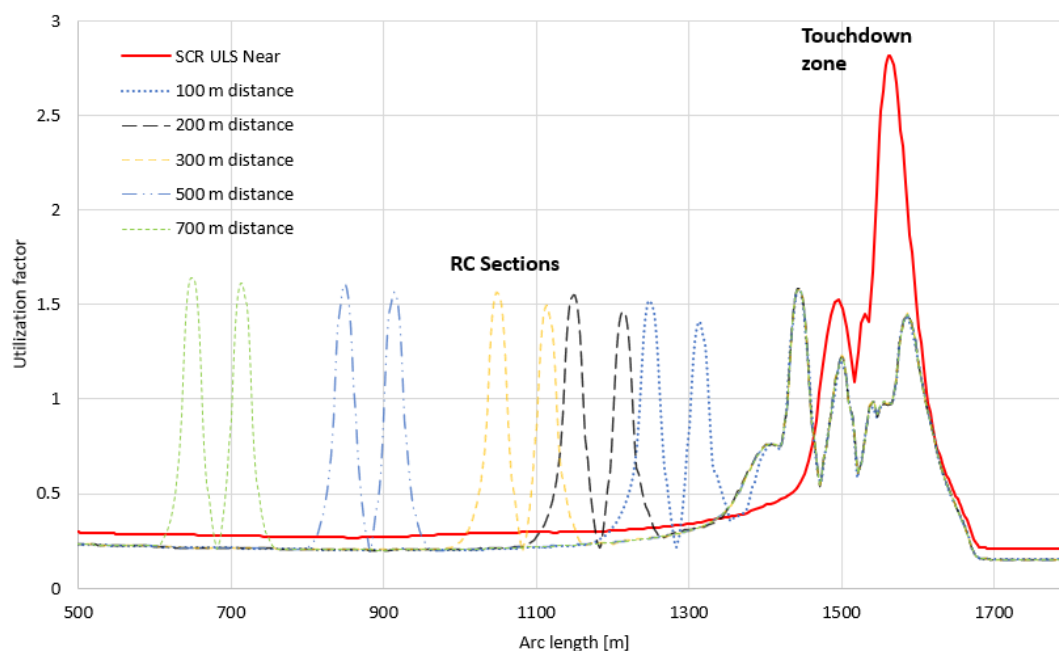


Figure 9.15: Sensitivity analysis of multiple 60 m sections of RC in spread out locations

9.5.2 Analysis of 140 m section

The utilization for this section is at the maximum in the lowest residual curvature section, at just above 1.5, as seen in Figure 9.16. Likewise to the 60 m section, the second section with residual curvature implemented higher up in the riser does not result in an improvement in the TDZ.

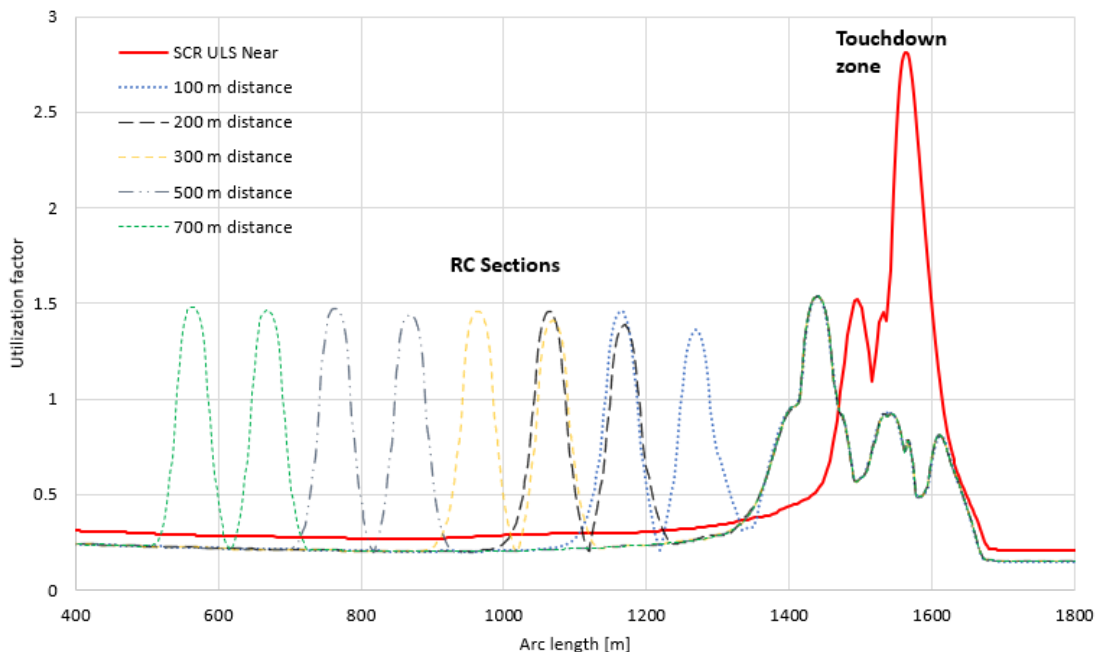


Figure 9.16: Sensitivity analysis of multiple 140 m sections of RC in spread out locations

Based on this sensitivity analysis, it can be concluded that having more than one section of RC with the same parameters does not impact the utilization factor for the TDZ. The length of the section of residual curvature also does not affect significantly, though it can be seen from the graphs in Figure 9.15 and Figure 9.16 that the utilization is lower for the 140 m section.

9.6 Different curvature for the residual curvature sections

Given that the analysis for the 140 m section in the other sensitivity analyses provides a better configuration based on the utilization factor, this analysis was only performed for this section. This analysis considers that the upper section with residual curvature maintains a constant curvature while the bottom section changes. The study showed a massive increase in utilization factor using two different curvatures for the under and over-straightened sections. Table 9.7 shows that the lowest utilization factor of 1.04 can be obtained by having a curvature of 0.01 for the upper section and 0.02 for the lower section, by increasing the upper curvature the utilization increases, which are to be expected. The upper section is under-straightened. This results in a curve opposite to the sagbend. Thus, by increasing the curva-

ture, the bending moment also increases, causing the utilization to go beyond the acceptable limit.

The analysis showed that the variation of curvature has a high impact on the utilization factor. It can be concluded that a configuration that utilizes a combination of curvatures has an overall positive effect on the Utilization Factor (UF) in the TDZ, with a lower curvature for the upper section.

Table 9.7: Sensitivity to different residual curvature for each of the sections

Lower section curvature [1/m]	Radius of curvature [m]	Upper section curvature [1/m]									
		Max compression [kN]					Max UF				
		0.01	0.0125	0.015	0.02	0.025	0.01	0.0125	0.015	0.02	0.025
0.01	100.0	333.08	299.76	269.31	220.40	178.37	1.32	1.26	1.25	1.55	1.85
0.0125	80.0	315.56	287.64	260.40	213.90	179.05	1.20	1.14	1.25	1.55	1.85
0.015	66.7	293.90	271.83	248.51	206.18	172.87	1.14	1.10	1.24	1.54	1.85
0.016	62.5	284.38	264.65	243.10	202.60	170.30	1.13	1.09	1.24	1.54	1.85
0.017	58.8	274.95	257.19	237.25	199.05	167.41	1.11	1.09	1.24	1.54	1.84
0.0175	57.1	270.05	253.21	234.35	197.06	165.98	1.10	1.09	1.24	1.54	1.84
0.018	55.6	265.07	249.42	231.23	195.03	164.52	1.09	1.09	1.24	1.54	1.84
0.019	52.6	255.46	241.51	224.90	190.93	161.47	1.07	1.09	1.24	1.54	1.84
0.02	50.0	245.64	233.48	218.47	186.58	158.23	1.04	1.09	1.24	1.54	1.84
0.0225	44.4	222.17	213.26	201.70	175.07	149.62	1.07	1.09	1.24	1.54	1.84
0.025	40.0	200.02	193.51	184.76	162.59	140.42	1.22	1.22	1.24	1.53	1.83
0.0275	36.4	200.02	193.51	184.76	162.59	140.42	1.22	1.22	1.24	1.53	1.83
0.03	33.3	160.81	157.06	151.65	136.82	120.44	1.51	1.51	1.50	1.53	1.83

9.7 Response analysis of the RCSCR

From the sensitivity analysis for the configuration of the residual curvature sections, the optimal setup parameters for reducing the utilization factor in the riser are:

- Length of section = 140 m(5 m - 5 m - 5 m- 2.5 m - 35 m - 2.5 m - 5 m - 5 m - 5 m - 5 m - 5 m- 2.5 m - 35 m - 2.5 m - 5 m - 5 m)
- Curvature = $0.01 m^{-1}$ for the upper section and $0.02 m^{-1}$ for the lower section
- Single section (including the under-straightened and over-straightened sections)
- Distance from the seabed for the near static offset position = 11 m

The results of this configuration reduces the utilization factor to 1.04, down from 2.81 for the steel catenary riser without any residual curvature. All of the sensitivity analyses were performed for hurricane conditions with a 3-hour sea state resulting in a downward velocity of 3.81 m/s at the hang-off point.

Table 9.8: Strength response for the RCSCR

Parameters	ULS		ALS	
	Near	Far	Near	Far
Max. Bending moment [kNm]	669.49	1079.38	693.13	1089.05
Max. Effective tension [kN]	2463.68	5006.95	2426.06	5359.93
Max. Compression [kN]	245.64	388.34	227.56	413.48
Max. Utilization LRFD	1.04	1.54	1.09	1.40

A summary of the strength responses for the RCSCR are presented in Table 9.8. Opposite to the conventional SCR, the offset for the ULS far offset position results in the highest utilization factor. The bending moment and effective tension increases, where the effective tension was expected due to the increase in free span of the riser. On the other hand, the bending moment results were unexpected. The increase in bending moment was also due to the increase in free span, as the sections with the residual curvature were more parallel to the seabed caused by the rise in the effective tension. The residual curvature sections experience the full downward velocity of the vessel while reducing it for the TDZ. Thus, the bending moment was distributed over a shorter section compared to the near offset configuration, resulting in a higher bending moment for the far offset.

The utilization decreases by over 1 in the TDZ for both the ULS near and far offset for the RCSCR as shown in Figure 9.17 compared to the conventional SCR. Nevertheless, for both cases, it is over the acceptable limit of one.

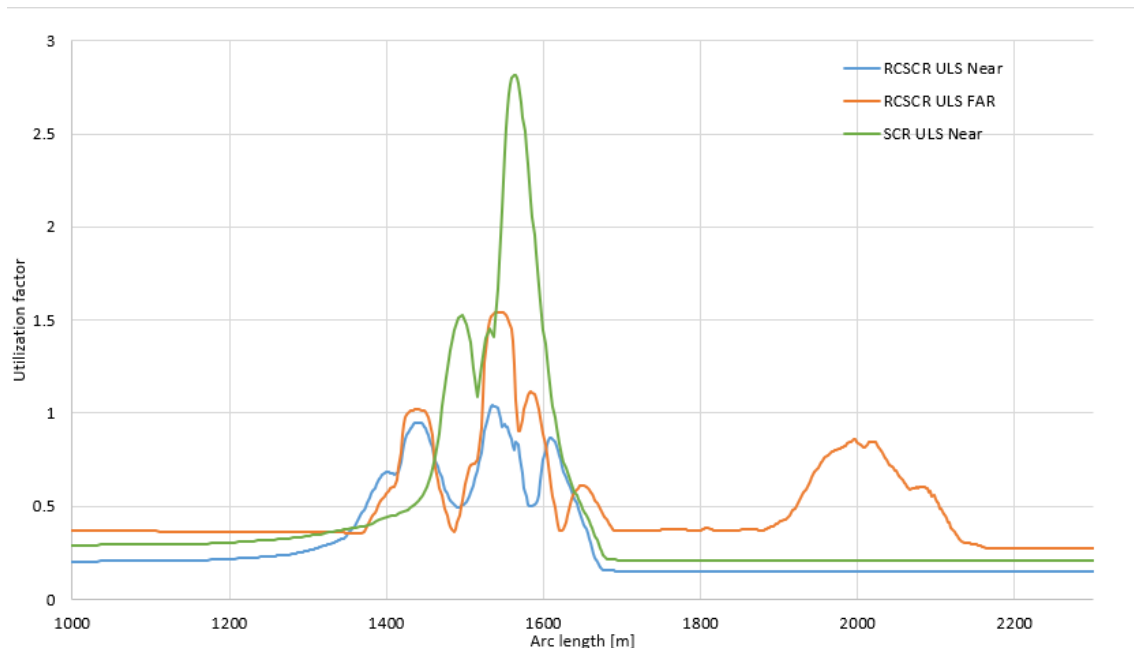


Figure 9.17: RCSCR and SCR utilization factor comparison

In Figure 9.18, a comparison for the compression for the ULS cases for the SCR and RCSCR are shown. Implementing the section with RC has increased the minimum effective tension in the riser for both offsets. Subsequently, the compression for the riser in the TDZ has been reduced. This reduction is due to the section's behaviour as a geometrical spring, previously described by Ramiro and Vesga [45][44], where the compression forces along the riser are propagated due to the local rigidity of the riser. This resulted in energy absorption from the vessel motions, effectively reducing the impact in the TDZ [46].

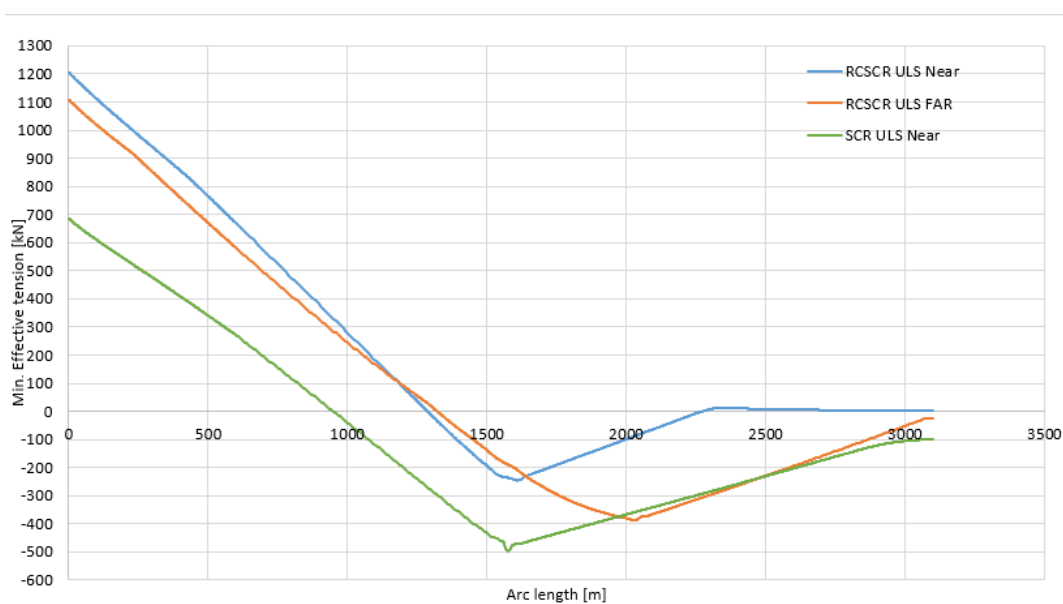


Figure 9.18: The minimum effective tension for RCSCR and SCR

9.8 Fine tuning of parameters

Since the preliminary results did not provide acceptable results, fine-tuning of the parameters and lowering the downward velocity were performed. The downward velocity was decreased to find the maximum velocity where the configuration would have a utilization below one for both near and far offsets.

9.8.1 Downward velocity of 3.63 m/s

As the RCSCR could not cope with a downward velocity of 3.81 m/s, a new seed with a maximum downward velocity of 3.63 m/s was analyzed. The strength responses are summarized in Table 9.9.

Table 9.9: Dynamic strength responses for the RCSCR with a downward velocity of 3.63 m/s

Dynamic results for the RCSCR	Offsets			
	ULS		ALS	
	Near	Far	Near	Far
Max. Bending moment [kNm]	828.48	1320.60	797.71	1331.62
Effective tension [kN]	3245.48	5233.85	3244.11	5505.99
Max. Compression [kN]	132.79	355.33	125.81	390.18
Max. DNV LRFD Utilization	0.959	1.496	0.841	1.365

The maximum utilization of 1.496 was observed in the ULS far design. The compression was highest in the ALS far design due to the extended free span of the riser. While the ULS near design had decreased to 0.959, within the acceptance criteria. With the ULS far design having a UF above 1, it shows that the RCSCR cannot cope with a downward velocity of 3.63 m/s.

9.8.2 Downward velocity of 3.42 m/s

As the result of the RCSCR were outside the allowable design criteria, an analysis of a slightly lower velocity of 3.41 m/s for the same configuration was performed. These results are presented in Table 9.10.

Table 9.10: Dynamic strength responses for the RCSCR with a downward velocity of 3.42 m/s

Dynamic results for the RCSCR	Offsets			
	ULS		ALS	
	Near	Far	Near	Far
Max. Bending moment [kNm]	834.40	1134.84	804.61	1152.62
Effective tension [kN]	3294.96	5046.16	3280.24	5376.81
Max. Compression [kN]	122.28	399.71	119.09	439.19
Max. DNV LRFD Utilization	0.943	1.359	0.814	1.278

The RCSCR had a maximum utilization in the far ULS design with 1.359. Still above the utilization factor limit, thus, the configuration cannot cope with a downward velocity of 3.42 m/s.

9.8.3 Downward velocity of 3.35 m/s

For the next analysis the velocity were reduced to 3.35 m/s and the summary of the results are presented in Table 9.11.

Table 9.11: Dynamic strength responses for the RCSCR with a downward velocity of 3.35 m/s

Dynamic results for the RCSCR	Offsets			
	ULS		ALS	
	Near	Far	Near	Far
Max. Bending moment [kNm]	803.89	1089.67	804.53	1103.44
Effective tension [kN]	3246.19	4871.36	3191.06	4906.64
Max. Compression [kN]	105.17	330.25	76.27	370.35
Max. DNV LRFD Utilization	0.913	1.214	0.806	1.149

It was clear that reducing the downward velocity improved both the compression and utilization. For the ULS near design, it was below one, while the far ULS design was unacceptable. The residual curvature peaks at the lower RC section, especially for the far ULS and ALS offsets as shown in Figure 9.19. It is clear that the residual curvature aids in reducing the UF for the riser overall and transitions the worst responses from the sagbend in the TDZ to the sections with RC.

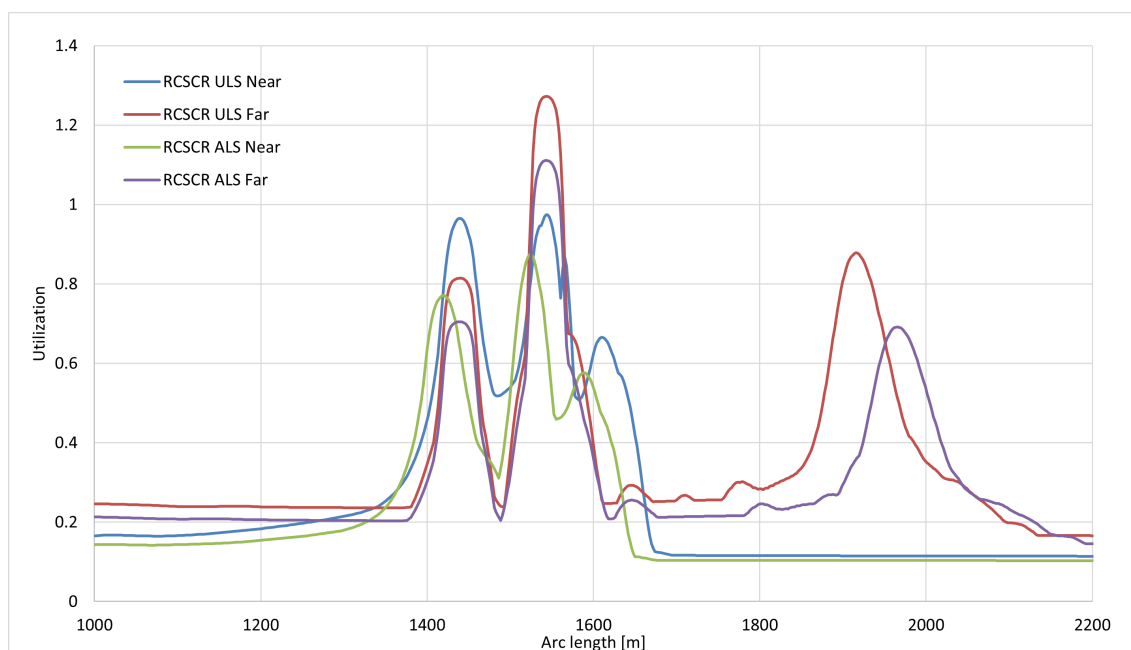


Figure 9.19: Strength response for RCSCR with for a downward velocity of 3.35 m/s

As decreasing the downward velocity has some impact on the utilization, the curvature of the sections had to be fine-tuned. The sensitivity analyses showed that the different curvatures for the under-and over-straightened sections saw the best utilization improvement. Having a higher curvature for the bottom section improved the UF for the near offsets, while on the other hand, increasing it for the far offset. Thus, the curvature for sections had to be altered to satisfy both offsets.

The analysis for different curvatures to the sections were performed where the results are presented in Table 9.12 and Table 9.13 for the near and far offsets. It can be seen that the optimal curvature for the upper section was 0.01 m^{-1} for both offsets, as this provided the lowest utilization. The upper section has the highest utilization for both offsets. Thus, the results for maximum utilization do not change for most combinations as the lower curvature section was altered.

Using a curvature of 0.01 m^{-1} for the upper section and 0.012 m^{-1} for the lower section, the utilization was reduced to 0.98 and 0.997 for the near and far offsets respectively. This corresponds to a radius of curvature of 100 m and 83.3 m. Moreover, the residual strain for the section was calculated using Equation 9.2, resulting in 16.2 % for the upper section and 19.4 % for the lower section.

$$\epsilon = r \times k = \frac{d}{2} \times k \quad (9.2)$$

Where: ϵ = Residual strain

r = Radius

d = Diameter

k = Curvature

Table 9.12: Fine tuning of residual curvatures section for the near offset position

Lower section curvature [1/m]	Radius of curvature [m]	Upper section curvature [1/m]									
		Max compression [kN]					Max UF				
		0.01	0.0125	0.015	0.02	0.025	0.01	0.0125	0.015	0.02	0.025
0.01	100.0	251.46	232.52	214.11	181.23	141.24	1.23	1.20	1.24	1.54	1.84
0.012	83.3	216.73	210.27	195.14	166.49	142.36	0.98	1.09	1.24	1.54	1.84
0.0125	80.0	234.61	219.16	203.17	172.73	146.87	1.12	1.09	1.24	1.54	1.84
0.015	66.7	216.42	204.18	190.79	163.42	139.15	1.03	1.09	1.24	1.54	1.84
0.016	62.5	208.89	197.99	185.44	159.57	135.96	0.99	1.09	1.24	1.54	1.84
0.017	58.8	201.51	191.65	179.99	155.66	132.73	0.95	1.09	1.23	1.54	1.84
0.0175	57.1	197.76	188.31	177.26	153.55	131.17	0.94	1.09	1.23	1.54	1.84
0.018	55.6	193.92	185.16	174.45	151.53	129.56	0.94	1.09	1.23	1.53	1.84
0.019	52.6	186.61	178.62	168.84	147.28	126.07	0.94	1.08	1.23	1.53	1.84
0.02	50.0	179.20	172.11	163.24	143.04	122.80	0.94	1.08	1.23	1.53	1.83
0.0225	44.4	161.36	156.02	148.96	132.05	114.21	1.06	1.08	1.23	1.53	1.83
0.025	40.0	144.63	140.45	135.01	120.96	105.39	1.20	1.20	1.23	1.53	1.83
0.0275	36.4	144.63	140.45	135.01	120.96	105.39	1.20	1.20	1.23	1.53	1.83
0.03	33.3	114.77	112.24	108.68	99.11	87.50	1.49	1.49	1.48	1.52	1.82

Table 9.13: Fine tuning of residual curvatures section for the far offset position

Lower section curvature [1/m]	Radius of curvature [m]	Upper section curvature [1/m]									
		Max compression [kN]					Max UF				
		0.01	0.0125	0.015	0.02	0.025	0.01	0.0125	0.015	0.02	0.025
0.01	100.0	432.94	406.14	387.29	312.54	314.65	1.05	1.15	1.32	1.49	1.87
0.012	83.3	389.80	389.85	366.59	320.43	283.33	0.997	1.15	1.31	1.49	1.87
0.0125	80.0	398.47	380.13	367.78	312.60	293.36	1.02	1.15	1.32	1.49	1.87
0.015	66.7	367.08	354.06	346.60	312.66	260.18	1.17	1.17	1.32	1.49	1.87
0.016	62.5	354.88	343.46	337.58	312.69	248.24	1.24	1.24	1.32	1.49	1.87
0.017	58.8	343.28	332.95	328.04	312.72	237.97	1.31	1.31	1.32	1.49	1.87
0.0175	57.1	337.19	327.53	323.53	312.73	232.68	1.34	1.34	1.35	1.49	1.87
0.018	55.6	331.21	322.13	319.01	312.75	227.04	1.37	1.37	1.39	1.49	1.87
0.019	52.6	318.94	311.35	310.22	312.78	220.08	1.44	1.44	1.45	1.49	1.98
0.02	50.0	306.65	300.59	301.59	312.81	262.66	1.51	1.51	1.52	1.49	1.98
0.0225	44.4	280.75	276.65	280.56	312.89	248.62	1.67	1.67	1.68	1.51	1.98
0.025	40.0	256.70	254.17	260.45	312.98	234.61	1.84	1.84	1.85	1.67	1.98
0.0275	36.4	256.70	254.17	260.45	312.98	234.61	1.84	1.84	1.85	1.67	1.98
0.03	33.3	215.93	214.71	223.00	313.16	206.09	2.17	2.17	2.18	1.98	2.18

9.9 Static analysis of the revised RCSCR configuration

Taking into consideration the sensitivity analysis and fine tuning of the RCSCR configuration, a new static analysis were performed to verify the compliance towards the DNV standards acceptance criteria. The parameters used were:

- Length of riser = 3100 m
- Length of section with curvature = 140 m (5 m - 5 m - 5 m- 2.5 m - 35 m - 2.5 m - 5 m - 5 m - 5 m - 5 m - 5 m- 2.5 m - 35 m - 2.5 m - 5 m - 5 m)
- Curvature upper section = 0.01 m^{-1}
- Curvature lower section = 0.012 m^{-1}
- Lowest RC section 11 m above the seabed in the static near offset position
- Downward velocity of 3.35 m/s

For the static analysis of the RCSCR, the DNV's acceptance criteria of keeping a utilization below one were achieved for all of the offsets as presented in Table 9.14. The effective tension were at its lowest for the near offset and highest for the far offset, as were expected due to the increased free span for the far offset. Similarly, the maximum bending moment was at the near offset, as the hang-off angle was smaller, creating a larger bend of the riser in the TDZ.

Table 9.14: Static result for revised RCSCR configuration

ULS Static for the RCSCR	Offsets		
	Near	Mean	Far
Effective tension [kN]	2671.15	2983.64	3409.36
Max. Bending moment [kNm]	754.34	741.26	732.69
Hang off angle [degrees]	8.22	10.01	16.10
Max. DNV LRFD Utilization	0.87	0.86	0.86

There was no compression along the riser for any of the offsets, visualized in Figure 9.20. As for the bending moment shown in Figure 9.21, the largest static moments were located in the residual curvature sections. It was also shown that the bending moment in the TDZ was far lower than for the RC section, as intended.

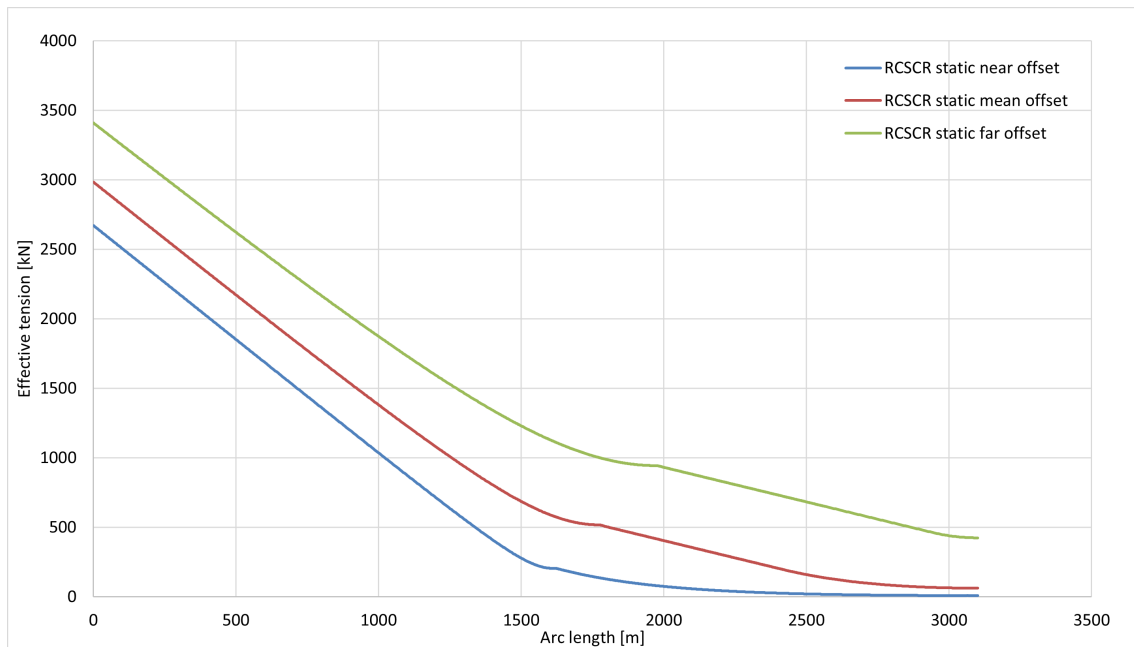


Figure 9.20: Effective tension for the RCSCR

As previously mentioned, the driving parameter for the utilization is the bending moment. While comparing Figure 9.21 and Figure 9.22, one can see that the maximum utilization occurs at the maximum bending moment as the graphs are almost identical. This clearly indicates that the critical response for the riser with residual curvature is the bending moment.

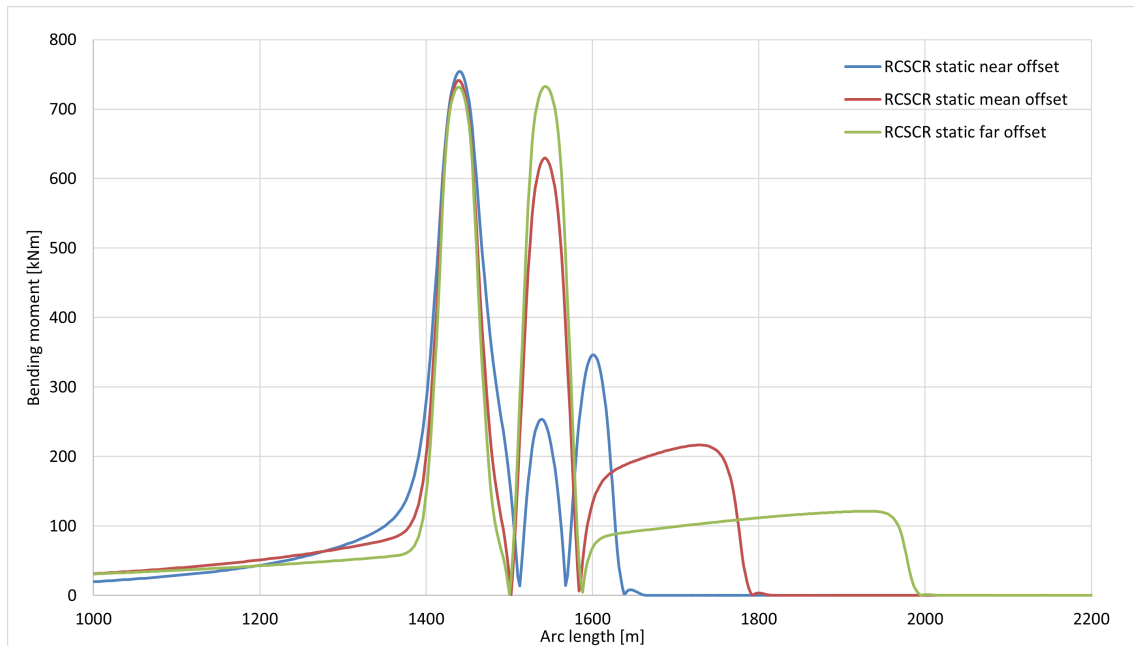


Figure 9.21: Bending moment for the RCSCR

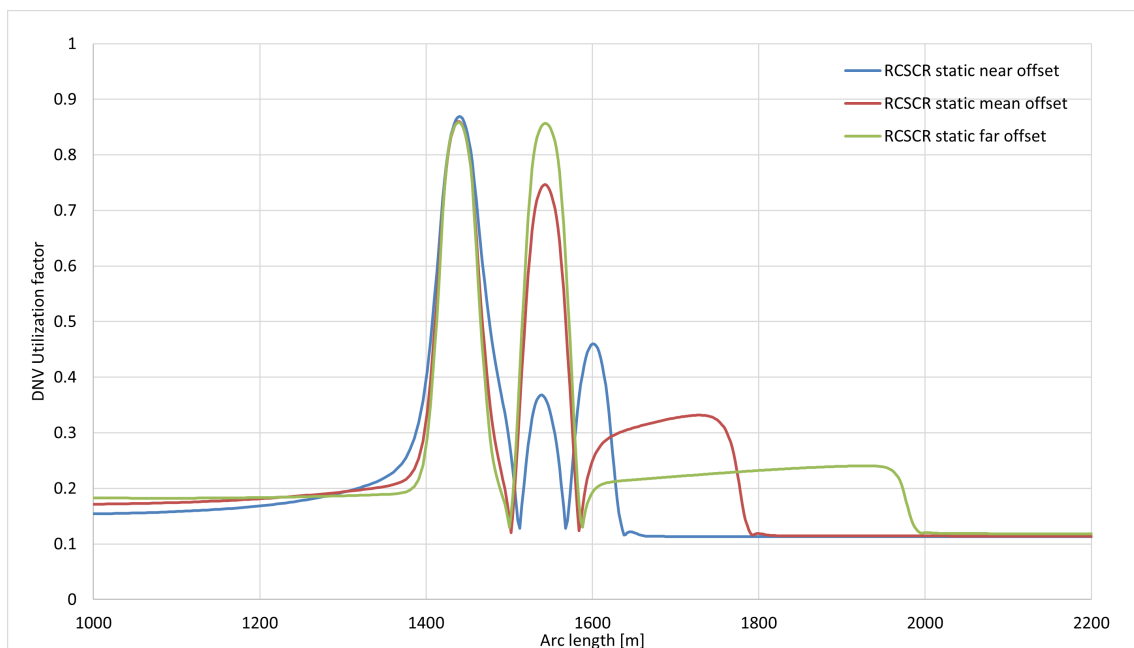


Figure 9.22: DNV utilization factor for the RCSCR

9.10 Dynamic analysis of the revised RCSCR configuration

Continuing the analysis for the RCSCR, this section covers the dynamic analysis of the riser with the revised configuration. This is in order to properly evaluate the responses from the extreme conditions, and to confirm that the acceptance criteria

are met. The parameters used for the dynamic analysis, are identical to the ones described in the static analysis for the RCSCR which were:

- Length of riser = 3100 m
- Length of section with curvature = 140 m (5 m - 5 m - 5 m- 2.5 m - 35 m - 2.5 m - 5 m - 5 m - 5 m - 5 m - 5 m- 2.5 m - 35 m - 2.5 m - 5 m - 5 m)
- Curvature upper section = 0.01 m^{-1}
- Curvature lower section = 0.012 m^{-1}
- Lowest RC section 11 m above the seabed in the static near offset position
- Downward velocity of 3.35 m/s

A summary of the dynamic response analysis for the revised RCSCR are presented in Table 9.15 for both ULS and ALS design.

Table 9.15: Dynamic strength responses for the revised RCSCR with a downward velocity of 3.35 m/s

Dynamic results for the RCSCR	Offsets			
	ULS		ALS	
	Near	Far	Near	Far
Max. Bending moment [kNm]	826.26	778.71	800.06	778.18
Effective tension [kN]	3196.63	5465.87	3156.29	5811.43
Max. Compression [kN]	204.76	389.53	186.33	421.43
Max. DNV LRFD Utilization	0.966	0.997	0.843	0.882

The RCSCR had a maximum utilization in the far ULS design with a value of 0.997 and are observed to be in the TDZ. It was observed that the bending moments were largest for the near offsets for both design cases. The effective tension and maximum compression were in the far offset similar to the SCR and were expected. This has shown that this configuration can cope with a downward velocity of 3.35 m/s.

9.11 Summary of the parametric study and response analyses

For the extreme analysis, the conventional SCR and the RCSCR responses have been studied to find a configuration able to handle the downward velocity in very harsh

North Sea environmental conditions. The DNV LRFD Utilization factor was used to assess the riser's capability to cope with the environmental and design conditions considered in this study.

The analyzes focused on finding a configuration for the RCSCR that is suitable to cope with a downward velocity of 3.81 m/s, as previous work has established that the conventional SCR cannot cope when it is higher than 2.33 m/s [7]. A parametric study of the parameters below impacting the residual curvature was performed.

- Section length
- Radius of curvature
- Distance to the seabed
- Number of sections in a row
- Separated sections

The results from the sensitivity study provided a configuration that reduced the utilization factor from 2.81 for the SCR to 1.54 for the RCSCR, still outside the allowable design criteria. Furthermore, it was proven that the utilization improves more when the implementation of the RC was closer to the sagbend in the TDZ. Additionally, the increased radius of curvature improved the attenuation of the compression forces. On the other hand, the utilization reduction stopped at 0.02 m^{-1} , before it increased again. The number of sections with residual curvature in a row or divided into separated sections was found to have no significant impact in reducing the utilization compared to having only one section.

In order to find a configuration working for both the near and far ULS design, the configuration had to be fine tuned and the downward velocity had to be reduced from 3.81 m/s to 3.35 m/s.

After the fine tuning, the optimal parameters for the RCSCR were as follows:

- Length of section with curvature = 140 m
- Curvature upper section = 0.01 m^{-1}
- Curvature lower section = 0.012 m^{-1}
- Lowest RC section 11 m above the seabed in the static near offset position

The feasible RCSCR, obtained a utilization factor of 0.966 and 0.997 for the ULS near and far designs respectively. Thus, proving that the residual curvature method aids in reducing the stress in the touchdown zone to acceptable limits. This extreme analysis on the RCSCR proved that the implementation of residual curvature to a conventional SCR could make it a feasible configuration for downward velocities up to 3.35 m/s with these environmental conditions.

Chapter 10

Fatigue analysis

10.1 Introduction

The riser is subjected to waves and currents, creating oscillatory motions that impact both the riser and the vessel. These environmental loads repeatedly produce cyclic stresses on the riser system by raising and lowering the riser on the seabed due to the vessel heaving. For riser fatigue design, there are three main stress cycles to consider as described by DNV [11]:

- Wave induced stress
- Low frequency stress
- Vortex induced stress

For both the SCR and RCSCR, the critical area for evaluating the fatigue is in the TDZ, caused by the vessel motions and soil-riser interaction. Due to time constraints, these fatigue analyses will only consider wave-induced fatigue damage. The calculations were performed using a non-linear time domain using an irregular wave model, which increases the numerical integration in small steps of the incremental dynamic equilibrium equations [11].

10.2 S-N curves

The fatigue calculation method in this thesis follows the S-N curve methodology, which defines the number of cycles to failure (N), while the riser is repeatedly cycled through a given stress range (S). Where the curves are expressed by Equation 10.1 and Equation 10.2.

$$\log N = \log \bar{a} - m \log S \quad (10.1)$$

$$S = S_0 \times SCF \times \left(\frac{t_3}{t_{ref}} \right)^k \quad (10.2)$$

Where:

N = Number of stress cycles to failure

S = Stress range

\bar{a} , m = Empirical constants

S_o = Nominal stress range

SCF = Stress concentration factor

$\left(\frac{t_3}{t_{ref}} \right)^k$ = Thickness correction factor, only applicable for $t_3 > t_{ref}$

t_3 = Pipe wall thickness

t_{ref} = Reference wall thickness

k = Thickness exponent

Figure 10.1 presents the various S-N curves used for risers in seawater using cathodic protection. For this thesis and fatigue calculations, only the D and C2 curves are considered. The D curve is less tolerant compared to the C2 curve and is expected to result in a higher fatigue damage for the riser, while the riser fatigue life for the D curve is also expected to be less, as previously established by Karunakaran et al. [18]. The curve parameters are highlighted in Table 10.1 and Table 10.2.

Table 10.1: Parameters for D-curve in seawater with cathodic protection

S-N Curve	$N < 10^6$ cycles		$N > 10^6$ cycles $\log \bar{a}_2$ $m_2 = 5.0$	Fatigue limit at 10^7 cycles [MPa]	Thickness exponent [k]
	m_1	$\log \bar{a}_1$			
D	3.0	11.764	15.606	52.63	0.20

Table 10.2: Parameters for C2-curve in seawater with cathodic protection

S-N Curve	$N < 10^6$ cycles		$N > 10^6$ cycles $\log \bar{a}_2$ $m_2 = 5.0$	Fatigue limit at 10^7 cycles [MPa]	Thickness exponent [k]
	m_1	$\log a_1$			
C2	3.0	11.901	15.835	58.48	0.15

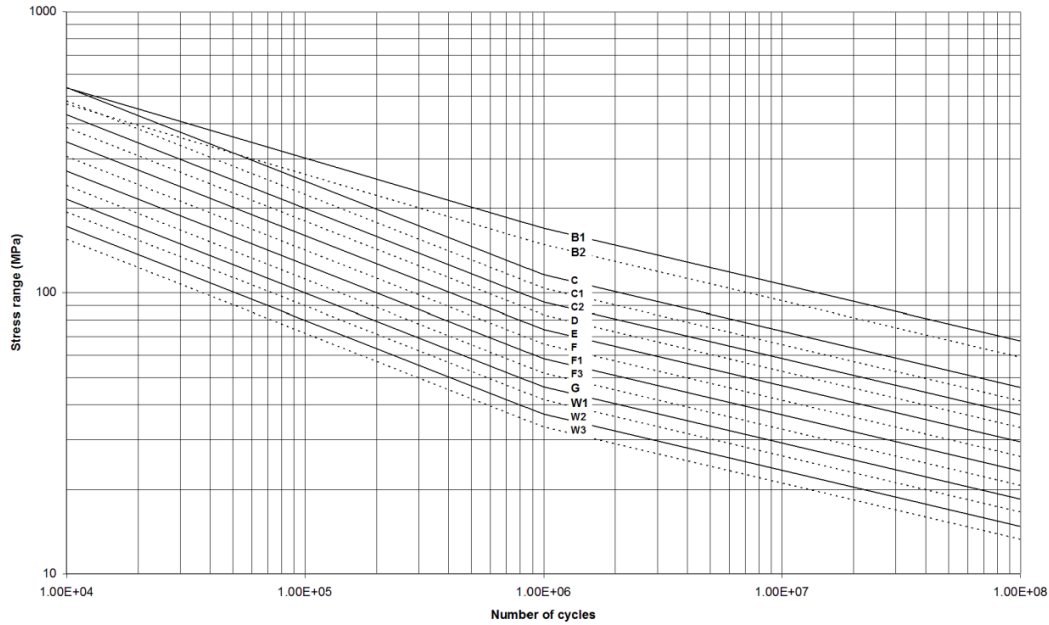


Figure 10.1: S-N curves in seawater with cathodic protection [47]

10.2.1 Stress concentration factor

The Stress Concentration Factor (SCF) is the local stress component divided by the nominal stress. This is taken into account when the stresses increases due to the geometric stress amplifiers that occur between two joints in the riser [47] In principle, two methods exist to obtain the SCF, either by performing finite element analyses or using a closed-form expression. The closed-form expression is described by Equation 10.3 for welded riser joints.

$$SCF = 1 + \frac{1e}{t_3} \exp\left(-\left(\frac{D}{t_3}\right)^{-0.5}\right) \quad (10.3)$$

Where:

D = outer diameter of the pipe

t_3 = Wall thickness of the pipe

e = Eccentricity caused by the imperfections in the geometry of the pipe

Based on this expression, a SCF of 1.2 is considered for the damage fatigue calculations for both D and C2 curves.

10.3 Wave induced fatigue

For wave-induced fatigue, the response is mainly induced by the vessel motions, making the vessel design and hang-off location on the FPSO the main contributors to mitigating the impact on the riser. For the fatigue damage calculations performed in this study, the FPSO and the risers are considered to be in the mean offset position.

In this study, there are a total of 12 wave directions considered for the wave-induced fatigue, based on metocean data for a typical North Sea area. Where the wave scatter diagram is defined by the spectral peak period (T_p), the significant wave height (H_s), covering a 100-year period, given a 3-hour storm sea state. Furthermore, the H_s in the wave scatter diagram covers a range between 0 to 16 meters, while the T_p ranges from 0 to 25 seconds.

For each of the 12 wave directions, a set of H_s and T_p combination must be considered, thus generating a total of 216 load cases for the fatigue damage calculations. The frequency of occurrence for the 12 directions is listed in Table 10.3, based on the global coordinate system of Orcaflex. These probabilities are used to determine the total fatigue damage from each wave direction.

Table 10.3: Sector probability for each of the wave directions

Wave direction [°]	Sector probability [%]
0	12.61
30	19.98
60	14
90	4.61
120	2.64
150	1.41
180	1.16
210	2.72
240	10.5
270	11.89
300	9.8
330	8.68
Sum	100

The fatigue damage calculation is based on the accumulation law by Palmgren-Miner [48] using Equation 10.4.

$$D_{fat} = \sum_{i=1}^{M_c} \frac{n_i}{N_i} \leq \eta \quad (10.4)$$

Where:

D_{fat} = Accumulated fatigue damage

η = Allowable damage ratio, considered to be 0.1

n_i = Number of stress cycles with stress range in block i

N_i = Number of cycles to failure at the i th stress range as defined by the S-N curve

For wave-induced fatigue damage calculations, the following procedures described by DNV [11] are considered:

- The wave scatter diagram is divided into a number of representative blocks.
- For each block, a single sea state representing all the sea states in the block is selected. The blocking of the wave scatter is shown in Figure 10.2, where the blue crosses mark the representative sea state for that block.
- The blocks are used to lump the probabilities of occurrence, defined as a percentage for all occurrences in each block over the total number of occurrences, as shown in Table 10.4.
- Calculation of the fatigue damage for every representative sea-state in all of the blocks. The simulation time for this analysis was 45 minutes (2700 seconds), to get a representative and accurate picture of the fatigue damage. In order to capture the damage at each weld along the total length of the riser, the damage is calculated at 8 equally spaced points around the circumference of the riser.
- The accumulated weighted fatigue damage for each of the sea states are calculated using Equation

$$D_L = \sum_{i=1}^{N_s} D_i P_i \quad (10.5)$$

Where:

D_L = Long term fatigue damage

N_s = Number of discrete sea states presented in the wave scatter diagram

D_i = Short term fatigue damage

P_i = Sea state probability

- The fatigue life can be estimated as the reciprocal of the total fatigue damage

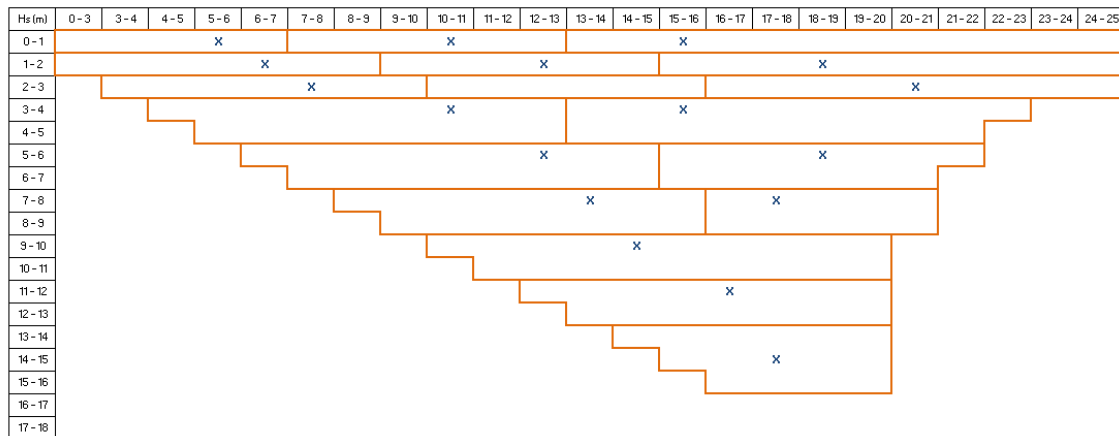


Figure 10.2: Blocking of the wave scatter diagram

Table 10.4: Lumped probability of occurrence for the representative sea states

S/N	Hs [m]	Tp [s]	Gamma	Lumped probability
1	0.5	5.5	1.00	2.83
2	0.5	10.5	1.00	3.52
3	0.5	15.5	1.00	0.14
4	1.5	6.5	1.00	18.53
5	1.5	12.5	1.00	14.04
6	1.5	18.5	1.00	0.43
7	2.5	7.5	1.34	16.08
8	2.5	14.5	1.00	12.03
9	2.5	20.5	1.00	0.27
10	3.5	10.5	1.00	20.26
11	3.5	15.5	1.00	3.57
12	5.5	12.5	1.00	5.79
13	5.5	18.5	1.00	0.47
14	7.5	13.5	1.08	1.49
15	7.5	17.5	1.00	0.12
16	9.5	14.5	1.40	0.36
17	11.5	16.5	1.17	0.07
18	14.5	17.5	1.59	0.01
Total probability				100

10.4 Results of the fatigue analysis

10.4.1 Conventional SCR

Two locations are critical to the fatigue performance of the SCR, the TDZ and just below the flex joint at the hang-off point. For this study, only the fatigue performance at the TDZ has been considered without the modeling of a flex joint. The implementation of the RCM to the SCR, which purpose is to absorb some of the energy generated by the floater motion, reducing the impact on the TDZ. For this reason, only the fatigue life in the TDZ is evaluated.

A summary of the fatigue performance for the C2 and D curves is presented in Table 10.5. The minimum life for the risers fatigue life required was 250 years. Thus, for both curves, it is way below the acceptance criteria. From Figure 10.3 and Figure 10.5 which shows the total damage of the riser and its expected life respectively, shows that the TDZ are very critical to wave-induced fatigue damage. As the minimum expected life for both curves is less than 250 years, it can be concluded that the SCR was not feasible for this location.

Table 10.5: SCR Fatigue life at the critical location

SCR location	C2-Curve	D-Curve
TDZ [years]	1.42	0.24

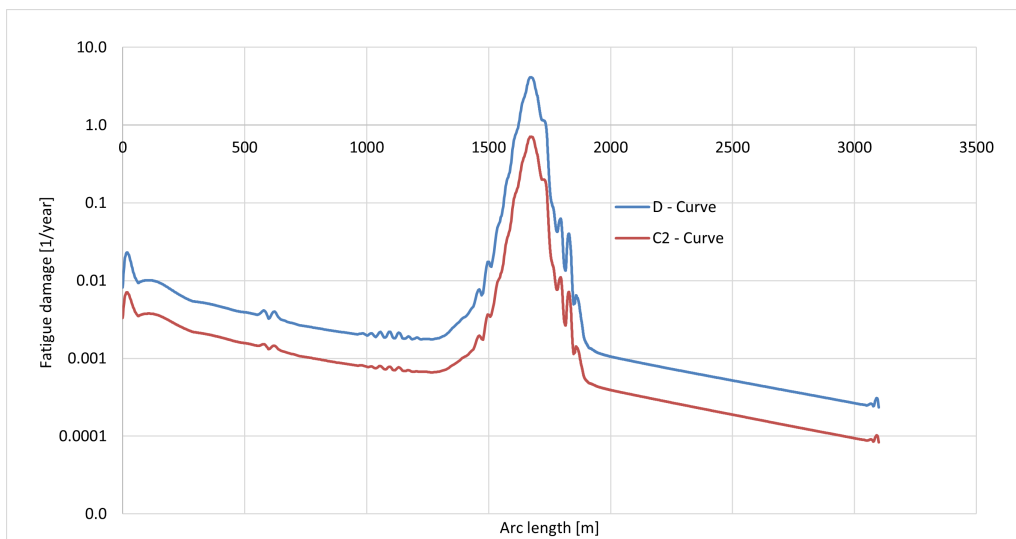


Figure 10.3: Total fatigue damage of the SCR

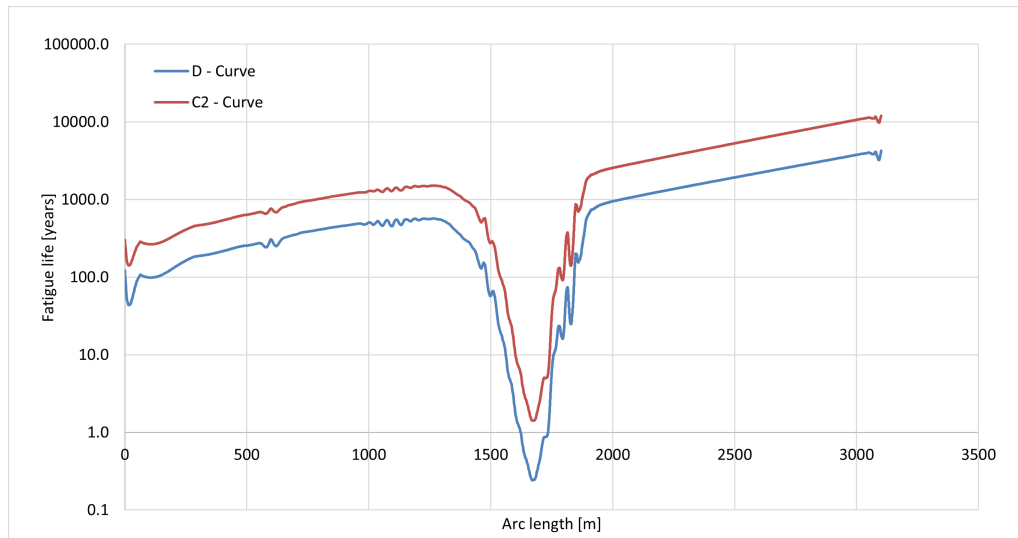


Figure 10.4: Fatigue life for the SCR

10.4.2 RCSCR

The RCSCR critical location for fatigue performance was also in the TDZ, similarly to the SCR. With the implementation of residual curvature to sections of the riser, it was expected to improve the fatigue performance. However, as can be seen from Table 10.6, there was some improvement, but still far off the minimum acceptance criteria. Figure 10.5 and Figure 10.6 the total damage along the risers total length and the expected fatigue life are presented.

It was observed that there was an improvement in the fatigue damage in the TDZ. Nonetheless, the peak of the fatigue damage was still in the area of contact between the riser and the seabed. The residual curvature section relieves some of the energy from the top of the riser to the TDZ, resulting in a fatigue enhancement. Moreover, it was noticed that with a higher radius of curvature, there was an increase in fatigue damage in the area, corresponding to lower fatigue life. The RCSCR cannot handle the fatigue loads for these environmental conditions.

Table 10.6: RCSCR Fatigue life at the critical location

SCR location	C2-Curve	D-Curve
TDZ [years]	11.74	1.65

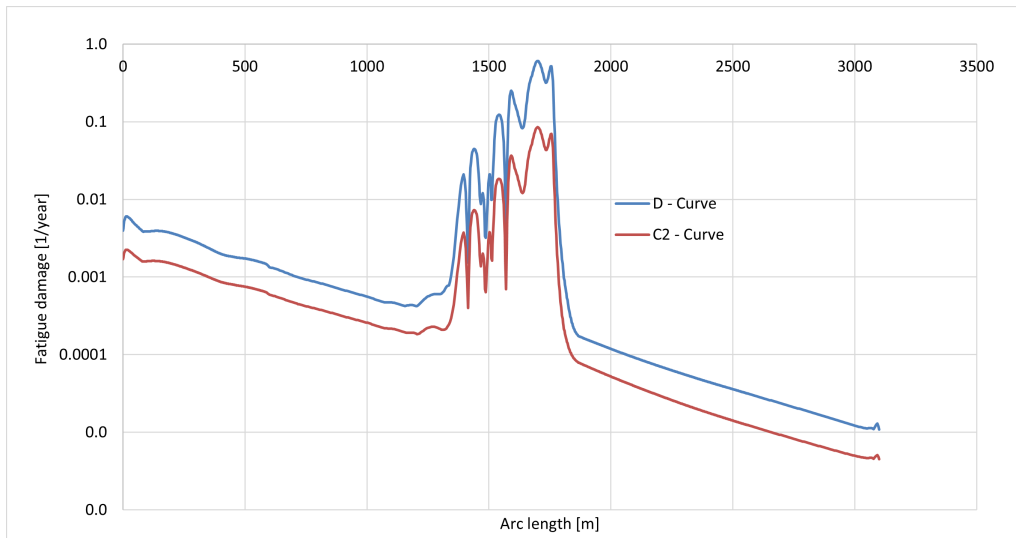


Figure 10.5: Total fatigue damage of the RCSCR

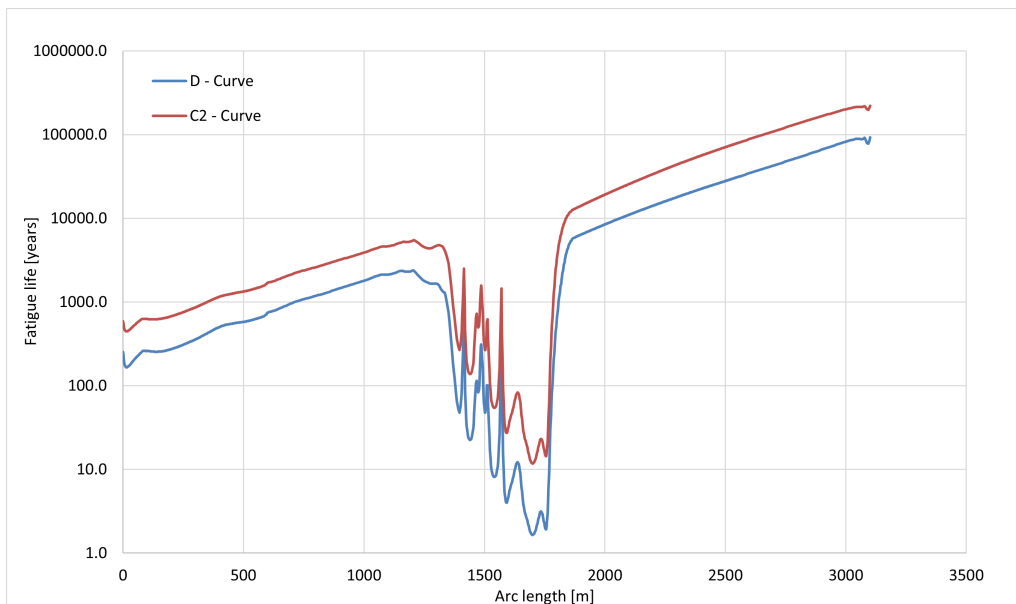


Figure 10.6: Fatigue life for the RCSCR

The fatigue performance for the RCSCR has been challenging. Similar to the SCR it is very sensitive to the vessel heave motion, which induces excessive cyclic stresses along the riser length. Particularly in the TDZ where the risers are affected by the soil-riser interaction. The low fatigue life in the TDZ is suspected due to the relatively low effective tension causing the riser to experience larger movements. Since the fatigue performance was not the main focus of the study, more extensive analyses were not executed to verify this assumption.

However, in order to improve the fatigue life, there has been several concepts discussed in previous published work and theses. As discussed by Ramiro et.al [4],

for a RCSCR at Santos Basin just outside Brazil, the RCM demonstrated a slight improvement in the fatigue performance compared to the SCR similarly to the results presented in this thesis. The paper also discusses alternative combinations for fatigue enhancements, such as weight distribution in the sagbend [16]. Moreover, a more detailed analysis on a weight distributed RCSCR was discussed by Vesga [44], which could handle both a higher downward velocity in addition to a significant improvement of the fatigue behavior.

Chapter 11

Conclusion and recommmendations

11.1 Conclusion

This thesis presents the application of the Residual Curvature Method for a 10” production SCR and its ability to cope with large vessel motions in deepwater and harsh environments. The variation of the SCR, named Residual Curvature Steel Catenary Riser (RCSCR), is compared to the conventional SCR in order to evaluate the effect of the implementation of residual curvature to the riser.

The location considered for the analyses is in the North Sea. As the location is remote and with limited existing infrastructure, a ship-shaped FPSO with an internal turret mooring system was selected as the preferred vessel. The metocean data for the location and the FPSO RAO’s are used to perform simulations and analyses for the strength, fatigue, and the parametric study of the SCR and RCSCR. All of the modeling and simulations were performed using Orcaflex.

Extreme response analysis

One of the main challenges for a SCR riser system is to cope with the large motion of the host platform due to deepwater applications and harsh environment. These motions may induce excessive buckling and fatigue in the TDZ, due to the riser and vessel being coupled together. This makes the downward velocity at the hang-off point at the top end of the riser attached to the vessel critical in the design. The downward velocity in the TDZ is heavily impacted by the downward velocity at the hang-off point. Thus, for the SCR, the critical sections of the riser is at the hang-off and in the TDZ.

For the conventional SCR, the analysis showed that the bending moment was the main design parameter as this had more impact on the DNV Utilization factor than the effective tension. Previous work showed that the conventional SCR with coating

could only cope with a maximum of 2.33 m/s of downward velocity. Thus, for a downward velocity of 3.81 m/s, which was used in the analysis, the utilization factor for near and far offsets in ULS and ALS were above the allowable limit. Thus, it was reaffirmed that the conventional SCR configuration would not be feasible in the extreme conditions of this location.

The parametric study of the RCSCR analyzed five parameters impacting the residual curvature; the section length, radius of curvature, distance to the seabed, number of sections in a row, and separated section. It was discovered that the section lengths had the lowest utilization below 200 m. The increase in radius of curvature improved the attenuation of compression forces in the riser. However, the reduction was lowest at 0.02 m^{-1} , and by increasing the radius of curvature, the utilization also increased. Moreover, the analysis showed that implementing the residual curvature sections closer to the seabed positively impacted the utilization factor, with the best result obtained at 11 m above the seabed in the near static offset position. On the other hand, the analyzes for the number of sections in a row and the separated sections proved to have no significant improvement over one section.

Implementing the residual curvature using the RCM on the SCR was proven to increase riser capacity to withstand higher downward velocities, thus improving the strength capacity. After the implementation, the RCSCR was able to cope with a maximum downward velocity of 3.35 m/s at the hang-off point, an increase of 43% compared to the SCR. The utilization factor for the ULS near and far offset were 0.966 and 0.997 respectively, reduced from 2.81 and 2.19 for the conventional SCR.

Fatigue performance

The wave-induced fatigue performance analysis for the SCR and the RCSCR considered twelve wave directions. A total of 18 load cases were generated for each wave direction. Thus, a total of 216 load cases were considered for the analyses.

The critical regions for fatigue for the risers are at the hang-off point and in the TDZ. However, the fatigue damage at the hang-off is mitigated by installing a flex joint at the top end of the riser. Moreover, the fatigue near the hang-off point does not directly impact the fatigue in the TDZ. As the study aimed to analyze the fatigue response in the TDZ the model did not include a flex joint.

The conventional SCR analysis only had a fatigue life of 0.24 years considering the D-curve. There was a tiny improvement by considering the C2 - Curve, increasing

the expected life to 1.42 years. For both, it was below the acceptance criteria of 250 years. The total fatigue damage of the riser peaked in the TDZ, going above the critical value of one.

A reduction in fatigue damage was observed for the RCSCR. The total fatigue damage did not exceed the critical value of one at any section of the riser. Moreover, some damage was transitioned from the TDP to the residual curvature sections. However, even with this improvement, the expected fatigue life did not improve significantly, with 1.65 and 11.74 years for the D and C2-curves, respectively, still below the acceptance criteria for fatigue design.

11.2 Recommendations

The studies performed in this thesis have investigated the feasibility of implementing residual curvature to the conventional SCR with the RCM. The results showed improvement in the strength and fatigue analyses compared to the SCR in harsh environmental conditions. However, the results also demonstrated that further work still needs to be done in order to cope with a higher downward velocity and especially analyze the fatigue performance. Thus, the following recommendations are made for further studies.

- A more comprehensive study for the parametric study can be performed using a Python algorithm in Orcaflex. This may optimize the RC configuration in the SCR for strength and fatigue damage reductions.
- Implementation of residual curvature to a weight distributed SCR. As the WDSCR has been proven to increase the riser's ability to cope with higher downward velocities, a comprehensive study to find its limitations in these harsh environments is recommended.
- A more exhaustive analysis of wave-induced and vortex-induced fatigue should be performed. The fatigue saw the least improvement and is a critical component for a feasible RCSCR.

References

- [1] IEA. *Key World Energy Statistics 2021*. Report. 2021. URL: <https://www.iea.org/reports/key-world-energy-statistics-2021>.
- [2] Offshore Magazine. *2019 DEEPWATER TECHNOLOGIES SOLUTIONS FOR CONCEPT SELECTION*. Report. 2019.
- [3] Yong Bai Qiang Bai. “Subsea Engineering Handbook”. In: (2012). ISSN: 9780123978059 012397805X 0123978041 9780123978042.
- [4] Andre Amorim Ramiro, Adekunle Peter Orimolade, and Daniel Nalliah Karunakaran. “Feasible SCR Configuration from FPSO with Large Motions, by Applying Residual Curvature Methods”. In: *Offshore Technology Conference*. Vol. Day 4 Thu, August 19, 2021. D041S045R003. DOI: 10.4043/31037-ms. URL: <https://doi.org/10.4043/31037-MS>.
- [5] E.H. Phifer et al. “Design And Installation Of Auger Steel Catenary Risers”. In: *Offshore Technology Conference*. Vol. All Days. OTC-7620-MS. DOI: 10.4043/7620-ms. URL: <https://doi.org/10.4043/7620-MS>.
- [6] Adekunle Peter Orimolade. “Steel lazy wave risers from turret moored FPSO”. Thesis. 2014.
- [7] Gilang M. Gemilang. “Feasibility study of selected riser concepts in deep water and harsh environment”. Thesis. 2015.
- [8] D. Karunakaran, N.T. Nordsve, and A. Olufsen. “An Efficient Metal Riser Configuration For Ship And Semi Based Production Systems”. In: *The Sixth International Offshore and Polar Engineering Conference*. Vol. All Days. ISOPE-I-96-106.
- [9] Geir Endal et al. “Reel-Lay Method to Control Global Pipeline Buckling Under Operating Loads”. In: *ASME 2014 33rd International Conference on Ocean, Offshore and Arctic Engineering*. Vol. Volume 6B: Pipeline and Riser Technology. V06BT04A005. DOI: 10.1115/omae2014-24062. URL: <https://doi.org/10.1115/OMAE2014-24062>.

- [10] Geir Endal and PR Nyström. “Benefits of Generating Pipeline Local Residual Curvature during Reel-lay and S-lay Installation”. In: *OPT Conference, Amsterdam*.
- [11] DET NORSKE VERITAS AS. *DNV-ST-F201: Dynamic Risers*. Standard. 2020. URL: <https://rules.dnv.com/docs/pdf/dnvpmp/codes/docs/2001-01/0s-F201.pdf>.
- [12] Chiemela Victor Amaechi. “Bonded Marine Hoses for Floating Offshore Structures (FOS)”. In: (2021).
- [13] DET NORSKE VERITAS AS. *DNV-SE-0476 Offshore riser systems*. Standard. 2017.
- [14] D. Karunakaran. *Pipelines and Risers Lecture Slides*. Generic. 2015.
- [15] Dr Frank Lim Howells and Dr Hugh. *DEEPWATER RISER VIV, FATIGUE AND MONITORING*. Conference Paper. 2000.
- [16] D. Karunakaran et al. “Weight-Optimized SCRs For Deepwater Harsh Environments”. In: *Offshore Technology Conference*. Vol. All Days. OTC-17224-MS. DOI: 10.4043/17224-ms. URL: <https://doi.org/10.4043/17224-MS>.
- [17] Dr Hugh Howells Hatton and Stephen A. “CHALLENGES FOR ULTRA-DEEP WATER RISER SYSTEMS”. In: *Floating Production Systems IIR* (1997).
- [18] Jean-Luc Legras, Daniel Karunakaran, and Richard Jones. “Fatigue Enhancement of SCRs: Design Applying Weight Distribution and Optimized Fabrication”. In: (2013). ISSN: 9781613992418. DOI: 10.4043/23945-MS.
- [19] Bjarte Kvamme et al. *Marine Operation Windows Offshore Norway*. 2016, V007T06A038. DOI: 10.1115/OMAE2016-54840.
- [20] C.R. Enze et al. “Auger Tlp Design, Fabrication, And Installation Overview”. In: *Offshore Technology Conference*. Vol. All Days. OTC-7615-MS. DOI: 10.4043/7615-ms. URL: <https://doi.org/10.4043/7615-MS>.
- [21] Ruxin Song, Basim Mekha, and Abhilash Sebastian. *Independent Design Verification of SCRs for Ultra Deepwater IHF Development*. 2006. DOI: 10.1115/OMAE2006-92502.

- [22] Jean-Luc Legras, Daniel N. Karunakaran, and Richard Lloyd Jones. “Fatigue Enhancement of SCRs: Design Applying Weight Distribution and Optimized Fabrication”. In: *Offshore Technology Conference*. Vol. All Days. OTC-23945-MS. DOI: 10.4043/23945-ms. URL: <https://doi.org/10.4043/23945-MS>.
- [23] Stael Ferreira Senra et al. “Challenges Faced in the Design of SLWR Configuration for the Pre-Salt Area”. In: *ASME 2011 30th International Conference on Ocean, Offshore and Arctic Engineering*. Vol. Volume 4: Pipeline and Riser Technology, pp. 67–75. DOI: 10.1115/omae2011-49096. URL: <https://doi.org/10.1115/OMAE2011-49096>.
- [24] American Petroleum Institute. *Recommended Practice for Design, Selection, Operation and Maintenance of Marine Drilling Riser Systems*. Standard. 1993.
- [25] Ian Frazer. *DEVELOPMENT OF METALLIC RISER SYSTEMS FOR DEEP WATER APPLICATIONS*. Conference Paper. 1998.
- [26] OFFSHORE ENERGY. *BP to develop two new North Sea projects*. Web Page. 2018. URL: <https://www.offshore-energy.biz/bp-to-develop-two-new-north-sea-projects/>.
- [27] Arvind Keprate. “Appraisal of riser concepts for FPSO in Deepwater”. Thesis. 2014.
- [28] NOV. *Submerged Turret Production*. Web Page. URL: <https://www.nov.com/products/submerged-turret-production>.
- [29] NOV. *External Turret Production*. Web Page. URL: <https://www.nov.com/products/external-turret-production>.
- [30] MCS Advanced Subsea Engineering. “IMPACT OF MARINE GROWTH ON PIPELINE RISERS FOR FLOATING PRODUCTION FACILITIES”. In: (2009).
- [31] Subsea 7. *Residual Curvature Method*. Standard. 2021.
- [32] Venu Rao et al. “Residual Curvature Method of Mitigating Lateral Buckling for HPHT PIP System – A case study”. In: *Offshore Technology Conference*. Vol. Day 3 Wed, May 08, 2019. D031S038R007. DOI: 10.4043/29603-ms. URL: <https://doi.org/10.4043/29603-MS>.

- [33] Andrew C. Palmer. *Subsea pipeline engineering*. 2nd. Tulsa, Okla: PennWell, 2008. ISBN: 9781593701338.
- [34] Tewolde Abraham. “Pipelay with Residual Curvature”. Thesis. 2017.
- [35] *Bending moments and beam curvatures*. Web Page. 2004.
- [36] Alan Roy et al. *Straightener Settings for Under-Straight Residual Curvature of Reel Laid Pipeline*. 2014, V06BT04A046. DOI: 10.1115/OMAE2014-24513.
- [37] Philip Cooper, Tao Zhao, and Ferry Kortekaas. *Residual Curvature Method for Lateral Buckling of Deepwater Flowlines*. 2017.
- [38] Subsea 7. *ST-GL-ENG-RP-010 Pipeline Spooling (Reeling) and Straightening Analysis*. Standard. 2015.
- [39] Per R. Nystrøm, Geir Endal, and Odd M. Lyngsaunet. “Lay Method to Allow for Direct Tie-in of Pipelines”. In: *The Twenty-fifth International Ocean and Polar Engineering Conference*. Vol. All Days. ISOPE-I-15-488.
- [40] Geir Endal, Per R. Nystrøm, and Odd M. Lyngsaunet. “Lay Method to Make Pipelines Conform to Uneven Seabed Topography”. In: *The Twenty-fifth International Ocean and Polar Engineering Conference*. Vol. All Days. ISOPE-I-15-489.
- [41] DET NORSKE VERITAS AS. *DNV-RP-F204 Riser fatigue*. Standard. 2019.
- [42] DET NORSKE VERITAS AS. *DNVGL-OS-E301 Position mooring*. Standard. 2018.
- [43] T.Moros R.Thethi. “Soil Interaction Effects on Simple Catenary Riser Response”. In: (2001).
- [44] Jeison Leandro Vesga Hernandez. “Feasibility Study of Application of Residual Curvature Method in Deepwater Free Hanging Risers”. Thesis. 2019.
- [45] Andre Ramiro. “Estudo da Curvatura Residual Aplicada ao Problema da Compressão Dinâmica em Risers Rígidos em Catenária Livre”. Thesis. 2018.

REFERENCES

- [46] Andre Amorim Ramiro, Adekunle Peter Orimolade, and Daniel Nalliah Karunakaran. “Feasible SCR Configuration from FPSO with Large Motions, by Applying Residual Curvature Methods”. In: *Offshore Technology Conference*. Vol. Day 4 Thu, August 19, 2021. D041S045R003. DOI: 10.4043/31037-ms. URL: <https://doi.org/10.4043/31037-MS>.
- [47] DET NORSKE VERITAS AS. *DNV-RP-C203 Fatigue design of offshore steel structures*. Standard. 2019.
- [48] Yong Bai and Qiang Bai. “Subsea Pipelines and Risers”. In: *Subsea Pipelines and Risers* (2005). DOI: 10.1016/B978-0-08-044566-3.X5000-3.
- [49] Orcina. *Orcaflex Web Help*. Web Page.

Appendices

Appendix A - Description of the ORCAFLEX Software

Introduction

Orcaflex is the main analysis software used in the thesis work. It is primarily design for static and dynamic analysis for offshore structures, such as rigid and flexible risers and mooring systems. The software is developed by Orcina, and the information presented is based on the software user manual.

The analyzes are performed using a non-linear time domain, which can be executed for certain parts of a system or the whole system. Moreover, it can be utilized for extreme response analyses in various sea-states and for fatigue analyses of marine risers among others.

In design and analyzes of an offshore system, there are several code checks included in the software such as [49]:

- DNV-OS-F201
- DNV-OS-F101
- API RP 2RD
- API STD 2RD
- API RP 1111

Overview of the software

The graphical user interface of Orcaflex is user friendly, intuitive and robust. It provides a solid visual representation of all parts of an offshore system as it is modeled.

Orcaflex is based upon a main window that contains menus, a toolbar, a status bar and at least one 3D view as presented in Figure A-1. The menu bar contains commands for opening and saving a file, editing a file, modeling creation, perform calculations, analyzes and batch processing. It may also be used to access different views of the model, and open multiple workspace windows.

The toolbar contains a variety of buttons that provide quick access to the most frequently used menu items [49]. It contains shortcuts for modeling of a system, analyzes and obtaining the results as shown in Figure A-2.

The status bar provides status information on the current action that is being performed, which displays the current iteration, number, time and completion of action for an simulation.

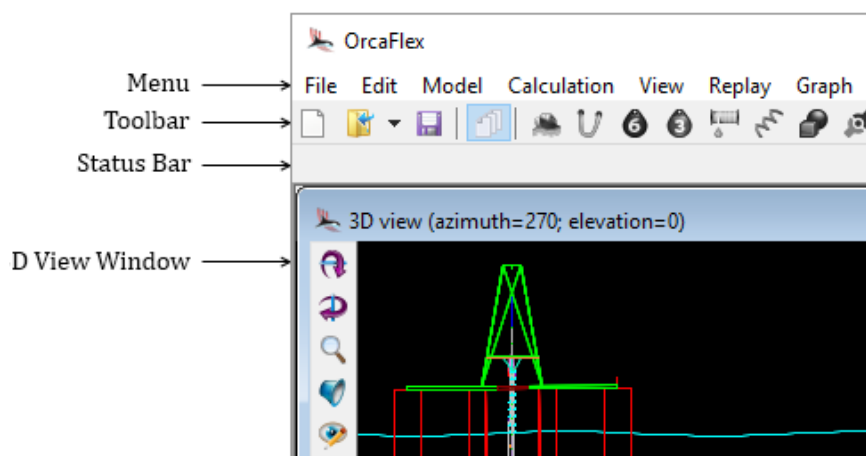


Figure A-1: The Orcaflex main window [49]




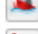



















Button	Action	Equivalent menu item
	Open	File Open
	Save	File Save
	Model browser	Model Model browser
	New vessel	Model New vessel
	New line	Model New line
	New 6D buoy	Model New 6D buoy
	New 3D buoy	Model New 3D buoy
	New winch	Model New winch
	New link	Model New link
	New shape	Model New shape
	New constraint	Model New constraint
	New turbine	Model New turbine
	Calculate statics	Calculation Statics
	Run dynamic simulation	Calculation Run dynamic simulation
	Pause dynamic simulation	Calculation Pause dynamic simulation
	Reset	Calculation Reset
	Start replay	Replay Start replay
	Stop replay	Replay Stop replay
	Step replay forwards	Replay Step replay forwards
	Edit replay parameters	Replay Edit replay parameters
	Add new 3D view	Window Add 3D view
	Examine results	Results Select results
	Help contents and index	Help OrcaFlex help

Figure A-2: Orcaflex toolbar [49]

Modeling and analyzes

Orcaflex build a mathematical model of the system being analyzed, where the model is comprised of a series of interconnected objects, such as lines, vessel and buoys [49]. The sequence of the analyzes is shown in Figure A-3. Iff the static analyzes are unable to complete, the dynamic analyzes will not be performed. Thus, the model has to be modified or time steps decreased.

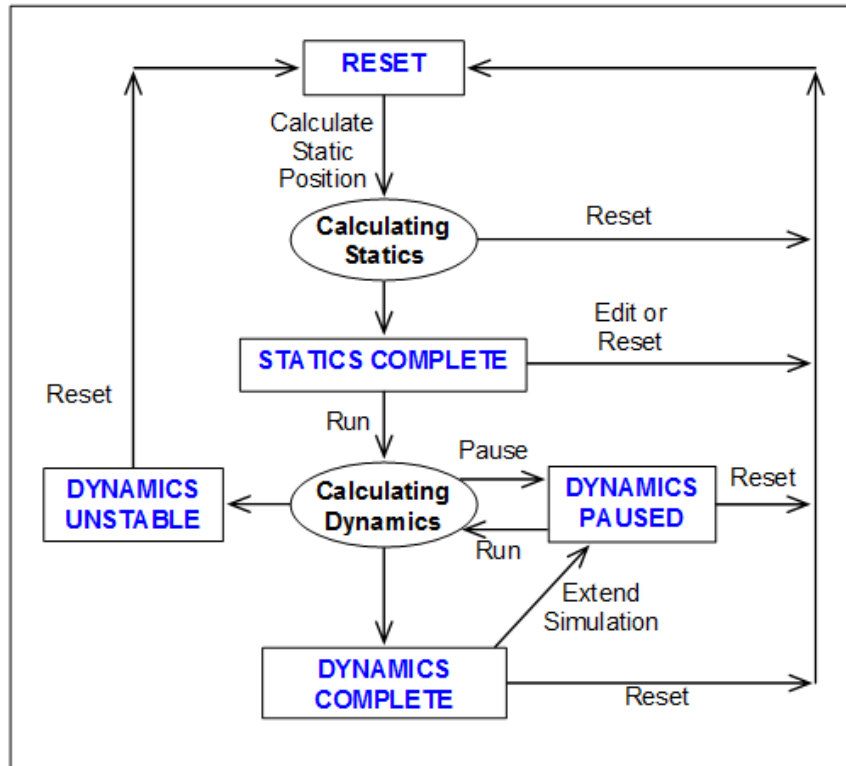


Figure A-3: Orcaflex model states [49]

Coordinate systems

Orcaflex consists of a number of frames of reference, each of which has a reference origin and a set of axes directions that represents the different coordinate systems. The global frame of reference denoted G_{XYZ} , where the global axis directions are denoted G_X , G_Y and G_Z . The local coordinate systems, which is usually generated for each object of the model are denoted L_{xyz} , with local axes L_x , L_y and L_z . For line end orientations it has a coordinate system denoted E_{xyz} .

All of the coordinate systems are right-handed, where the positive rotations are clockwise. A representations of the the coordinate system and axes is shown in Figure A-4.

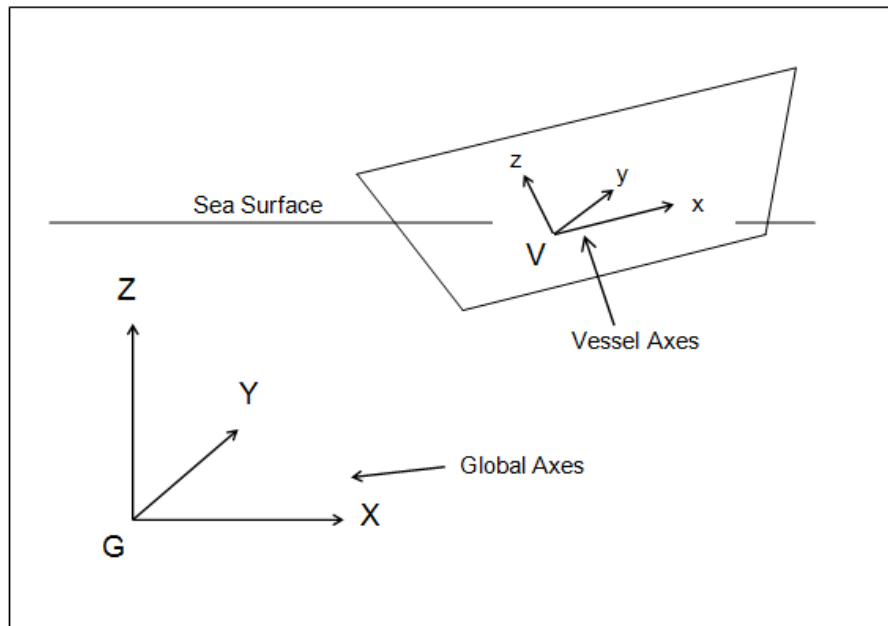


Figure A-4: Orcaflex coordinate system [49]

The directions and headings are defined in the horizontal plane in Orcaflex as the azimuth angle of the directions in degrees, measure positive from the x-axis towards the y-axis, as illustrated in Figure A-5 [49].

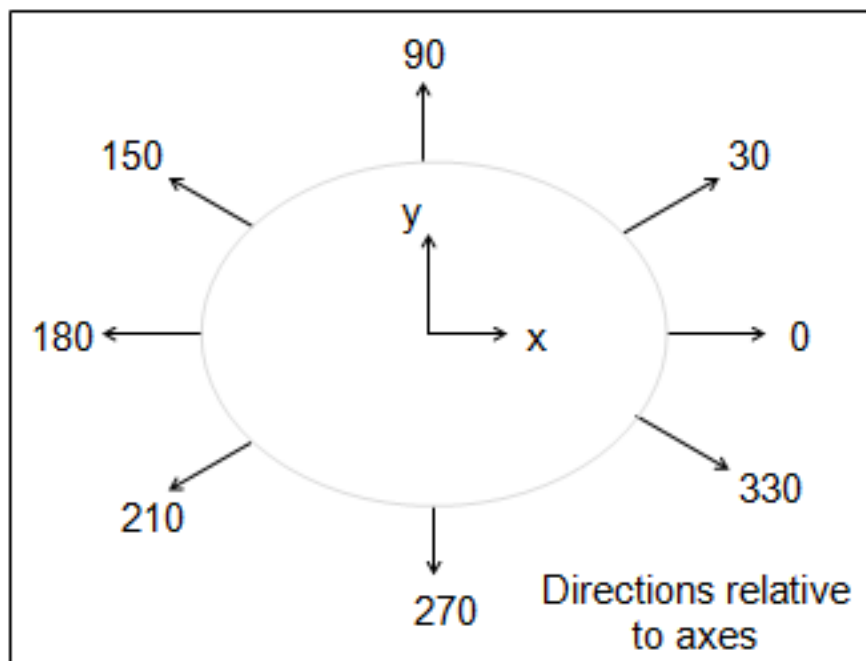


Figure A-5: Orcaflex headings and directions [49]

The directions for waves, current and wind are specified by giving the direction in which the wave, current or wind is progressing relative to the global axes. In other

words, the x and y-axes in Figure A-5 correspond to the global G_X and G_Y axes.

Simulation stages

The simulation period is defined as the number of consecutive stages. In which the duration are specified by the data. Before the main simulations stage, there is a build-up stage, where the wave and vessel motions are ramped up smoothly from zero to their full size. This helps reduce the transients that are generated by transitioning from the static position to full dynamic motion. The build up-stage is numbered 0, and its length should be at least one wave period [49]. A schematic of the simulation time and stages are shown in Figure A-6.

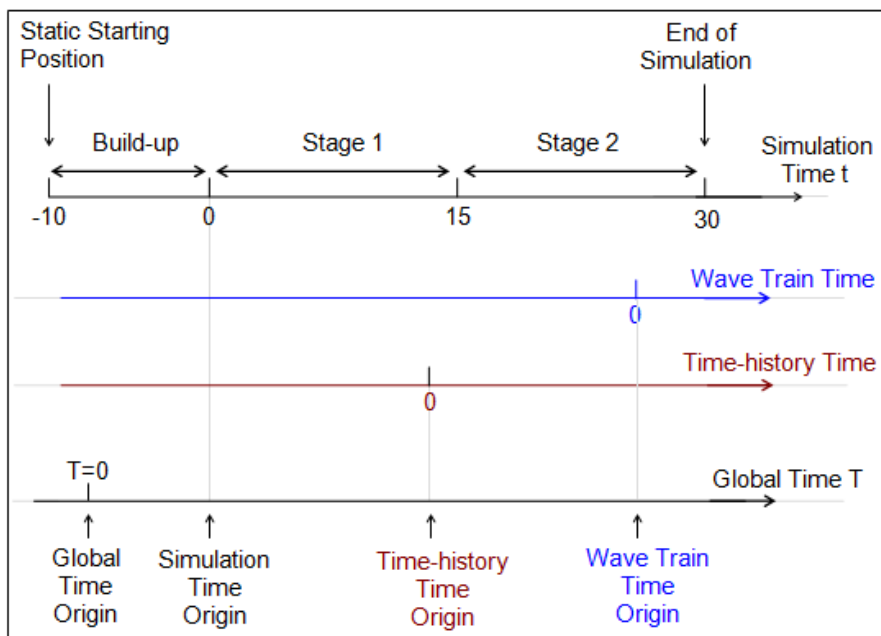


Figure A-6: Time and simulation stages [49]